GENETIC ANALYSIS OF PRY-1/AXIN IN CAENORHABDITIS BRIGGSAE

GENETIC ANALYIS OF PRY-1/AXIN FUNCTION IN THE NEMATODE CAENORHABDITIS BRIGGSAE

By

NAGAGIREESH BOJANALA, B.Sc. M.Sc.

A Thesis

Submitted to the School of Graduate Studies

In partial fulfillment of the Requirements

For the Degree

Master of Science

McMaster University

MASTER OF SCIENCE (2007) McMaster University
(Biology) Hamilton, Ontario.

TITLE: Genetic analysis of *pry-1*/Axin function in the nematode *Caenorhabditis briggsae*

AUTHOR: Nagagireesh Bojanala (McMaster University)

SUPERVISOR: Bhagwati P Gupta, Ph. D., Assistant professor, McMaster University

NUMBER OF PAGES: xi, 138

ABSTRACT

Evolutionary variations during vulval development in *C. elegans* and its related nematode species are well analyzed. The formation of *C. elegans* vulva involves many complex cell–cell interactions that are mediated through well conserved EGF/EGFR/RAS, LIN-12/Notch and WNT signaling pathways. These pathways specify distinct cell fates of the six epidermal vulval precursor cells (VPCs), P(3-8).p. *pry-1*/Axin in *C. elegans* is identified as a part of destruction box complex that mediates β-catenin degradation and is known to negatively regulate canonical Wnt signaling pathway during its development. I focused on the genetic analysis of *pry-1*/Axin function in *C. briggsae,* sister species to *C. elegans,* to study inter-species comparisons of vulva formation. Three alleles, *lin(sy5353), lin(sy5411) and lin(sy5270)* were genetically mapped to LG I using standard genetic and indel mapping techniques. Interestingly, a unique simultaneous Multivulva and Vulvaless (Muv-Vul) phenotype was observed during vulva formation in *Cbr-pry-1* alleles, resulting from the varying induction potentials of the VPCs along the A/P axis, compared to *Cel-pry-1* animals. In order to analyze these phenotypic differences between *Cel-pry-1*and *Cbr-pry-1* in greater detail, I dissected vulval development in *sy5353* animals. VPC competence analysis was done through cell lineages and ablations studies, while the *C. briggsae* vulval cell fate markers were used for cell fate specification analysis. Cell ablations revealed that P7.p and P8.p in *Cbr-pry-1* animals exhibited non-competence towards anchor cell signaling. Additionally, gonad-independent inductions was observed in P(3-8).p cells and they adopted 2^0 cell fate specifications. Using RNAi approach, *Cbr-pry-1* interactions with other vulval pathway genes were dissected and it was observed that *Cbr-lin-12* is involved in VPC competence of P7.p and *Cbr-pop-1* exhibited different regulatory levels during vulval development compared to *C. elegans.* Thus, it can be inferred that the mechanisms of vulva formation in *C. briggsae* has evolved through changes in the competence of VPCs.

Acknowledgements

I express my sincere gratitude to Dr. Bhagwati Gupta for introducing me to the 'wonderful worms'. I thank him for his patience during my initial learning process and for teaching genetics and cell biology aspects of the worm and his invaluable guidance during the present study. I would also like to thank Dr. Ana Campos for her suggestions and guidance towards my research during the committee meetings and Dr. Rama Singh for being part of my defense committee. I express my gratitude to the Department Of Biology, McMaster University for providing Teaching Assistantship and bursary during my graduate studies. I enjoyed myself as a lab instructor for 1A03, 1AA3 and 3MO3 courses and meanwhile had an opportunity to analyze my teaching abilities. I convey my special thanks to Pat, Barb and other administrative staff for their assistance. Furthermore, I will be really missing the fun I had during the BGSS Annual Picnic, Holy frolic, Halloween parties and Biology-Psychology Volleyball Club during my graduate life.

I convey my gratefulness to the past and present members of Dr. Gupta lab: Sujatha, Zobia, Joanna, Sushmita, Ajit, Mike, Renu, Tram, Cindy, Ashwin, Mark, Jhon, Prateek, Rajneet, Naved, Shyema and Hayoung, for their support and assistance in the wormlab. I would like to convey my special thanks to Pradeep and Sujatha for their cooperation and encouragement during their stay in Canada. I am deeply thankful to Ajit, Ashwin and Bijan for their patience and time during the final revisions of my thesis. My friendship with Renu and Ashwin always added more fun in the lab routine and in my personal life. I wish good luck to them in their future endeavors. Finally, I would like to appreciate the efforts of 'MacIndian Association' at McMaster in keeping our spirits high and for organizing cultural and religious activities at Mac. I am deeply thankful to Vipulbhai & family, Mukeshbhai, Mihir, the 301- 1716 Trio (Nilesh, Dharmesh and Yuvraj) and all other Indian friends at Mac for their friendship and support.

Finally, I thank my family for their encouragement and continuous support in all my endeavors. I did really miss my niece, Thanmai and all of my family members during my graduate life.

Table of Contents

List of Tables viii
List of Figures x
Chapter 1. Introduction 1
1.1 *C. elegans* as a model organism to study animal development 2
1.2 Vulval development in *C. elegans* 3
1.2.1 Cellular aspects 4
1.2.2 Genetic analysis 5
1.3 Signaling pathways involved in vulval development 5
1.3.1 Ras signaling 6
1.3.2 Lateral/Notch/ LIN-12 signaling 6
1.3.3 Synmuv signaling 7
1.3.4 Wnt signaling 8
1.4 Hox targets of Wnt signaling in vulval cell fate specification 8
1.5 Additional Wnt signaling components in *C. elegans* 9
1.6 Evolution of vulval development in *C. elegans* and related nematode species 10
1.7 Resources available for *C. elegans* - *C. briggsae* comparative studies 11
1.8 Present study 12
Chapter 2. Materials and Methods 25
2.1.1 Nematode strains used in the present study 25
2.1.2 Nomenclature and standard phenotypic description of the strains 25
2.1.3 Growth conditions and manipulations of the worms 26
2.1.4 Maintenance and cleaning of the mutant stocks 27
2.1.5 Calculating brood size 27
2.2 Genetic methods 28
2.2.1 Genetic crosses 28
2.2.2 Complementation study 28
2.2.3 Two-factor cross to assign new mutations to specific linkage groups 29
2.2.4 Cis two-factor self-cross for measuring recombination frequencies 30
2.2.5 Protocol for Indel mapping 30
2.3 Cell biology 31

2.3.1 Scoring vulval induction pattern 31
2.3.2 Scoring vulval cell lineages 31
2.3.3 Laser microsurgery technique for cell ablations 32
2.3.4 Microscopy and Photography 32
2.5 Molecular biology 32
2.5.1 DNA extraction from worms 33
2.5.2 Polymerase Chain Reaction 33
2.5.3 Agarose gel electrophoresis 33
2.5.4 RNAi 34
Chapter 3. Phenotypic characterization and genetic mapping of *pry-1* in *C. briggsae* ... 35
Background 36
3.1 Genetic characterization of *Cbr-pry-1*alleles 39
3.1.1 Complementation study 39
3.1.2 Genetic mapping 40
3.1.2a Linkage study 40
3.1.2b Indel mapping 40
3.1.2c Two-point mapping 41
3.2 Phenotypic characterization of *Cbr-pry-1* mutants 41
3.2.1 Q neuroblast migration defect in hermaphrodites 42
3.2.2 P12 cell fate transformation defect in hermaphrodites 42
3.2.3 Tail defects in the males 42
3.2.4 Vulval defects in the hermaphrodites 43
3.2.2e Brood size 43
Discussion 43
Chapter 4. Genetic analysis of *pry-1* function in *C. briggsae* vulval development 69
Background 71
4.1 Vulval development in *Cbr-pry-1* mutants 73
4.1.1 Vulval induction properties of *Cbr-pry-1* alleles 73
4.1.2 VPC lineage analysis in *Cbr-pry-1* animals 73
4.1.3 VPC fate specification studies in *Cbr-pry-1* animals 74
4.1.4 Vulval induction competence of P7.p and P8.p in *Cbr-pry-1* mutants 74

4.1.5 RNAi mediated knock down of *Cbr-pry-1* phenocopies *pry-1* alleles in *C. briggsae* 75
4.2 Gonad independent VPC fate specifications in *Cbr-pry-1* animals 75
4.3 Genetic interactions of *Cbr-pry-1*with LIN-12/Notch and Wnt signaling pathway and their targets 75
4.3.1 LIN-12/Notch pathway 76
4.3.2 Wnt pathway 76
4.3.3 The Hox gene *Cbr-mab-5* 77
Discussion 77
Cbr-pry-1 mutation is associated with a unique Muv-Vul phenotype in the vulva 78
VPC competence analysis in *Cbr-pry-1* mutants 78
LIN-12/Notch pathway interacts with *Cbr-pry-1* to regulate competence of P7.p towards vulval induction 79
Genetic specification of Wnt pathway in *C. briggsae* through RNAi interactions 80
Summary 122
Future Experiments 127
Appendix A: Preliminary phenotypic characterization of *C. briggsae* Muv mutants. 124
Appendix B: Genetic mapping of integrants *mfIs5* and *mfIs8* 127
Appendix C: Primers used in the present study 130
References 131

List of Tables

Table 1.1: Components of Wnt pathway orthologs in *C. elegans* 14
Table 3.1: Different classes of multivulva mutants in *C. briggsae* 45
Table 3.2: Linkage mapping data for *lin(sy5270)* and *lin(sy5353)* 46
Table 3.3: Percent recombination *(p)* values between *sy5353* and *sy5440* 47
Table 3.4: Expression pattern for *Cel-mec-7*::gfp in wild type *C. briggsae* 48
Table 3.5: P12 fate transformations in AF16 and *Cbr-pry-1* mutants 49
Table 3.6: Morphological defects in male tail development in *Cbr-pry-1* mutants 50
Table 3.7: Penetrance of Muv phenotype in *Cbr-pry-1* animals 51
Table 3.8: Statistical summary of *sy5353* and *sy5270* brood sizes 52
Table 4.1: Percentage of VPCs adopting vulval fates in and *Cel-pry-1* and *Cbr-pry-1* mutants 81
Table 4.2: VPC lineage pattern in *sy5353* 82
Table 4.3: VPC lineage pattern in *sy5270* and *mu38* 83
Table 4.4: Vulval cell fate marker expression in AF16 animals 84
Table 4.5: Vulval cell fate marker expression in *sy5353* 85
Table 4.6: Vulval cell fate marker expression in *sy5270* 86
Table 4.7: Cell fates adopted by the isolated P7.p and P8.p in wild type and *Cbr-pry-1* animals 87
Table 4.8: Gonad independent VPC inductions in *Cbr-pry-1(sy5353)* animals 88
Table 4.9: Summary of plate level phenotypes observed during RNAi experiments for *Cbr-pry-1* mutants 89
Table 4.10: VPC cell fates observed upon *Cbr-lin-12* inactivation by RNAi in *lin(sy5353)*;JU1018 90
Table 4.11: VPC cell fates observed upon *Cbr-bar-1* inactivation by RNAi in *lin(sy5353)*;JU1018 91
Table 4.12: VPC cell fates and gonad defects observed upon *Cbr-pop-1* inactivation by RNAi in JU1018 92
Table 4.13: VPC cell fates and gonad defects observed upon *Cbr-pop-1* inactivation by RNAi in *lin(sy5353)*;JU1018 93

Table 4.14: RNAi phenotype of *Cbr-pry-1* in *C. briggsae* 94
Table 4.15: Summary of *bar-1* and *lin-12* RNAi interactions of *Cbr-pry-1* and its comparisons to *Cel-pry-1* 95
Table 4.16: Summary of *pop-1* RNAi interactions of *Cbr-pry-1* and its comparisons to *Cel-pry-1* 96
Table 4.17: Model for *Cbr-pry-1* VPC competence 97

List of Figures

Figure 1.1: VPC cell fate patterning in *C. elegans* 15
Figure 1.2: Interplay among the signaling pathways during *C. elegans* vulva formation 17
Figure 1.3: Regulation of Canonical wnt pathway in metazoans 19
Figure 1.4: Phylogeny of the genus Caenorhabdits within phylum Nematoda 21
Figure 1.5: *C. briggsae* genetic linkage map (v9.0)(Phenotypic marker based) 23
Figure 3.1: Q lineages and *mec-7* expression pattern in N2 and *Cel-pry-1* animals 53
Figure 3.2: P11.p and P12.pa cell anatomy in N2 and in *Cel-pry-1(mu38)* animals 55
Figure 3.3: Genetic cross scheme for complementation test between *sy5270* and *sy5353* 57
Figure 3.4: The genetic cross scheme for the Indel mapping of *sy5353* 58
Figure 3.5: Validation of indel mapping for *sy5353* for bhP7 and bhP3 polymorphisms 59
Figure 3.6: Genetic cross scheme for calculating recombination frequencies between *sy5353* and *sy5440* 61
Figure 3.7: Expression pattern of *Cel-mec-7::gfp* in AF16 animals 62
Figure 3.8: Expression pattern of *Cel-mec-7::gfp* in *sy5353* animals 64
Figure 3.9: P7.p-P10.p morphology in wild type *C. briggsae* and *Cbr-pry-1* mutants 66
Figure 3.10: Male tail morphology in AF16 and *Cbr-pry-1* mutants 68
Figure 4.1: pattern variation among the VPC fates upon cell ablations in *C. elegans* 98
Figure 4.2: Morphological features of the vulval phenotypes of AF16 and *Cbr-pry-1* mutants 100
Figure 4.3: DIC images of the VPC cell lineage analysis in AF16 102
Figure 4.4: VPC cell lineage analysis in *sy5353* 104
Figure 4.5: Expression of 1^0 and 2^0 cell fate markers, *mfIs8* and *mfIs5*, respectively in AF16 106
Figure 4.6: Expression pattern of *Cbr-egl-17::gfp* in *sy5353* animals 108
Figure 4.7: Expression pattern of *Cbr-egl-17::gfp* in *sy5270* animals 110
Figure 4.8: *Cbr-egl-17::gfp* expression pattern in isolated P7.p and P8.p in AF16 112
Figure 4.9: DIC images of isolated P7.p and P8.p VPCs in *sy5353* showing non-competence towards inductive signal 114
Figure 4.10: Gonad independent vulval fate specifications in *sy5353* animals 116

Figure 4.11: RNAi phenotypes of JU1018 and *Cbr-pry-1* mutants in *lin-12*/ Notch pathway background in *C. briggsae* 118
Figure 4.12: RNAi phenotypes of JU1018 and *Cbr-pry-1* mutants in wnt pathway background in *C. briggsae* 120

Chapter 1: Introduction

One of the challenges of evolutionary biology is to understand the mechanisms of morphological diversity among animals. Earlier comparative studies have revealed the conserved role of regulatory genes during animal development. However, it has been identified that molecular changes in the spatio-temporal control of regulatory genes have resulted in morphological diversity. On the other hand, it is largely unknown how these molecular changes evolved across animals.

It is expected that by analyzing developmental processes (either at the genetic, cellular or molecular levels) among closely related species will illuminate the evolution of control mechanisms regulating molecular changes during development (Simpson 2002). For example, a comparative developmental study between a model species and a closely related sister species, provides us with an opportunity to observe the origin of novel phenotypic traits during evolution. Thus, hypotheses regarding the kind of molecular changes resulting in novel phenotypes can easily be formulated and experimentally verified among closely related species. In practice, such a comparative study is only possible when there is an availability of a handful of closely related species to model developmental organisms (such as, fly, worm and mouse). *C. elegans* with its handful of closely related species provides a valuable resource for comparative evolutionary studies. In this thesis, the development of the female reproductive system (vulva) in *C. elegans* and its related nematode species *C. briggsae,* was chosen for comparative studies.

1.1 *C. elegans* as a model organism to study animal development

It is interesting to consider a simple question: why a small millimeter-long nematode, *Caenorhabditis elegans* (popularly known as *C. elegans*), is elevated to the prestige of a model organism? The possible explanation lies in the unique and special attributes the worm possesses compared to other living creatures. *C. elegans* was first identified as a model organism by Sydney Brenner to pursue his interests in neurobiology and developmental biology. It has an un-segmented, cylindrical body and occurs as a non-parasitic, free-living nematode species. Moreover, the transparency of the animals allowed observation of division patterns of the cells during the development. The

complete cell lineages starting with an egg to adult are available for *C. elegans* (Horvitz and Sulston 1980). In addition, the complete neuronal circuitry consisting of 302 neurons has been mapped (White, Southgate et al. 1986; Wood 1988). Additionally, it can be easily and cheaply cultivated in large numbers (10^4 worms/ plate) in the laboratory by feeding *E. coli* strain. In favorable growth conditions the life cycle of *C. elegans* is relatively short (~3.5 days at 20^0). But, during extreme environmental conditions (such as lack of nurtrient, high temperature), the larvae can live for months in dauer stage. Finally, the *C. elegans* stock can be kept in frozen conditions indefinitely.

C. elegans is amenable to both forward and reverse genetic approaches. Its haploid genome has five autosomes and one sex chromosome and exists in two sexes, males (XO) and hermaphrodites (XX). The main organs include neurons, reproductive, digestive and muscles with simple anatomical features. The hermaphrodites and males have 959 and 1031 cells, respectively. The self-fertilizing hermaphrodite along with the occasional males (0.02%, in the wild populations) is very acquiescent to genetic analysis (Brenner 1974). Furthermore, suppressor and enhancer screens have identified a vast majority of mutants (>3000) with varying phenotypic repertoire, such as chemo, mechano-sensory, morphological, lethal, maternal effect, behavioral, and cell lineage mutants. More importantly, the completely annotated genome sequence (100 Mbp) of the worm has revolutionized reverse genetic studies and novel advanced genetic tools such as RNAi and targeted gene knock out technologies are being added to its tool kit (Tabara, Grishok et al. 1998; Fraser, Kamath et al. 2000; Kamath and Ahringer 2003). Thus, with the above mentioned features *C. elegans* allow rapid progress in understanding biological studies with minimal experimental time when compared to other model organisms (such as mice and the fly).

1.2 Vulval development in *C. elegans*

The *C. elegans* vulva, which is a non-essential organ (for survival) is required for egg laying and the copulation process, and has been well analyzed at the cellular, genetic and molecular levels (Wood 1988). Significant information regarding cell fates

specifications and cell differentiation processes that control morphological diversity during development were obtained from the studies focused on the nematode vulva.

1.2.1 Cellular aspects

The *C. elegans* vulva is formed from the descendents of the ventral epidermal cells that are usually referred to as the Pn.p cells (Sulston and Horvitz 1977). 12 Pn.p cells are formed during the mid L1 stage along the anterior-posterior axis of the body. Of these, P (1-2).p and P(9-11).p cells fuse with the hypodermal syncytium, hyp7. Descendents of P12.p develop into a special epidermal cell, hyp12. Only P3.p to P8.p cells have the potential to receive the signal from the somatic gonadal cell, anchor cell (AC), and are referred to as vulval precursor cells (VPCs). In wild type animals, the AC is usually positioned above the P6.p and induces P(5-7).p cells to form the vulva. After AC induction, the VPCs P(5-7).p acquire two types of cell fates, described as 1^0 and 2^0. The P6.p undergoes three rounds of cell divisions, giving 8 cells and acquires 1^o fate. Then, P6.p induces 2^o fate in P5.p and P7.p, resulting in 7 daughters from each cell through three rounds of cell divisions. Thus, the vulva is composed a total of 22 cells (Figure 1.1B). The P3.p, P4.p and P8.p acquire 3^o fate and produce two cells each, which ultimately fuse with hyp7. Thus, the VPCs exhibits an invariant pattern of cell fates, 3^0-3^0-2^0- 1^0- 2^0 -3^0 during vulval development in wild-type animals (Figure 1.1A) (Greenwald 1989; Kornfeld 1997).

The specification of VPC fates occurs during the L3 larval stage (Sulston and White 1980). 1^0 cell fates are characterized by [TTTT] division patterns of the P6.p whereas 2^0 cell fates consist of [LLTN] of P5.p and [NTLL] of P7.p cells (Figure 1.1B). The underline refers to the attached portion of the 2^0 lineage cells to the hypodermis. All the remaining VPCs (P3.p. P4.p and P8.p) adopt syncytial fate referred by [SS]. P3.p sometimes fails to divide and adopts an alternative [S] fate. The 1^0 and 2^0 cell lineages form seven cell types or toroidal rings, starting with VulA, VulB1, VulB2, VulC, VulD, VulE and VulF (Figure 1.1 B and C). Thus, vulval formation is a good model to study cell migrations, cell fusions and the formation of cell types during development (Sharma-Kishore, White et al. 1999).

1.2.2 Genetic analysis

One of the major advantages of studying vulva is its amenability to genetic studies (Brenner 1974). Forward genetic screens aimed towards identifying mutant animals with defects in the vulva, isolated many viable mutants with ease in *C. elegans*. They were generally described as egg-laying defective (Egl) mutants. Based on the induction properties of the VPCs, two main classes of vulval mutants were isolated: Vulvaless (Vul) and Multivulva (Muv) mutants (Ferguson and Horvitz 1985; Ferguson, Sternberg et al. 1987). In the first case, all the six VPCs adopt non-vulval fates or syncytial fates and as a result, no functional vulva is formed in these animals and the eggs that are produced from self-fertilization are not released into the exterior. Eventually they will hatch within the mother and are released by rupturing its cuticle. This phenotype is typically referred as 'the bag of worms' phenotype and is easy to score under the dissecting microscope. In the other case, the VPCs P3.p, P4.p and P8.p, which usually adopt the 3^0 non-vulval fates in wild type animals, acquire the vulval fates 2^0 or 1^0. The resulting differentiated cells form ectopic pseudovulvae along the ventral side of the body. Depending on the severity of Muv phenotype, these animals are also associated with the Egl phenotype Additionally, everted or protruding vulva (Pvul) mutants were also identified to be involved in VPC competence and fate specification processes (Eisenmann and Kim 2000).

1.3 Signaling pathways involved in vulval development

In the previous sections, I discussed about the cellular and genetic events that specify the VPCs to develop into the vulva. But how the VPCs and the AC interact with each other (ligand–receptor interactions) and the signals that mediate the communication processes during vulval development was largely unknown. Through integrating genetics, molecular biology and biochemical tools available for *C. elegans,* it was identified that four highly conserved and distinct signaling pathways are involved in vulval cell fate patterning: (1) An inductive signal mediated through EGF/RAS/MAPK (2) a lateral signaling system through LIN-12/Notch (3) an inhibitory signal from the surrounding

hypodermis (hyp7), and (4) a WNT mediated regulation of vulva fate specifications (Figure 1.2).

1.3.1 Ras signaling

The inductive signaling or EGF/RAS/MAPK signaling is the backbone of the vulval induction pathway and the somatic gonadal cell, anchor cell (AC), is the source of the signal. Anchor cell signal acts as a morphogen and the VPC that receives higher signal adopts 1^0 fate, while intermediate levels produce 2^0 fate and further low levels produce 3^0 cell fates. Thus, the activity of inductive signaling ensures 1^0cell fate in the P6.p, 2^0 in P5.p and P7.p, and 3^0 in the remaining cells (Figure 1.2). During this pattern formation, the anchor cell communicates to P6.p through LIN-3 (EGF homolog)/LET-23 (EGFR homolog) ligand/receptor interactions (Hill and Sternberg 1992). EGFR belongs to the receptor tyrosine kinase (RTK) family and upon its stimulation by LIN-3/EGF, triggers a conserved signaling cascade consisting of SEM-5 (Grb2 like adaptor protein), LET-60 (Ras GTP-binding protein), LIN-45 (Raf serine/threonine kinase), a MAPK kinase (mek-2) and a mitogen-activated protein kinase, SUR-1/MPK-1 in the VPCs (Aroian, Koga et al. 1990; Beitel, Clark et al. 1990; Han, Aroian et al. 1990; Wu and Han 1994; Wu, Han et al. 1995; Gupta, Liu et al. 2006). All these events involve protein-protein interactions through phosphorylation and de-phosphorylation events. Furthermore, through genetic epistatsis studies, LIN-3, LET-23 and SEM-5 were placed upstream of LET-60, LIN-45, MEK-2 and MPK-1, during vulval development (Sternberg and Han 1998). The loss of function (*lf*) mutations in these genes produce Vul phenotype, while gain of function *(gf)* mutations produce the Muv phenotype (Sternberg and Han 1998). More details regarding different components involved in inductive signaling can be obtained from the reviews by Greenwald and Kornfeld (Greenwald 1997; Kornfeld 1997).

1.3.2 Lateral/Notch/LIN-12 signaling

The graded and sequential model of the AC signal during pattern formation in the vulva was explained previously. In addition to promoting 1^0 cell fate in the VPCs,

inductive signaling also stimulates lateral signaling components in P6.p, which in turn antagonize 1^0 cell fates in P5.p and P7.p. The NOTCH family protein, LIN-12 was identified as a key member of the lateral signal in the VPCs (Greenwald 1997; Kornfeld 1997). Hyper-activation (*gf*) of *lin-12* results in the execution of 2^0 cell fates by all the six VPCs, while hypo-activations (*lf*) can lead to alterations in cell fates depending on the strength other signaling pathways (Greenwald 1997; Kornfeld 1997). Ras signal or inductive signal down-regulates LIN-12 activity in P6.p and is an important step in regulating lateral signaling (Shaye and Greenwald 2002). This process is mediated through a post-translational event in the di-leucine (HLH) motif in the C-terminal region of LIN-12, resulting in its increased endocytosis (Shaye and Greenwald 2002). Genetic evidence suggests that the DSL (Delta/Serrate/LAG-2) family of Notch ligands and LIN-12/Notch receptor interactions mediate 2^0 cell fate specifications in the VPCs (Greenwald, Sternberg et al. 1983; Sternberg and Han 1998). Thus, Ras is involved in both the transcription of genes involved in the activation of lateral signal and LIN-12 endocytosis. In a similar way, Notch antagonizes Ras in P5.p and P7.p, through the transcription of LAG-1, which in turn switches on transcription of *lst* genes (Yoo, Bais et al. 2004). This process results in the production of proteins LIP-1, ARK-1 and others involved in endocytosis and degradation of EGFR (Berset, Hoier et al. 2001; Yoo, Bais et al. 2004).

1.3.3 Synmuv signaling

The syncytial hypodermis, hyp7 that surrounds the VPCs is also known to antagonize Ras signaling in the VPCs and is described as the inhibitory signal (Herman R.K and Hedgehock 1990, 1995; Myers and Greenwald, 2005). The molecular basis for this inhibitory signal is not yet defined clearly, but it has been shown that hyp7 is the site of action for some *synmuv* genes (Herman and Hedgecock 1990; Myers and Greenwald 2005). Several *synmuv* genes were identified through genetic screens in *C. elegans* and were classified into three major classes, class A, B and C. They were known to encode homologs to transcriptional repressor and chromatin remodeling complex proteins, such as LIN-35Rb, HDAC-1 and HPL-2, Heterochromatin protein 1 (HP1)](Ferguson and Horvitz 1989; Ceol, Stegmeier et al. 2006).

1.3.4 Wnt signaling

In addition to the previously discussed signaling pathways, Wnt signaling also play a significant role in VPC cell fate specifications and P7.p polarity defect in *C. elegans* (Ferguson, Sternberg et al. 1987; Eisenmann, Maloof et al. 1998). β-catenin/ Armadillo related protein BAR-1 is identified as a key component of Wnt signaling and is involved in the positive regulation of VPC cell fates. In this process it regulates the expression of Hox gene *lin-39* in the VPCs through cooperating with LET-23/LET-60 pathway (Eisenmann, Maloof et al. 1998). But, Gleason and colleagues showed that hyperactivated Wnt signaling is sufficient to induce VPCs in Ras independent manner (Gleason et.al., 2002). They identified two key components, PRY-1 (Axin homolog) and APR-1 (APC homolog) as negative regulators of Wnt signaling in the VPCs. Mutations in *pry-1* and *apr-1* cause an overinduced or Muv phenotype, which is further suppressed by mutations in *lin-39* and *pop-1* (Gleason, Korswagen et al. 2002). Besides, Wnt ligands are also shown to function in specifying P7.p polarity in the vulva (Ferguson et al., 1987). More information regarding genetic specification of Wnt pathway during vulval development is described in Chapter 4 of the thesis.

1.4 Hox targets of Wnt signaling in vulval cell fate specification

In the nematode vulval cell fate patterning, two Hox genes *lin-39* and *mab-5* (homologs of Drosophila *Scr* (sex combs reduced) and *Antennapedia*, respectively), have been identified to play a significant role in VPC fate specification (Salser and Kenyon 1994; Hunter and Kenyon 1995; Clandinin, Katz et al. 1997; Eisenmann, Maloof et al. 1998). Both of them encode HOM-C class of transcription factors and are identified as the downstream targets of the vulval signaling pathways.

LIN-39 was identified to be involved in generation of Pn.p cells during the L1 stage and fate specification of P(3-6).p cells during the L3 stage in *C. elegans* development and interacts with both inductive signaling and Wnt signaling components (Clark, Chisholm et al. 1993; Maloof and Kenyon 1998). In mutants where LIN-3/LET-

23 pathway activity was decreased (due to loss-of–function mutations), *lin-39* gene expression was reduced in the VPCs, when compared to wild type animals (Maloof and Kenyon 1998). In LET-60/RAS gain-of-function mutations, increased *lin-39* expression was observed, revealing that it is the direct target of inductive signaling in the VPCs (Maloof and Kenyon 1998). The worm β- catenin, BAR-1 has been identified to target *lin-39* in the VPCs. It was also confirmed that BAR-1 co-ordinates with the inductive signaling pathway components in the regulation of *lin-39* expression (Eisenmann, Maloof et al. 1998). Genetic epistasis studies confirmed that *lin-39* acts downstream of Wnt and inductive signaling during vulval development.

The Hox gene *mab-5* has been identified to be involved the positioning or centering of anchor cell (above P6.p) during vulval development in *C. elegans* (Clandinin et al., 1997). In *lf* alleles of *mab-5* (*e1239* and *e2088*), it was observed that the anchor cell was positioned posterior to the vulva, which is formed form P(6-8).p cells. Furthermore, *lin-3* reporter gene expression studies in *mab-5* background suggested that the two posterior VPCs, P7.p and P8.p are less competent to inductive signaling (Clandinin et. al., 1997). Additionally, it was also involved in the fate specifications of the posterior Pn.p cells, P7.p to P11.p. Genetic epistasis studies confirmed that *mab-5* acts downstream of inductive and lateral signaling during the formation of vulva (Clandinin et. al., 1997). Thus, during VPC cell fate patterning, both *lin-39* and *mab-5* act in specific domains along the A/P axis, similar to segmentation genes in Drosophila (Clark, Chisholm et al. 1993; Clandinin, Katz et al. 1997; Eizinger and Sommer 1997; Eisenmann, Maloof et al. 1998; Chen and Han 2001).

1.5 Additional Wnt signaling components in *C. elegans*

Wnt proteins belong to glycoprotein family of secretion proteins and are usually involved in cell communication processes (Cadigan 1997). They are first identified in studies focused on mouse and Drosophila, *wnt*-1 and *wingless (wg)* genes, respectively (Varmus 1982; Van Ooyen 1984; Cabrera 1987). Two kinds of Wnt pathways have been identified to be involved in animal development, canonical Wnt pathway/β-catenin

pathway and β-catenin independent Wnt pathway/ non-canonical Wnt pathway (Figure 1.3) (Wodarz and Nusse, 1998; Peifer and Polakis, 2000).

Most of the canonical Wnt proteins identified in flies and vertebrates are found in *C. elegans* (Table 1.1) (Herman MA 2003). LIN-44 was identified as the first Wnt protein and involved in asymmetric cell divisions in the tail and posterior body region in *C. elegans* (Herman and Horvitz 1994; Herman, Vassilieva et al. 1995). In addition, a total of 5 ligands (LIN-44,CWN-1,CWN-2,EGL-20, and MOM-2) and 4 receptors (LIN-17/Fz, MIG-5/Dsh, Dsh-2 and MOM-5) were identified (Gleason, Szyleyko et al. 2006). PRY-1, APR-1 and POP-1 were identified as orthologs of AXIN, APC and TCF/LEF counterparts (in flies and vertebrates). BAR-1, WRM-1, HMP-2 and SYS-1 were identified as worm β-catenins (Korswagen, Herman et al. 2000; Natarajan, Witwer et al. 2001). Furthermore, KIN-19 and GSK-3 (*C. elegans* homologs of vertebrate destruction complex protein kinases, CKIα and GSK-3β, respectively) were identified as negative regulators of Wnt signaling.

1.6 Evolution of vulval development in *C. elegans* and related nematode species

Evolutionary variations are observed during the comparisons of vulval development among *C. elegans* and its related nematode species, both at inter-specific and intra-specific levels (Sommer R.J 2005) (Felix, 2007). *C. elegans* belongs to the genus *Caenorhabditis* of the family Rhabditidae (Kiontke and Fitch). In *Caenorhabditis* nematode species the vulva is located at the centre of the body and the anchor cell signal is only required once for proper vulval induction. However, in more distantly related nematode species, the genus *Oscheius*, it was observed that the anchor cell signal is required twice for vulva formation. This is usually referred to as 'two nested gonadal induction' (Felix and Sternberg., 1997). A Similar kind of two-step induction was observed in the genus *Panagrolaimus,* where the anchor cell is positioned between P6.p and P7.p, when compared to the *C. elegans* (above the P6.p). Furthermore, in *Pristionchus pacificus,* belonging to the phylum Diplogastridae, multiple signals originating from the gonad induce vulva formation. In this case, seven of the Pn.p cells (that usually fuse to hyp7 in *C. elegans*) undergo cell death and the remaining P(3-7).p

form the equivalence group (Sommer and Sternberg 1996). Thus, evolutionary variations are observed in the number of cells contributing to the vulval equivalence group, the requirement of induction by the anchor cell and the position of the vulva in nematodes (Felix and Sternberg 1996; Delattre and Felix 2001; Delattre and Felix 2001).

A total of 11 species are identified in the genus *Caenorhabditis,* with known phylogeny (Figure 1.4) (Kiontke and Fitch). Evolutionary variations are also observed within the genus *Caenorhabditis* during vulva formation. In *C. briggsae*, sister species to *C. elegans*, P3.p exhibits variable competence towards adopting syncytial fates (S) during vulval fate patterning (Delattre and Felix, 2001). For example, in *C. elegans,* P3.p acquires S fate in 50% of the animals and SS in other cases, but in *C. briggsae,* it adopts S fate in only 15% of the animals (Delattre and Felix, 2001). Notch family members LIN-12 and GLP-1, regulate lateral signaling in *C. elegans* (section 1.3.2). Interestingly, in *C. briggsae,* two *lin-12* genes are identified compared to *C. elegans* (only one *lin-12* gene) (Rudel and Kimble 2001; Rudel and Kimble 2002). In addition, *glp-1* in *C. briggsae* is not involved in vulval development (Rudel and Kimble 2001; Rudel and Kimble 2002). Furthermore, cryptic or silent changes are observed in vulval development in *C. remanei* and *C. briggsae,* due to minor variations in Ras and Notch pathways between (Felix 2007). Thus understanding vulva formation in the genus *Caenorhabditis* helps to dissect evolution of vulva at smaller evolutionary scales.

1.7 Resources available for *C. elegans* - *C. briggsae* comparative studies

The soil nematode, *C. briggsae* has emerged as a model organism in parallel to *C. elegans*, to facilitate inter-species comparative developmental studies (Gupta, Johnsen et al. 2007). The estimated divergence time between *C. elegans* and *C. briggsae* was found to be about 80-110 million years and presumably occurred in the Precambrian era (Blaxter 1998). Both species reproduce through self-fertilization, with an obvious hermaphroditism when compared to the gonochoristic mode of reproduction in the genus *Caenorhabditis* (Michael A. Miller et.al. 2004). Both species look alike in most of their morphological features, for example the vulval anatomy is very similar in both the species. However, minor anatomical differences were observed in the excretory duct and

male ray pattern formation (Fitch and Emmons 1995; Wang and Chamberlin 2002). In addition, the major advantages of comparative studies between *C. elegans* and *C. briggsae* is the availability of complete genome sequences for the two nematodes (Rachael Ainscough et.al. 1998; Stein, Bao et al. 2003). Recently, *C. elegans* - *C. briggsae* genome comparisons provided with us information regarding intron evolution, protein-coding regions, colinearity, and species-specific genes (Gupta, Johnsen et al. 2007).

Furthermore, many visible mutant phenotypes such as Dpy (Dumpy), Unc (Uncoordinated), Muv (Multivulva) and Rol (roller) were isolated for *C. briggsae*, through EMS screens (B. Gupta, P. Sternberg and D. Baillie, unpublished, www.briggsae.org.). From previous studies carried out on these mutants, a partial genetic map of *C. briggsae* was established and is organized into 5 autosomes (LG I-V) and one sex chromosome (LG X), similar to *C. elegans* (Figure 1.5). In addition, an alternative mapping approach was also carried out through SNPs (Single Nucleotide Polymorphisms) that are available for *C. briggsae* from genome comparisons with its polymorphic isolates, HK104 and VT847 (Hillier 2007). Efforts are under progress to integrate the mutant-based and SNP-based genetic maps in order to refine the genetic linkage map and to carry out epistasis and genetic interactions of specific genes of interest in *C. briggsae* (B. Gupta and R. miller, unpublished).

1.8 Present study

The main objective of my thesis is to dissect genetic control of development among closely related species in order to better understand evolution of developmental mechanisms. I focused on the genetic analysis of *pry-1/Axin* function in *C. briggsae,* sister species to *C. elegans,* to facilitate inter-species comparisons of developmental processes in the genus *Caenorhabditis*. *Pry-1* function in *C. elegans* has been well established and is known to negatively regulate canonical wnt pathways during its development. To identify evolutionary variations in *pry-1* function between *C. elegans* and *C. briggsae,* I focused on analyzing the phenotypic and genetic properties of *pry-1*

alleles in *C. briggsae* (Chapter 3), and also dissected *pry-1* function in *C. briggsae* vulval development (Chapter 4).

Table 1.1: Components of Wnt pathway orthologs in *C. elegans*

Component	Orthologs in *C. elegans*
Porcupine	*mom-1*
Wnt	*mom-2, lin-44, egl-20, cwn-1 and cwn 2*
Frz B	*mom-5, lin-17, mig-1*
Dishevelled	*mig-5, dsh-1 and dsh-2*
Caesin kinase I	*kin-19*
GSK-3β	*sgg-1*
Axin	*pry-1*
APC	*apr-1*
β - catenin	*wrm-1, bar-1, hmp-2 and sys-1*
TCF/LEF	*pop-1*
Groucho	*unc-37*
NLK	*lit-1*
TAK 1	*mom-4*

Table adapted from Wnt signaling in *C. elegans* (Herman MA 2003)

Figure 1.1: VPC cell fate patterning in *C. elegans*

(A) Of the 12 ventral hypodermal Pn.p cells born in the mid L1 stage in AF16, the central P3.p to P8.p form the vulval equivalence group (VEG). These six cells were referred as Vulval Precursor Cells (VPCs). (A) Cell patterning in AF16. The anchor cell always positions above the P6.p and restricts the vulval induction potential to the three central VPCs, P5.p to P7.p. Later, cells acquire 2^0-1^0-2^0 cell fate patterns represented by LLTN-TTTT-NTLL plane of cell divisions of their daughters and grand daughter cells, resulting in a total of 22 cells. The other three VPCs of the equivalence group (P3.p, P4.p and P8.p) undergo one round of cell division forming two cells, which will eventually fuse with the hyp7. These cells were represented by SS and represent 3^0 fate. Thus, vulval cell patterning in *C. elegans* is represented by, 3^0-3^0-2^0-1^0-2^0-3^0 invariant cell fates. In this cartoon VPCs are illustrated by oval drawings and the hexagonal blocks represent the specific cell types formed from them. The cell fates adopted by an individual VPC is presented within the oval boxes. Plane of cell divisions is referred as T- transverse, left/right; L- longitudinal, a/p; N- undivided or none; S- syncytial, fusion with the hypodermal syncitium. The horizontal solid black bar represents the hyp7 and the star symbol represents anchor cell. The vertical black bars represent the cell division pattern of the VPCs. All of the division patterns of the VPCs are observed from late L3 to mid L4 stages.

(B) This figure represents 7- epithelial toroids or rings formed during vulval formation, which are distinguished by 7 distinct cell types, represented by VulA, VulB1, VulB2, VulC, VulD, VulE, and VulF (in ventral to dorsal order). Each ring consists of four nuclei except VulB1 and VulB2, which possess only two nuclei each (represented by '0 or 00' within the syncitium of each cell type). VulE and VulF toroids represent cell lineages from 1^0 fate and VulA to D are of 2^0 fate. The star sign represents the anchor cell. (C) Nomarski image of the vulval morphology at midL4 stage. This stage is recognized by the typical bell shape morphology of the developing vulva. All the cell types are represented along with the anchor cell except VulE, VulF and VulC, which are not observed in the present focal plane.

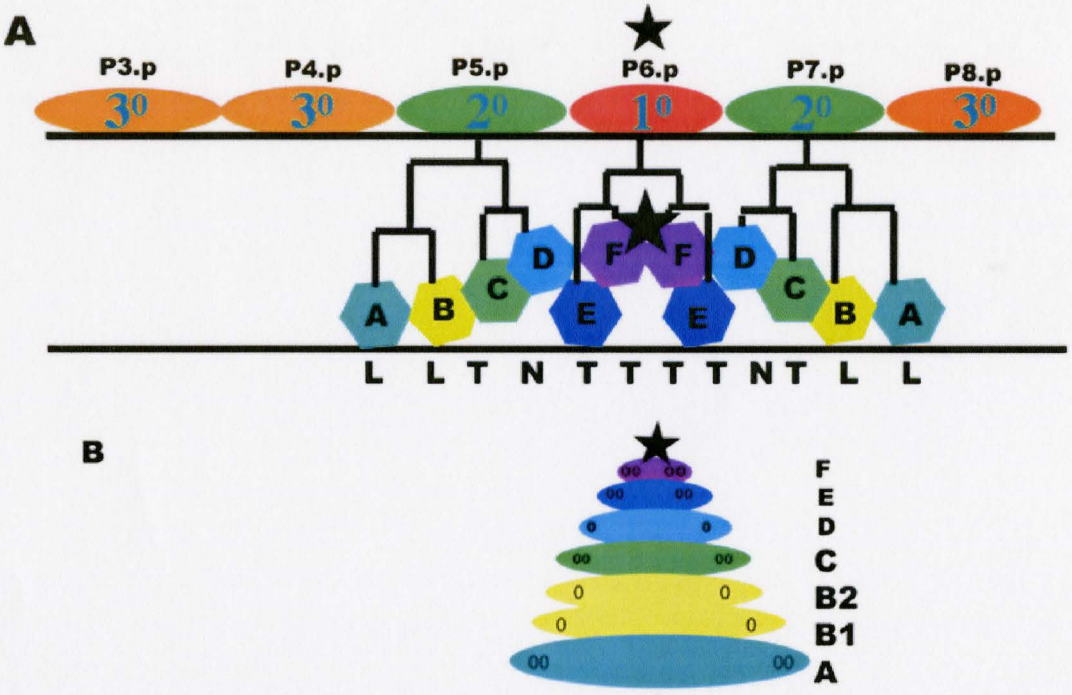
A
P3.p
P4.p
P5.p
P6.p
P7.p
P8.p
3°
3°
2°
1°
2°
3°
A
B
C
D
F
F
D
C
B
A
E
E
L L T N T T T T N T L L
B
F
E
D
C
B2
B1
A

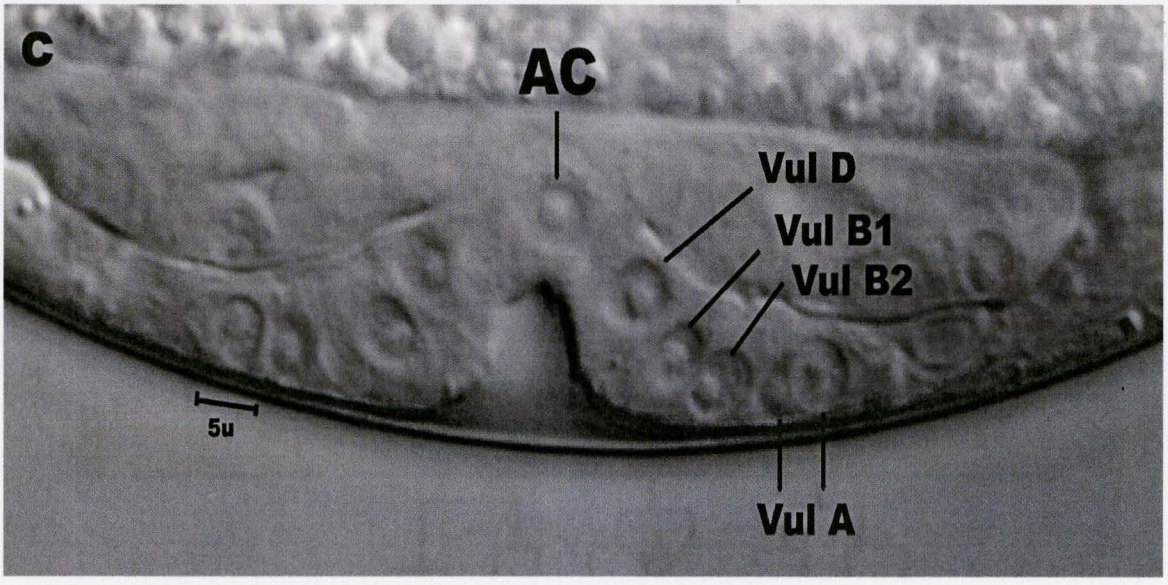
C
AC
Vul D
Vul B1
Vul B2
5u
Vul A

Figure 1.2: Interplay among the signaling pathways during *C. elegans* vulva formation

Vulva development in *C. elegans* is a paradigm to study cell-cell communication through signaling pathways. The role of anchor cell signal as a morphogen can be judged from the intensity of arrows towards VPCs. The lateral signal from P6.p to P5.p and P7.p was shown with horizontal black lines and the inhibitory signal from the hyp7 with black arrows. Figure modified and adapted from wormbook chapter: vulval development (www.wormbook.org; Paul Sternberg).

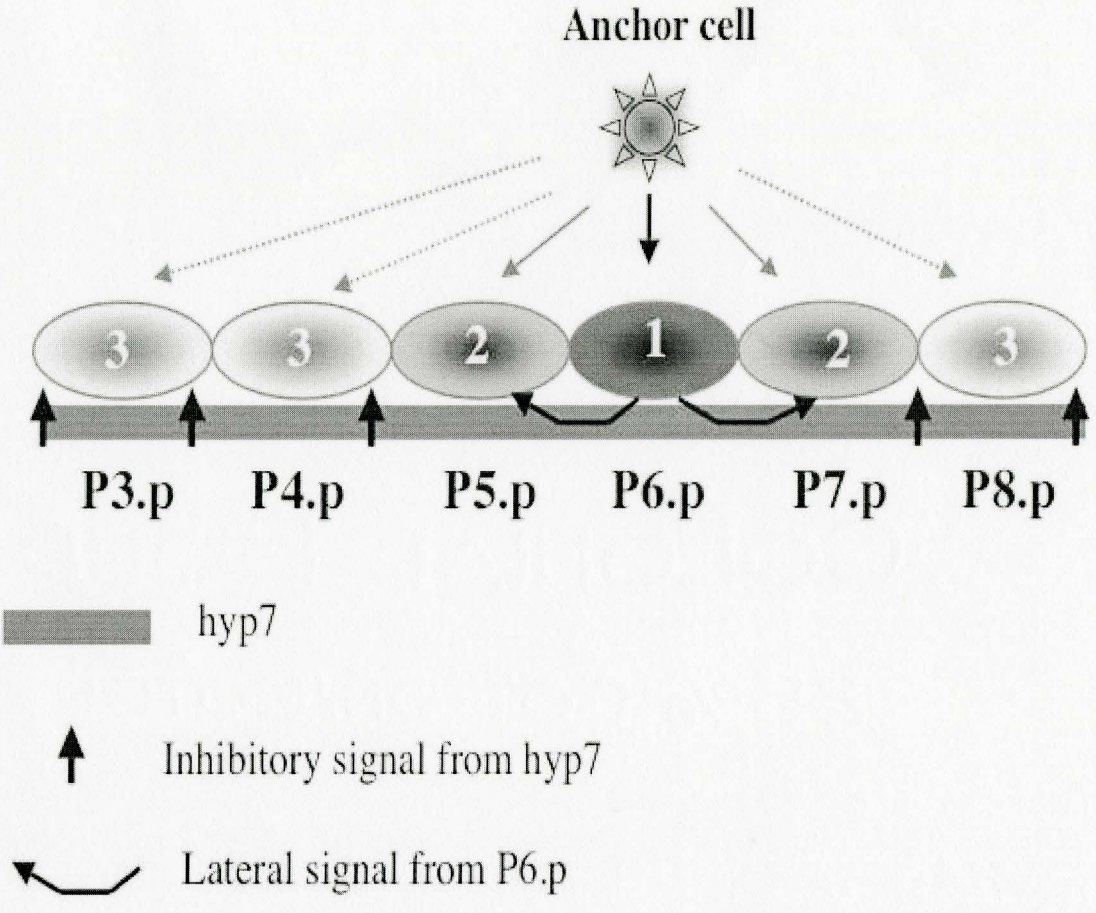
Anchor cell
3
3
2
1
2
3
P3.p
P4.p
P5.p
P6.p
P7.p
P8.p
hyp7
Inhibitory signal from hyp7
Lateral signal from P6.p

Figure 1.3: Regulation of Canonical Wnt pathway in metazoans

Two types of general scenarios of canonical Wnt pathway are presented: 1) In the absence of signal from the ligand (Wnt) the APC and AXIN proteins (Scaffold proteins) interact with the cytoplasmic β- catenin, which results in its phosphorylation mediated by protein kinases, CKIα and GSK3β. Later, the phosphorylated β- catenin is being degraded by the proteosome complex through the process of ubiquitination. This process leads to the trasciptional repression of Wnt target genes in the nucleus. 2) In the presence of Wnt ligand, the function of APC, AXIN, CKIα and GSK3β were inhibited, which results in the non-phosphorylation of β- catenin in the cytoplams. Thus, the non-phosphorylated form of β- catenin is freely transduced into the nucleus, allowing transcription of Wnt target genes. The LPR 5/6/arrow family coreceptor was identified to be involved in the inhibitory process and Wnt pathway converges at TCF/LEF family member transcription factors as the final target genes in the nucleus. Figure modified and adapted from wormbook chapter: Wnt signaling in *C. elegans* (www.wormbook.org) (Eisenmann).

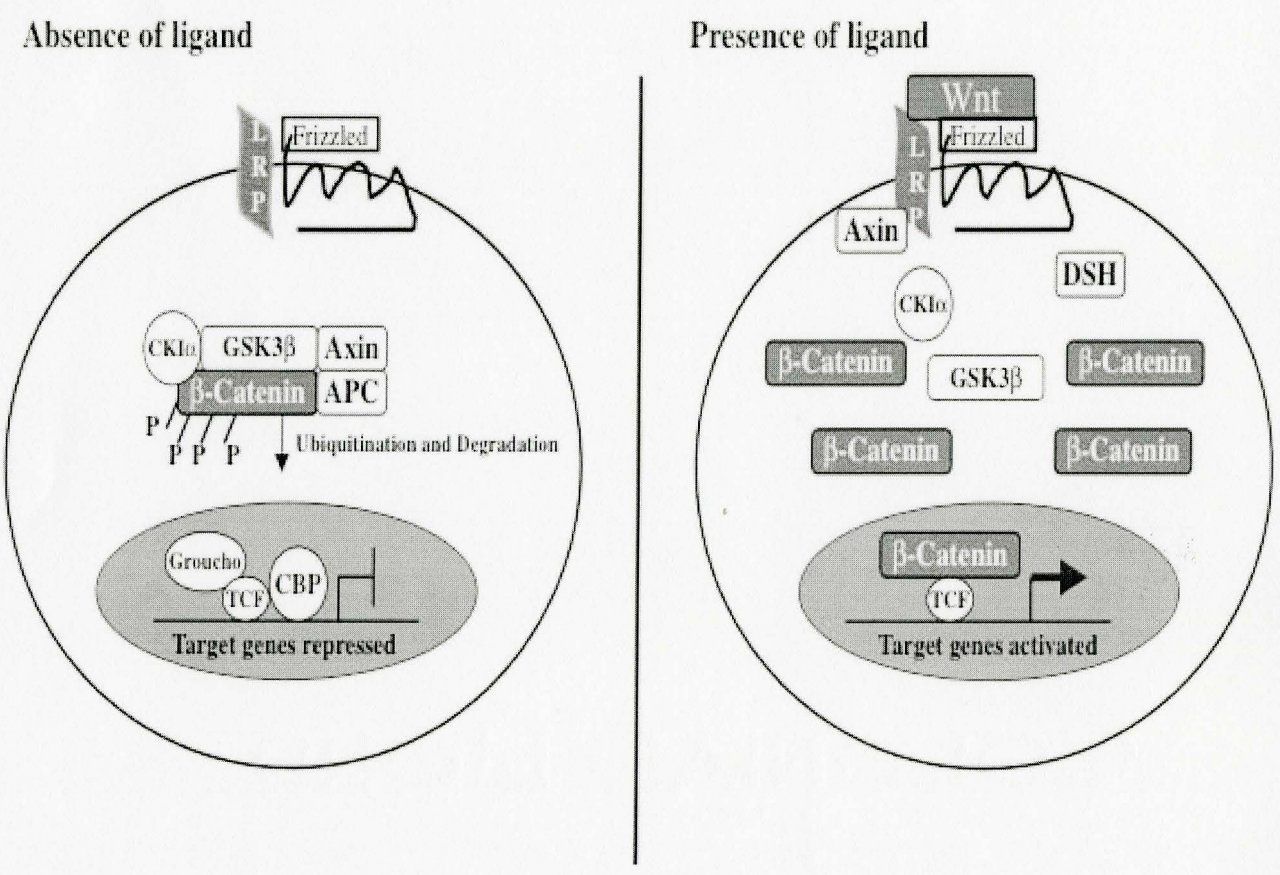
Absence of ligand
Presence of ligand
L
R
P
Frizzled
CKIα
GSK3β
Axin
β-Catenin
APC
P
P P P
Ubiquitination and Degradation
Groucho
TCF
CBP
Target genes repressed
Wnt
Frizzled
L
R
P
Axin
DSH
CKIα
β-Catenin
GSK3β
β-Catenin
β-Catenin
β-Catenin
β-Catenin
TCF
Target genes activated

Figure 1.4: Phylogeny of the genus *Caenorhabditis* within phylum Nematoda

Initially it was thought that *C. briggsae* is closely related to *C. elegans,* but recent phylogenetic analysis suggested that *C. remanei* and *C. brenneri* are much closer to *C. elegans* compared to *C. briggsae*. Refer to wormbook chapter "The phylogenetic relationships of *Caenorhabditis* and other rhabditids" by Kiontke and Fitch for more detailed phylogeny (www.wormbook.org).

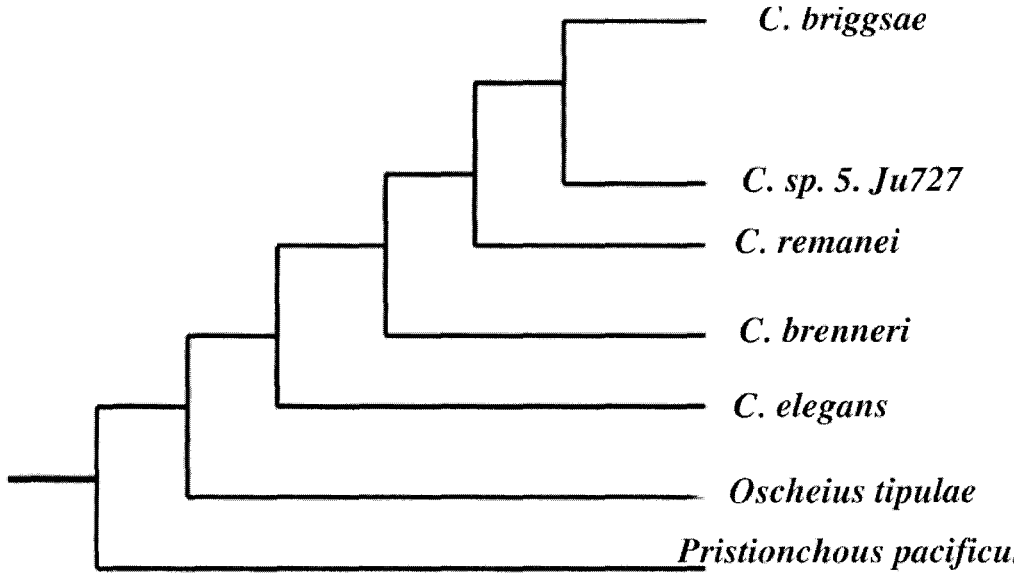
C. briggsae
C. sp. 5. Ju727
C. remanei
C. brenneri
C. elegans
Oscheius tipulae
Pristionchous pacificus

Figure 1.5: *C. briggsae* genetic linkage map (v9.0)(Phenotypic marker based)

The experimentally confirmed orthologs to *C. elegans* in *C. briggsae* are represented below the corresponding genes. The candidate loci assigned in '?' refer to their similarity in phenotype, allele frequency and map position and require additional information for further confirmation. This map is being referred from Gupta, B.P., et al., 2007, with permission.

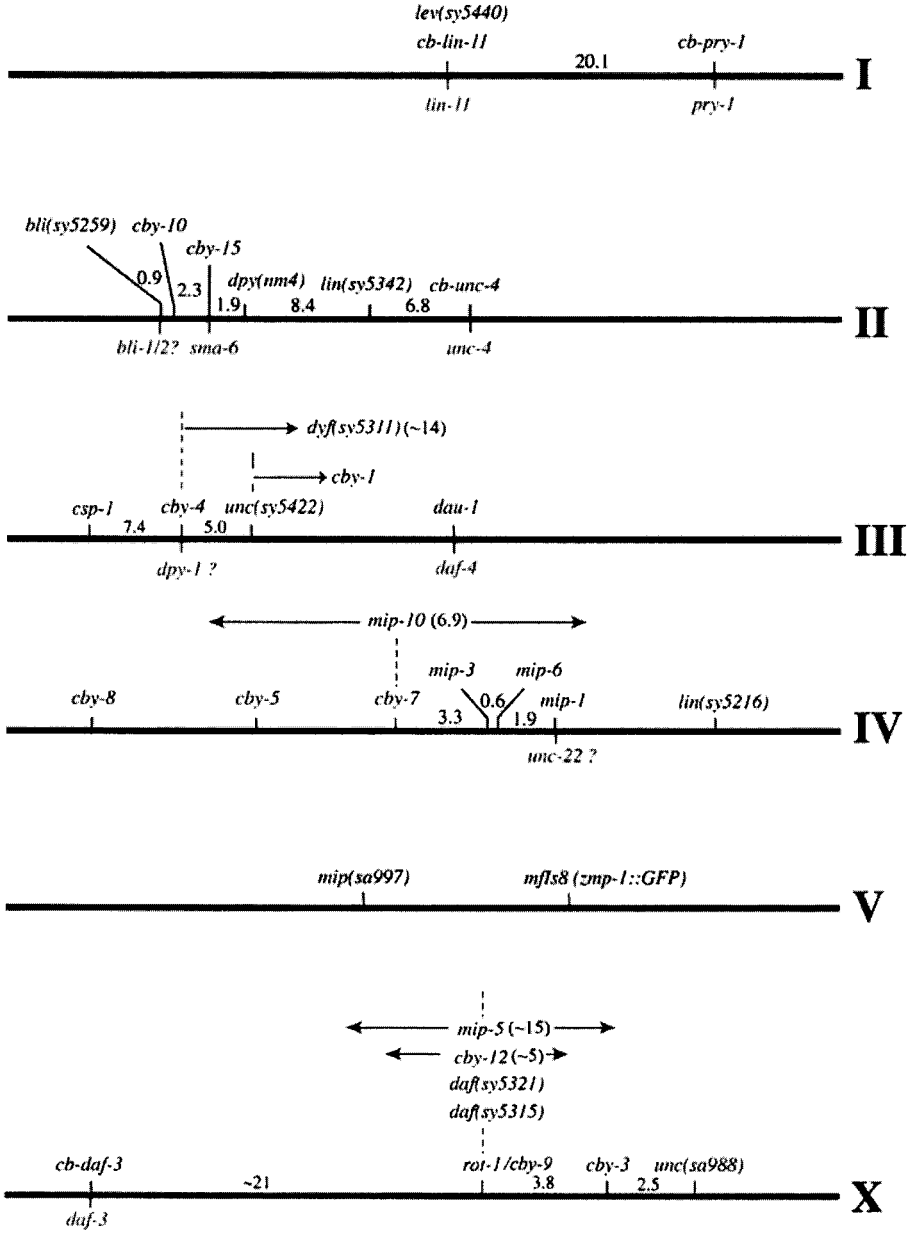
lev(sy5440)
cb-lin-11
cb-pry-1
20.1
I
lin-11
pry-1
bli(sy5259)
cby-10
cby-15
0.9
2.3
dpy(nm4)
lin(sy5342)
cb-unc-4
1.9
8.4
6.8
II
bli-1/2?
sma-6
unc-4
dyf(sy5311)(~14)
cby-1
csp-1
cby-4
unc(sy5422)
dau-1
7.4
5.0
III
dpy-1 ?
daf-4
mip-10 (6.9)
mip-3
mip-6
cby-8
cby-5
cby-7
0.6
mip-1
lin(sy5216)
3.3
1.9
IV
unc-22 ?
mip(sa997)
mfIs8 (zmp-1::GFP)
V
mip-5 (~15)
cby-12 (~5)
daf(sy5321)
daf(sy5315)
cb-daf-3
rol-1/cby-9
cby-3
unc(sa988)
~21
3.8
2.5
X
daf-3

Chapter 2: Materials and Methods

2.1 General

2.1.1 Nematode strains used in the present study

***C. elegans* specific**: N2 (Wild type), *pry-1(mu38)* (LG I)

***C. briggsae* specific:** AF16, wild-type *Caenorhabditis briggsae* (obtained from Caenorhabditis Genetics Centre). All the strains described here are in AF16 background. HK104 a polymorphic variant to AF16 was specifically used in In-del mapping technique along with the following mutations:

LGI: *lin(sy5411), lin(sy5353), lin(sy5270), lev(sy5440), lev(sy5436)*

LGII: *dpy(nm4), Cb-Unc-4(sy5341), lin(sy5342), dpy(sy5148)* [AKA (*cby-15*)]

LGIII: *dpy(s1281)* [AKA(*cby-1*)]

LGIV: *unc(s1270)*[AKA(*mip-1*)], *lin(sy5216), lin(sa993)*

LGV: *unc(sy5415), unc(sa997)*

LGX: *dpy(nm3)*

Transgenic strains: *mfIs5* [*Cbr-egl-17:: gfp + Cel-myo-2::gfp*], *mfIs8* [*Cbr-zmp-1::gfp +Cel-myo-2::gfp*], PS4078; *unc-119(ed4);syIs95*[*mec-7::gfp+unc-119(+)*], *mec-7::*GFP(*bhEX25*)[*mec-7::gfp+-myo-2::gfp*], *sy5353*; *bhEX25*[*mec-7::gfp + myo-2::gfp*], JU1018 (*mfIs42* [*sid-2;myo-2*::dSRED]), *sy5353*; *mfIs5* [*Cbr-egl-17:: gfp + Cel-myo-2::gfp*], *sy5353*; *mfIs8* [*Cbr-zmp-1::gfp + Cel-myo-2::gfp*], *sy5270*; *mfIs5* [*Cbr-egl-17:: gfp + Cel-myo-2::gfp*], *sy5270*; *mfIs8* [*Cbr-zmp-1::gfp + Cel-myo-2::gfp*].

All the transgenic strains are obtained from MA. Felix, Jaques Monad Institute, Paris, France.

2.1.2 Nomenclature and standard phenotypic description of the strains

The guideline for the nomenclature of *C. briggsae* strains was followed as mentioned in the guidelines for the nomenclature of *non – C. elegans* strains (www.briggsae.org). In general, the known orthologs for *C. elegans* can be referred with the same gene name as described to as *Cbr-unc-4* (the *C. briggsae* ortholog of *C. elegans unc-4* gene). For the other genes whose orthology has not been established, different gene/phenotype name was used. Nomenclature and phenotypes of some of the strains used in this study are as follows:

dpy(sy5148): These animals are described as "Chubby or Dumpy" based on their small and fat appearance compared to AF16. Similar kinds of mutants were isolated and were mapped on to different chromosomes in *C. briggsae.*

unc(sy5415): These animals are described as " Uncoordianted, Coiler" based on their inability to move as swiftly as AF16 animals. They spend most of the time in curled up posture. Their movement defect was obvious when a single AF16 and mutant worm were placed in the same plate with full of bacterial lawn. The mutant worms follow a zig-zag path compared to AF16 sinusoidal path.

Cbr-unc-4 (sy5341): These animals are described as "Uncoordianted, Shrinker" based on their inability to move backwards compared to AF16. They display normal forward movement compared to AF16. However if we oppose its forward movement it exhibit characteristic shrinking of the body and fails to follow backward movement compared to wild-type animals. This strain was identified as an ortholog of *C. elegans unc-4* mutant.

lev(sy5440): These animals are described as "Levamisole drug resistant". In contrast to the wild type AF16 that are paralyzed in the presence of 1 mM levamisole these animals are active. In addition they also exhibit slight uncoordinated behavior.

lin(sy5353): These animals are described as "Lineage defect, Muv (Multi-vulva)". Adult animals will have more than one ventral protrusion along with the central vulva, described as pseudovulvae. Only the central vulva can lay eggs in these animals. In the present study this allele was being identified as an ortholog of *Cel-pry-1* and is described as *Cbr-pry-1.*

2.1.3 Growth conditions and manipulations of the worms

All the strains were grown on NGM agar plates (usually 5-cm plates) by applying standard growth conditions at 20° C (Brenner, 1974). The E. coli bacterial strain OP50 (Uracil deficient) was used as a source of food for the worms. Few drops of OP50 culture was placed on the NGM agar plates, and within a period of 1-5 days a thick bacterial lawn will be obtained and was used for the cultivation of worm populations. A platinum wire (~30 gauge), which was sealed into the broken neck of a Pasteur pipette will be flattened at the opposite end and was used as a worm pick. The worm pick was sterilized by flaming through a Bunsen burner before picking the worms. After sterilization the

pick was cooled down and then a scoop of bacterial lawn was taken and was used as a bait to pick the worms. Alternatively, a 2 cm Pasteur pipette (a narrow passage was made at one end by flaming it through Bunsen burner) connected to a water aspirator was also used to suck up large homogeneous populations of the worms.

2.1.4 Maintenance and cleaning of the mutant stocks

The working stock can be maintained by transferring few worms or a chunk of agar along with worms (chunking) to a fresh plate with a well-grown bacterial lawn. Furthermore, to avoid desiccation, the plates were kept in covered plastic boxes. The working stock lasts for a week or two and then they were backed up by covering them with parafilm and were kept at 15° C. Additionally for long-term storage purposes the stocks were maintained in liquid nitrogen as frozen cultures. During the culturing process, due to the repeated transferring of the stocks and also depending on the surroundings, there exists a possibility of contamination by bacterial and fungal mycelia. To de-comtaminate them sodium hypochlorite solution was used and the process was described as bleaching technique. 5 µl of freshly prepared sodium hypochlorite (2 vol 2N NaOH: 3 vol 10-20% NaOCl) was placed between the bacterial lawn and the edge of the NGM agar plate. Then 6-8 gravid hermaphrodites (adults with full of eggs in the uterus) were placed on the bleach spot. The bleach kills most of the bacterial and fungal contaminations through tissue degradation in adult animals leaving behind the resistant eggs and the debris. The hatched larvae from these eggs will crawl to the bacterial lawn and they were transferred to fresh uncontaminated plates and cultured.

2.1.5 Calculating brood size

Individual L4 worms were placed on separate NGM agar plates and were allowed to lay eggs. Eggs laid from an individual animal during a period of 12 to 24 hour intervals were allowed to become larvae stages (L2 or L3 or L4). Thus the progeny obtained from an individual within a period of 3-4 days is quantified and generally described as brood size.

2.2 Genetic methods

2.2.1 Genetic crosses

All the mutations analyzed in the present study are recessive. Standard genetic methods are followed up in all the genetic experiments and worms were grown at 20 ^{0} (Brenner 1974). Keeping 8 or 12 young males and 3 or 5 virgin hermaphrodites in a plate ensures good mating and subsequently to the success of the genetic cross. Frequently crosses were carried out with males and hermaphrodites in similar developmental stages, such as L3 or L4 animals. Selfing was done in a similar manner to brood size, which favors maintenance of homogeneous populations of the working stocks. Self and cross progeny were distinguished by the fact that the mutant being recessive for a given visible phenotype display wild type phenotype in heterozygous condition (m/+, where m refers to mutant gene and + wild type) and mutant phenotype in homozygous condition (m/m). Alternatively gfp expression was also used as a marker phenotype where animals (carrying gfp integrants) heterozygous for the mutation express low gfp or no gfp compared to homozygous condition.

Backcrossing was done by selfing F_1 heterozygous hermaphrodites (mutant/+) obtained by crossing wild type males to *sy5270* hermaphrodites. The frequency of *sy5270* phenotype was observed in the next generation (F_2's). F_3's exhibiting the observed mutant phenotype was isolated from F_2's. This was represented as 1X outcross (First outcross). Subsequent backcrosses were done in as similar manner, as necessary.

2.2.2 Complementation study

Complementation test is the standard method to assign allelism among the mutations under study. Similarity in phenotype of the isolated mutants may cause difficulty in the distinction of cross and self-progeny during recombination events. So, usually one of the tester mutants under observation was crossed to a completely different phenotypic marker mutant. For example, Dpy or Unc markers were crossed to Muv and the resulting DpyMuv or UnvMuv double mutant, which can be distinguished easily from the single mutants. The complementation test between two mutants with similar

phenotype, m1 and m2 is as follows: m1 hermaphrodites are crossed with wild type males to obtain m1/+ males. Then these males are crossed with N hermaphroites (marker mutant expressing non-m phenotype) and in the subsequent generations the double mutant 'm1N' was isolated and cultured. Later, m2 /+ males (wild type in phenotype) obtained from crossing m2 hermaphrodites to wild type males (+/+) were mated with 'm1N' hermaphrodites. In the next generation 40-60 wild-type hermaphrodites were cloned and observed for either all wild-type or both mutant and wild-type phenotypes. If the two mutations were on the same chromosome then there exists a possibility of 50% of the cross progeny in F2 will segregate 'm non N'. The possible genotypes were m1/m2. On the other hand if they were on different chromosomes then the entire cross progeny will be wild type. The possible genotypes were (m1/+; m2/+) or (m1/+; +/+). Thus, for two recessive mutations, the trans-heterozygote in F_2 looks wild-type, if the two mutations were on different genes and appears as a mutant phenotype if they were allelic.

2.2.3 Two-factor cross to assign new mutations to specific linkage groups

Different phenotypic markers like Dpy, Unc and Lev that are genetically mapped onto *C. briggsae* genetic linkage map are used as phenotypic markers to map newly isolated mutants to their corresponding chromosomes. The markers are chosen to be different from the tester mutant, like Muv and Unc or Dpy and Unc, where Muv and Dpy are the tester mutant phenotypes under observation. Two-factor cross to map a tester mutant that exhibits Muv phenotype to LG II by using the Dpy marker is as follows: First Muv/+ males [obtained from crossing Muv hermaphrodites to wild type males (+/+)] were crossed to Dpy hermaphrodites. From the F1 progeny 10-12 wild type looking hermaphrodites were cloned to individual plates. The possible genotypes of the hetetozygotes are, (Muv/+; Dpy/+) and (+/+;+/Dpy). Later, the plates that segregate both Dpy and wild-type worms (+/+; +/Dpy) were discarded and from the plates that segregate both Muv and Ddpy worms (Muv/+; Dpy /+), 40-50 Muv non-Dpy or Dpy non-Muv worms were cloned to separate plates. The F2 generation was observed for the mendilian segregation of 3:1 for Muv non-Dpy [Muv/Muv;+/+] or [Muv/Muv;Dpy/+] : MuvDpy [Muv/Muv;Dpy/Dpy] animals, respectively. Deviations from this ratio confer possible

linkage between the two mutants. The obtained double mutant MuvDpy will be preserved for future experiments.

2.2.4 Cis two-factor self-cross for measuring recombination frequencies

Recombination frequencies are calculated by applying cis two-factor self-cross. Two-factor cross between tester mutant that is Muv the phenotypic marker mutant, Lev present on the same LG is as follows: The homozygous double mutant hermaphrodites, which are MuvLev in phenotype (obtained through cross scheme 2.2.4) were mated with wild type males (+/+) and the obtained hermaphrodite cross-progeny [(MuvLev)/++, phenotypically wild-type] were allowed for selfing. Two types of phenotypes are possible from the selfing, parental and recombinants. The parental phenotypes are MuvLev and wild type. The possible recombinants are Muv non-Lev [Muv/Muv Lev/+] and non-Muv Lev [Muv/+ Lev/Lev]. The recombination frequencies are calculated by " total number of recombinants/ total number of parents + recombinants". 50% recombination frequency confers independent assortment.

2.2.5 Protocol for Indel mapping

Specific Insertions and Deletions (In-dels) are identified in sequence comparison with polymorphic variant strain HK104 and AF16. These indels are assigned to specific chromosomes and tested for their corresponding DNA amplifications in the genome through PCR. For example the Indel type I-10 present on *C. briggsae* chromosome 1(Cb1) amplifies 253 bp in AF16 and 263 bp in HK104, thus revealing 10bp insertion in the latter. The cross scheme carried out for Indel mapping is as follows: HK104 males were mated with AF16 (or *sy5353*) hermaphrodites and the resulting hermaphrodite cross progeny [HK104/AF16] were selfed. The genotypes of F2 populations were AFF16/AF16, HK104/HK104 and HK104/AF16 and their segregation ratio will be 1; 1; 2 ratio, respectively, for independent assortment. The genomic DNA was isolated from each genotype populations and was used as a template in PCR reactions (40 cycles program was applied with denaturation cycle at 94^0 for 2', annealing cylce at 45^0 for 15''

and extention cycle at 68^0 for 45'' followed by a final extention cycle at 68^0 for 7') using chromosome specific primer pairs (Appendix c).

2.3 Cell biology

2.3.1 Scoring vulval induction pattern

Vulval induction pattern in hermaphrodites is generally analyzed through quantifying the number of VPCs adopting vulval fates vs non-vulval fates. 1^0 and 2^0 fates are described as vulval fates and 3^0 as non-vulval fates. The VPC that adopts 1^0 or 2^0 fates will produce 8 or 7 cells, respectively and was referred to acquire 1.0 cell induction or complete induction. Thus the VPC induction pattern in AF16 animals was generally inferred as 3.0 cell induction, where P5.p and P7.p adopt 2^0 fate and P6.p adopted 1^0. In multivulva animals the cell induction will be always >3, as they often possess ectopically induced VPCs. In the other cases, where one of the daughter fuses with the hyp7 and the other follow cell division to produce 2 to 4 cells to form vulval invaginations are counted as 0.5 cell induction or partial induction. Alternatively, ectopic pseudovulvae observed anterior and posterior to the central vulva are also used as a criterion. But L4 stage observations were unbiased and reliable for dissecting individual VPC induction potentials.

2.3.2 Scoring vulval cell lineages

The Pn.p cell lineages were analyzed as mentioned by Sulston and Horvitz (1977). The complete Pn.p lineages of the VPCs of the animal were observed in a period of 2-3 hr continuous observations under Nomarski optics. Worms were picked in early-mid L3 stages where all or most of the Pn.p cells have more than two cells i.e., after second round of cell division and mounted on 5% agar pads with 5-10 µl of S-basal [(0.1 M NaCl and 0.05M H_3PO_4 (pH6) and cholesterol (5mg/ml in EtOH)] mixture solution without adding sodium azide. A lot of bacteria were scraped on to the agar pad as a food source for the worms during the study. To avoid any possible desiccation during DIC observations water was added at regular intervals of 15-30' to the agar pad. The division patterns of Pn.p cells were observed by following the corresponding nuclear divisions

and careful effort was taken to draw nuclear positions in a paper with an interval of 5-10'. In this way any possible misinterpretations of division pattern were avoided and the drawings were recorded for future reference. The nuclear divisions were labeled as L-longitudinal, T- transverse, O-oblique, S-syncytial, N- undivided and D- ambiguous, based on the plane of nuclear division axis. The cell fates 1^0, 2^0 and 3^0 were characterized based on the criteria described by Sternberg and Horvitz (1986). Alternatively, cell expression markers *mfIs5* and *mfIs8* expression pattern is observed in the mutant background and their respective cell fates were observed.

2.3.3 Laser microsurgery technique for cell ablations

Cell ablations were carried out by the use of a photonic Instruments laser system which fires a coumarin dye laser microbeam that is capable of damaging a given cell without disturbing its neighbors. The animals at L1stage where the gonad has only 4 cells (Z1-Z4) were picked and mounted on 5% agar pads. All the four cells were ablated and the worms after ablation were recovered immediately on to a fresh NGM plate and observed for the developmental defect within 2-3 days. In a similar way individual VPC ablations were done.

2.3.4 Microscopy and Photography

Plate level observations were carried out using light microscopes, Nikon SMZ645 or Leica MZ75 and Leica MZFLIII is used for GFP observations. For detailed anatomical studies live animals were anesthetized with sodium azide (NaN3 – final concentration of 300-500 pm) on 5% agar pads and Nomarski images were taken using either ZEISS Imager.D1 or Nikon Eclipse 80i dissecting microscopes. Images were captured with either Nikon digital camera Dxm1200F or Hamamatsu ORCA-ER digital camera. DIC images and GFP fluorescence images were taken with automatic exposure. All the images were saved in jpeg or tiff format and were processed using Adobe Photoshop v8.0.

2.5 Molecular biology

2.5.1 DNA extraction from worms

One to two eggs (or L1/L2 worms) were picked on to the cap of a 0.7 microfuge tube containing a previously aliquoted 5 μl worm lysis buffer [50mM KCl, 10mM Tris (pH 8.2), 2.5mM MgCl, 0.45% NP-40, 0.45%Tween 20, 0.001%Gelatin] and proteinaseK mixture(13 μl of 10mg/ml concentration is added to 1ml of worm lysis buffer). The transfer of worms was observed through microscope and necessary care was taken to minimize bacterial transfer. The tubes were all kept on ice until all the required population of worms were collected. Then they were centrifuged briefly and incubated at -70^0 C for 15' to overnight. After the incubation step 25 μl of mineral oil was added to each tube and heated for 1hr @ 60^0 C and then 15' @95^0C. This final step ensures the extraction of DNA from the tissues and was analyzed further. For bulk DNA isolation 20 worms were picked and lysed in varying amounts of lysis buffer (20 μl - 50 μl) depending on the required concentration of DNA.

2.5.2 Polymerase Chain Reaction

All the polymerase chain reactions were carried out using Peltier thermal cycler PTC-200 system. Primers for PCR were obtained from either SigmaAldrich or Mobix laboratory (McMaster University) and re-suspended in water (RNase or DNase free) to obtain 150 pmole /μl stock. This was diluted to obtain working stock of 15 pmole/μl. PCR master mix was prepared by adding 2μl of dNTPs, 1μl up and down primer each, 10μl of buffer, 1μl of $MgSO_4$, 0.5μl of polymerase to 2μl of DNA and the final volume was adjusted to 50μl using water. In general, 30-40 cycle extensions were followed through a denaturation temperature of 94^0C followed by 68^0C elongation step. The annealing temperature ranges from 40^0C to 56^0C. Final extension cycle at 68^0C for seven minutes was followed. Routinely, 2-5 μl of PCR product was analyzed by agarose gel electrophoresis.

2.5.3 Agarose gel electrophoresis

Agarose gels of 0.8 to 2% (1X TBE or TAE) are routinely prepared in EasyCast™ Model B1 horizontal minigel systems. 1μl of 10mg/ml EtBr (Ethidium Bromide) was

used as a staining agent. 2-20 µl of DNA was loaded into the wells and 80-100V voltage was applied through Lightning volt™ power supply model OSP-500. The separated DNA fragments were visualized through UV illuminator from AlphaDigidoc™ RT.

2.5.4 RNAi

All RNAi experiments were carried out in the *C. briggsae* RNAi sensitive strain JU1018, obtained from MA. Felix. Mark Hindle – An undergraduate thesis student in Dr. Gupta lab carried out transformation experiments for *Cbr-pry-1* construct and *Cbr-lin-12* and *Cbr-bar-1* constructs were obtained from MA.Felix. Ashwin (M.Sc student) carried out transformation experiments for *Cbr-pop-1* and *Cbr-mab-5* constructs. 80 ul of *E. coli* (HT115) transformed with the respective constructs (produce dsRNA of genes of interest) was placed on the six well RNAi agar plates and 3-4 adult worms were placed on them. The progeny was observed for the detectable phenotypes, in adults (plate level observations) and earlier stages, L3 to L4 (Nomarski observations), resulting from the partial inactivation of the gene under observation.

Chapter 3: Phenotypic characterization and genetic mapping of *pry-1* in *C. briggsae*

Background

Pry-1 in *C. elegans (Cel-pry-1)* was isolated in genetic screens aimed at identifying genes involved in Q neuroblast migration in *C. elegans* (Maloof et al., 1999). It was mapped to LG I close to *lin-11* (WormBase). Two alleles (*mu38* and *nc1*) are currently known for *Cel-pry-1* and both behave similarly (Maloof et al., 1999). The genetic and molecular studies of *Cel-pry-1* revealed that it encodes a homologue of vertebrate Axin protein (Korswagen, 2002). Axin interacts with GSK3β and adenomatous polypopsis protein (APC) to form a destruction box complex that targets β-catenin for degradation (See chapter 1, Figure 1.3). *Cel-pry-1* protein contains RGS and DIX domains and is distantly related to Axin/Conduction (Korswagen, 2002). In *C. elegans*, BAR-1 was identified as the worm β-catenin and mutations in PRY-1 caused constitutive activation of Wnt signaling by causing BAR-1 to accumulate in the nucleus where it interacts with TCF/LEF factor POP-1 (Korswagen, 2002).

During *C. elegans* development, canonical Wnt pathway regulates VPC cell fate, sensory ray formation, posdeireid formation, P12 cell fate and Q neuroblast migration (QL and QR pair) (Herman MA, 2003). Genetic, cellular and molecular events occurring during vulval development in *C. elegans* was explained in Chapter 1 and mutations in pry-1(Axin) causes an overinduced or multivulva (Muv) phenotype that results from the ectopic inductions by P3.p, P4.p and P8.p cells to adopt vulval fates (Gleason et.al., 2002).

In *C. elegans*, the descendents of QR cells migrate towards the anterior region, while the progeny of QL cells migrate towards the posterior region (Figure 3.1B) (Sulston and Horvitz 1977; Sulston, Albertson et al. 1980; Hedgecock, Culotti et al. 1987). This migration process depends on the Hox gene *mab-5* which is the target of Wnt signaling pathway (Kenyon 1986; Hedgecock, Culotti et al. 1987; Salser and Kenyon 1992). Mutations in *pry-1* cause ectopic expression of *mab-5* in QR, such that QR behaves like its siser QL leading to the migration of its progeny towards the posterior (Figure 3.1C) (Maloof et al., 1999). This process can be visualized by a GFP reporter

driven by the MEC-7 (The *C. elegans* β-tubulin) gene promoter (Figure 3.1) (Hamelin, Scott et al. 1992).

P11 and P12 are the two posterior hypodermal P cells in *C. elegans* (Sulston and Horvitz 1977). In wild-type animals, the posterior daughter of P11, P11.p, will fuse with the syncytial hypodermis hyp7. While, the posterior daughter of P12 (P12.p) produces two cells named P12.pa and P12.pp. The P12.pp undergoes programmed cell death whereas P12.pa adopts hyp12 fate (Figure 3.2A). Mutations in *lin-3/let-23* pathway resulted in fate transformation of P12.pa into P11.p, resulting in two P11.p like cells (Fixsen, Sternberg et al. 1985). Mutations in Frizzled receptor LIN-17 cause transformation of P12.pa into P11-like cell (Jiang and Sternberg, 1998). A similar phenotype is observed in BAR-1 and POP-1 mutants. In contrast, mutations in PRY-1 cause cell fate transformation such that P11 is transformed towards P12-like cell (Figure 3.2B) (Eisenmann, Maloof et al. 1998; Jiang and Sternberg 1998; Gleason, Korswagen et al. 2002; Korswagen 2002).

In *C. elegans,* Wnt signaling also regulates the fates of the lateral seam cells, V cell lineages that give rise to postdereid sensillum in hermaphrodites and sensory rays in males (Sulston, Albertson et al. 1980). The canonical Wnt signaling components EGL-20 (Wnt), LIN-17 (Fz) and BAR-1(β-catenin) are required for the proper fate specification of V cells. Mutations in PRY-1 (Axin) cause ectopic activation of MAB-5 in V cells leading to the formation of external rays (poly-rays) in males and missing postdereid in hermaphrodites (Maloof, Whangbo et al. 1999).

Previous research carried out in Gupta Lab identified 2 alleles of *C. briggsae pry-1* (*sy5353* and *sy5411*) (Table 3.1). My present work lead to the identification of another *Cbr-pry-1* allele, *sy5270* and the present chapter discusses experiments aimed towards the following objectives:

1. Genetic analysis of *Cbr-pry-1* alleles such as mapping and complementation studies.

2. Characterization of the phenotypes of *Cbr-pry-1* mutants and their comparison with *Cel-pry-1* animals.

Results

3.1 Genetic characterization of *Cbr-pry-1* alleles

3.1.1 Complementation study

Previous genetic screens carried out by Dr. Gupta had identified several multivulva mutants in *C. briggsae* (Table 3.1). While two of these, *sy5353* and *sy5411* were found to be alleles of *Cbr-pry-1*. I carried out complementation studies to search for additional *cbr-pry-1* alleles (refer to Materials and Methods). This exercise revealed that sy5270, a previously uncharacterized Muv mutant, is allelic to sy5353 and sy5411 and is as described below:

First, *lin(sy5270)* hermaphrodites were mated with *lev(sy5440)* males to obtain MuvLev double mutant [*lin(sy5270) lev(sy5440)*], where lev or unc phenotype was used to distinguish between self and cross-progeny. The *lin(sy5353)* /+ males (wild-type in phenotype), obtained from crossing *lin(sy5353)* hermaphrodites to wild-type (AF16) males, were mated with the above MuvLev hermaphrodites. In the subsequent generation, the progeny were screened for the Multivulva phenotypes. If *sy5270* was present on a different linkage group compared to *sy5353* then both wild type and Muv phenotype animals will appear in the F2 progeny. However, if the two alleles belong to the same linkage group then the 'het' animals will appear mutant i.e., Muv. Thus there exists a possibility that 50% of the F2 cross progeny that segregate Muv will be non-Lev. The possible genotypes were (*sy5270/sy5353*). On the other hand, if they were on different chromosomes then the entire cross progeny will be wild type. The possible genotypes were (*sy5270/+; sy5353/+*) or (*sy5270/+; +/+*). 30% (n=59) Muv non-Lev animals were recovered in the F2 generation for the above cross scheme. A similar cross scheme was applied between *sy5270* and *sy5411* and 40% (n=46) Muv non-Lev worms were observed in the F2 generation. Though the observed segregation patterns were comparatively less than the expected 50%, the presence of Muv worms in the F2 generation suggests that the two mutations were failing to complement each other, suggesting that *sy5353*, *5270* and *5411* belong to the same complementation group.

3.1.2 Genetic mapping

3.1.2a Linkage study

Many visible mutant phenotypes such as Dpy (Dumpy), Unc (Uncoordinated), Muv (Multivulva) and Rol (roller) were isolated for *C. briggsae*, through EMS screens and a partial genetic map was made available for *C. briggsae* through standard genetic mapping procedures (B. Gupta, P. Sternberg and D. Baillie, unpublished, www.briggsae.org.) (Figure1.5). These phenotypic marker mutants available for *C. briggsae* were utilized for linkage mapping of *sy5270* and *sy5353* (see Materials and Methods). *lin(sy5270)/+* males [obtained from crossing *lin(sy5270)* hermaphrodites to AF16 males(+/+)] were crossed to *cby-15* hermaphrodites (LG II marker). The possible genotypes of the heterozygotes in the F2 were, [*lin(sy5270)/+;cby-15/+)* and *(+/+;+/cby-15)*]. Subsequently, the plates that segregate both Dpy and wild-type worms *(+/+; +/cby-15)* were discarded. From the plates that segregate both Muv and Dpy worms [*lin(sy5270)/+;cby-15/+*], 40-50 Dpy non-Muv worms were cloned onto separate plates. The F3 generation was observed for the mendelian segregation of 3:1 for Muv non-Dpy [*lin(sy5270)/lin(sy5270);+/+*] or [*lin(sy5270)/lin(sy5270);cby-15/+*]: MuvDpy [*lin(sy5270)/lin(sy5270);cby-15/cby-15*)] animals, respectively. Deviations from these ratios indicate possible linkage between the two mutations. In a similar way, linkage tests were carried out between *sy5270* and other marker mutants on the remaining chromosomes. The results suggested linkage of *sy5270* with *lev(sy5440)* present on LGI (Table 3.2). Similarly, linkage for *lin(sy5353)* was verified with the *lev(sy5440)* marker mutant present on LG I and the results confirmed that *sy5353* also maps to LGI.

3.1.2b Indel mapping

In addition to the phenotypic markers, several SNPs (Single Nucleotide Polymorphisms) and indels (insertions–deletions) are made available for *C. briggsae* from genome comparisons with its polymorphic isolates, HK104 and VT847 (Hillier

2007). So, I made an effort to confirm linkage mapping of *sy5353* through indel mapping technique (see Materials and Methods). Linkage was tested with indels available for chromosome 1 and 3 (see Figure 3.4 for genetic cross). The primer pairs, GL 66 and 67 (Cbin1-2L/R) and GL 43 and 44 (Cbin3-1L/R) were used to identify polymorphisms bhP7 and bhP3 on Cb1 and Cb3, respectively (Appendix C). GL 66 and 67 pimers amplify 246 bp fragment in AF16 and 239 bp in HK104. GL 43 and 44 primers amplify 251 bp fragments in AF16 and 259 bp in HK104. The F2 generation homozygous *sy5353* animals (obtained from a cross between *sy5353* and HK104, refer to Figure 3.4) were tested for the presence/absence of desired polymorhisms. The results showed that GL 66 and 67 primers amplified both *sy5353* and HK104 fragments in 3 out of 13 cases and GL 43 and 44 in 11 out of 13 in F2 populations (Figure 3.5). For independent assortment, 50% of the F2 *sy5353* worms should segregate both *sy5353* and HK104 polymorphisms and the results from the indel mapping suggest that sy5353 is linked to Cb1, where only 23% of F2 *sy5353* segregated both polymorphisms (Figure 3.5).

3.1.2c Two-point mapping

Once *sy5353* and *sy5270* were mapped to LG I, an attempt was made to calculate recombination frequencies between *sy5353* and *lev(sy5440)* (see Materials and Methods; Figure 3.6). Double mutant hermphrodites [*lin(sy5353)lev(sy5440)*] that were phenotypically MuvLev, were mated with wild type males (+/+). The subsequent cross-progeny hermaphrodites [*lin(sy5353)lev(sy5440)*/++, phenotypically wild-type] were allowed to self. In the next generation two kinds of progeny were obtained from: parental- MuvLev and wild type and recombinants - Muv non-Lev and non-Muv Lev (Figure 3.6B). By screening for these two mutant phenotypes from the selfing of MuvLev, the percent recombination (*p*) between the two mutations was calculated. An average *p* value of 16.8 cM (centi-Morgans) was obtained for *lin(sy5353)* and *lev(sy5440)* (Table 3.3).

3.2 Phenotypic characterization of *Cbr-pry-1* mutants

3.2.1 Q neuroblast migration defect in hermaphrodites

Mec-7::gfp transgenic animals (provided by Dr. Gupta) were used to analyze Q cell migration defect in *C. elegans* (Figure 3.1). Expression pattern of *syIs95* was observed in *Cel-pry-1(mu38)* under Nomarski otpics and 53 % (n= 88) of animals QR migrated towards posterior. To analyze Q cell migration defect in *C. briggsae,* DNA of *mec-7::gfp* was transformed into *C. briggsae* AF16 animals (microinjections were carried out by Dr. Bhagwati Gupta). One of the stable line exhibited higher penetrance for *mec-7::gfp* in Q cells under Nomarski optics and was used in further studies (bhEX25, Table 3.4). To observe Q neuroblast migration defect in *Cbr-pry-1*animals, *mec-7::gfp* expression was observed in *sy5353* animals. Of the observed 60 animals only 41 animals expressed *mec-7::gfp* and a total of 36.5% (15/41) animals exhibited QR migration defect (Figure 3.8). Thus it can be inferred that *Cbr-pry-1* gene functions similar to *Cel-pry-1* in the context of Q cell migration.

3.2.2 P12 cell fate transformation defect in hermaphrodites

P12 cell fate in *Cbr-pry-1* alleles and *Cel-pry-1(mu38)* was analyzed under Nomarski optics. In *Cel-pry-1(mu38)* animals P11.p was transformed into P12.pa like cell in 88% (n=48) cases. In the case of *Cbr-pry-1* alleles the penetrance of similar transformation was found to be and 100% (Table 3.5). In addition, P7.p – P10.p cells also displayed a morphology similar P12.pa cell (Figure 3.2 and 3.9).

3.2.3 Tail defects in the males

To observe defects in male reproductive system in *Cbr-pry-1*animals, mutant males are obtained through heat shock treatment (6 hrs of heat shock treatment at 31^0 C) to plates containing 10-15 L4 mutant hermaphrodites. This causes non-disjunction during meiosis and results in more male populations. Later, phenotypic defects in *Cbr-pry-1* males were observed under Nomarski optics (Table 3.6 and Figure 3.10). The poly-ray phenotype was recognized by their capillae or bumpy tips along the mid body region (Figure 3.10C and D). Interestingly, in some cases ectopic pseudovulvae were observed

due to Pn.p induction similar to hermaphrodites (Table 3.6) (Sulston and Horvitz, 1985). In addition, few of the sensory rays were missing in mutant background (Figure 3.10D)

3.2.4 Vulval defects in the hermaphrodites

Depending on the vulval induction potentials of P3.p, P4.p and P8.p cells, ectopic pseudovulvae are observed in Muv mutants, located either anterior or posterior to the central vulva compared to wild type animals. Both *Cel-pry-1* and *Cbr-pry-1* adult hermaphrodites were observed for the Muv penetrance using a dissecting microscope. For *Cel-pry-1(mu38),* 40% (n=55) Muv penetrance was observed. A higher Muv penetrance was observed and for sy5270 and sy5353 (90% and 99%, respectively) (Table 3.7).

3.2.2e Brood size

Calculating brood size counts of wild type animals and mutants helps in understanding defects associated with their egg-laying behavior. Therefore, brood size was calculated for *Cbr-pry-1*animals (see Materials and Methods). Mean values of 170 and 109 are obtained for the brood size of *sy5353* and *sy5270*, respectively (Table 3.8). These values are much less when compared to AF16 animals (~300) and suggest that these mutants are associated with egg-laying defects (egl). In addition, *Cbr-pry-1* mutants are healthier compared to *Cel-pry-1(mu38).*

Discussion

This chapter summarizes work focused towards characterizing the genetic and phenotypic properties of *C. briggsae pry-1* mutants, *sy5270, sy5353* and *sy5411.* These mutants were identified in gentic screens aimed for mutations that affect vulval cell proliferation. Complementation studies described in this chapter revealed that all three alleles dirupt the *pry-1* locus. Results from the complementation confirmed allelism among them (section 3.1.1). Genetic mapping of *sy5270* was done through standard linkage mapping through phenotypic markers. The Indel mapping technique was applied for genetic mapping of *sy5353* (section 3.1.2). Both *sy5270* and *sy5353* were mapped to LG I through our linkage studies. Furthermore, I attempted to specify *Cbr-pry-1* locus on

LG I by calculating recombination frequencies between *lev(sy5440)* and *lin(sy5353)* (section 3.1.2b). However, a lack of phenotypic markers with established map positions on LG I largely hindered our positional cloning studies. But our genetic studies and molecular cloning of *sy5353* (Dr. Gupta, personal communication) confirmed that class III mutltivulva mutants are indeed *Cbr-pry-1* alleles.

Futhermore, I analyzed their phenotypes and compared them with *Cel-pry-1* animals, except postdeireid formation. Simple Nomarski observations of tail defects (poly-ray) and P12.pa cell fate defects revealed similarities between *Cbr-pry-1* and *Cel-pry-1* alleles (section 3.2.2 and 3.2.3). Furthermore, QL and QR migrations were observed through *mec-7::gfp,* and both *Cbr-pry-1* and *Cel-pry-1* alleles the QR stayed posterior in position compared to wild type animals (section 3.2.1). Thus, Q neuroblast migration defect was conserved in *Cbr-pry-1* and *Cel-pry-1* alleles. Though penetrance for P11 cell fate transformation and Q neuroblast migration defect were higher in *Cbr-pry-1* alleles, these phenotypes are also observed in *Cel-pry-1* animals suggesting that Wnt signaling controls similar developmental processes between *C. elegans* and *C. briggsae.* Additionally, a higher penetrance was observed for Muv phenotype between *Cbr-pry-1* and *Cel-pry-1* alleles (section 3.2.4). In addition, our preliminary L4 observations of *Cbr-pry-1* alleles suggested that P7.p and P8.p cells are rarely induced in these animals. I analyzed vulval development in *Cbr-pry-1* alleles in greater details (such as VPC lineages and ablations) in chapter 4 and significant variations were observed, when compared to *Cel-pry-1* alleles. Thus, Wnt signaling involved in vulval formation may differ between *C. elegans* and *C. briggsae* and is explained in greater detaisl in Chaper 4.

Table 3.1: Different classes of multivulva mutants in *C. briggsae*.

Class	Allele	Comments[a]
I	*sa993*	P3.p is not induced at all
II	*sy5216* *sy5392*	Resembles to *lin-1* mutant phenotype
III[b]	*sy5353* *sy5411* *sy5270*	P7.p and P8.p exhibit reduced induction
IV	*sy5342* *sy5344*	Resembles to *lin-31* mutant phenotype

Table was adapted and modified with permission from Dr. Gupta, unpublished work.

a - refers to the vulval induction pattern observed in the specific classes and compared with the established *C. elegans* Muv mutant phenotypes (the corresponding genes were referred in italics).

b – Complementation of *sy5270* with *sy5353* and *sy5411* was established in the present study.

Table 3.2: Linkage mapping data for *lin(sy5270)* and *lin(sy5353)*

Genotype	LG[a]	Genotype of selected marker	Phenotype of selected marker	Genotype of heterozygote in F1	Phenotype of heterozygote in F1	Phenotype of selected double mutants in F2 (n)	Genotype of selected double mutants in F2	% of double mutants observed in F2	Linkage
lin(sy5270)	I	*lev(sy5436)*	Unc	*sy5270/+; sy5436/+*	Wt	Unc non-Muv (36)	*sy5270;sy5436*	30	Yes
	II	*dpy(sy5148)*	Dpy	*sy5270/+; sy5148/+*	Wt	Dpy non-Muv (40)	*sy5270;sy5148*	62.5	No
	III	*dpy(s1281)*	Dpy	*sy5270/+; s1281/+*	Wt	Dpy non-Muv (38)	*sy5270;s1281*	60.5	No
	IV	*unc (s1270)*	Unc	*sy5270/+; s1281/+*	Wt	Unc non-Muv (38)	*sy5270;s1270*	57.5	No
	V	*unc(sa997)*	Unc	*sy5270/+; sa997/+*	Wt	Muv non-Unc (28)	*sy5270;sa997*	71	No
	X	*dpy(nm3)*	Dpy	*sy5270/+; nm3/+*	Wt	Dpy non-Muv (27)	*sy5270;nm3*	62	No
lin(sy5353)	I	*lev(sy5440)*	Unc	*sy5353/+; sy5440/+*	Wt	Lev-non-Muv (36)	*sy5353;sy5440*	43%	Yes

a– the corresponding linkage groups for whom linkage with *sy5270* was observed

n- the number of double mutants segregated from the F1 heterozygote in F2

Table 3.3: Percent recombination *(p)* values between *sy5353* and *sy5440*

S.No[a]	Progeny obtained from *lin(sy5353) lev(sy5440)/ + +* in F2				R	*p(cM)*	*% p*
	Parental		Non-parental or recombinants				
	Wild type	Unc Muv	Muv nonUnc	Unc non Muv			
1	149	19	25	33	0.25	0.3	30
2	182	17	25	27	0.20	0.23	23
3	208	16	24	30	0.19	0.22	22

a- the number of individual cases where progeny from selfing *lin(sy5353) lev(sy5440)/ + +* was observed.

p- Recombination frequency and is calculated by, $1-\sqrt{1-2R}$ and is expressed in cM (centi Morgans). *% p* is percent recombination.

R- Fraction of recombinant phenotypes and is calculated by, number of recombinants scored/ total number of animals scored (parental+recombinants).

Table 3.4: Expression pattern for *Cel-mec-7*::*gfp* in wild type *C. briggsae*

Animals scored	No fluorescence	GFP(+)	GFP(++)	GFP(+++)	n[a]
Less than six GFP expressing neurons	AVM(40) PVM(45)	AVM(9) PVM(1)	AVM(5) PVM(3)	AVM(16) PVM(21)	70
Six GFP expressing neurons	-	-	-	AVM(9) PVM(9)	9
No GFP expressing neurons	AVM(0) PVM(0)	-	-	-	37

All animals analyzed were at mid L4 to early adult stages. The cell positions were compared relative to the expression of *Cel-mec-7* in Q neuroblast cells (refer to Figure 3.1A).

GFP fluorescence was arbitrarily grouped into high (+++), medium (++) and weak (+). Zero (0) refers to no visible fluorescence.

n – refers to the number of animals expressing *Cel-mec-7* in the corresponding neuronal cells.

a-Due to mosaicism, of the observed 116 animals, 37 animals showed no GFP fluorescence. Of the remaining animals, 70 showed fluorescence in a subset of neurons, and 9 animals showed fluorescence in all the 6 neurons.

Table 3.5: P12 fate transformations in AF16 and *Cbr-pry-1* mutants

Genotype	% P11.p - P12.pa[a] (n)
AF16	0(43)
lin(sy5353)	100(35)
lin(sy5270)	100(36)
lin(sy5411)	100(28)

a- the transformation of P11.p to P12.pa like cell giving to two P12.pa cells (P11.P – P12.pa transformation). AF16 animals exhibit no penetrance and all the *Cbr-pry-1* alleles show 100% penetrance.

n- the number of animals observed

Table 3.6: Morphological defects in male tail development in *Cbr-pry-1* mutants

Mutant	Defective rays		Spicule	Hook	Polyray[a] phenotype	Pn.p induction[e] (n)	N
	morphology	pattern					
lin(sy5270)	2	23	23	23	13	1(8)	24
lin(sy5353)	6	17	17	17	2	1(2)	17
lin(sy5411)	4	16	16	16	4	1(6)	16

a- the animals where the typical poly ray (external rays) phenotype observed along he A/P axis. It should be noted that the poly ray phenotype was observed under Nomarski, unlike the MH27 or DAPI staining procedures carried out in *Cel-pry-1* animals and the numbers don't represent to the actual penetrance of the polyray phenotype.

e- the animals where one ectopic vulvae were observed similar to hermaphrodites.

n- the number of animals showing the ectopic vulvae

N- total number of males observed for the study

Table 3.7: Penetrance of Muv phenotype for *Cbr-pry-1* animals

lin(sy5270)					*lin(sy5353)*				
Clone	**Muv**	**Wt**	**total**	**penetrance**	**Clone**	**Muv**	**Wt**	**total**	**penetrance**
1	62	4	66	94%	1	46	0	46	100%
2	108	7	115	94%	2	55	0	55	100%
3	81	3	84	96%	3	51	2	53	97%
4	72	3	75	96%	4	89	2	91	98%
5	100	12	112	88%	5	145	2	147	99%
6	62	4	66	94%	6	46	0	46	100%
7	108	7	115	94%	7	55	0	55	100%
8	111	7	118	94%	8	51	3	54	97%
9	114	12	126	90%	9	110	2	112	98%
10	69	4	73	94%	10	162	3	165	98%
11	56	3	59	95%					
12	84	4	88	95%					
average	94%				99%				

Plate level Muv phenotype was counted against wild type animals in *sy5353* and *sy5270*

Table 3.8: Statistical summary of *sy5353* and *sy5270* brood sizes

Parameter:	*5353*brood
Mean:	170.42
# of points:	12
Std deviation:	45.560
Std error:	13.152
Minimum:	114.00
Maximum:	256.00
Median:	162.00
Lower 95% CI:	141.47
Upper 95% CI:	199.36

Parameter:	*5270* brood
Mean:	109.00
# of points:	16
Std deviation:	38.269
Std error:	9.5673
Minimum:	72.000
Maximum:	169.00
Median:	90.500
Lower 95% CI:	88.612
Upper 95% CI:	129.39

All the statistical analysis was done though Instat 2.00 program.

Figure 3.1: Q lineages and *mec-7* expression pattern in N2 and *Cel-pry-1* animals

Anterior is towards left in all the images. All animals observed at the stages of midL4 to early adults. (A) The cell lineages of the Q neuroblast and their descendents in N2 worms. Different shapes and color background were used to represent individual cell lineages and their descendents. QL/R, oval circles; QL/R.a, large diamonds; QL/R.ap, small diamonds; QL/R.paa (PVM/AVM) and QL/R.pap, small circles and specifically PVM red color and AVM yellow circle to distinguish the position of the cells. X represents the cells that undergone programmed cell death. (B) This cartoon worm represents the positions of all the six chemosensory neurons in *mec-7* worms in N2. The star symbol refers to the position of the vulva. The AVM is anterior to the vulva and PVM is in the posterior. (C) This cartoon worm refers to the Q neuroblast migration defect in *pry-1*mutants. The big star represents central vulval invagination and small ones pseudovulvae, which is the typical feature of Muv. The AVM cells (small yellow circle) stays behind posterior in *pry-1*mutants compared to N2.

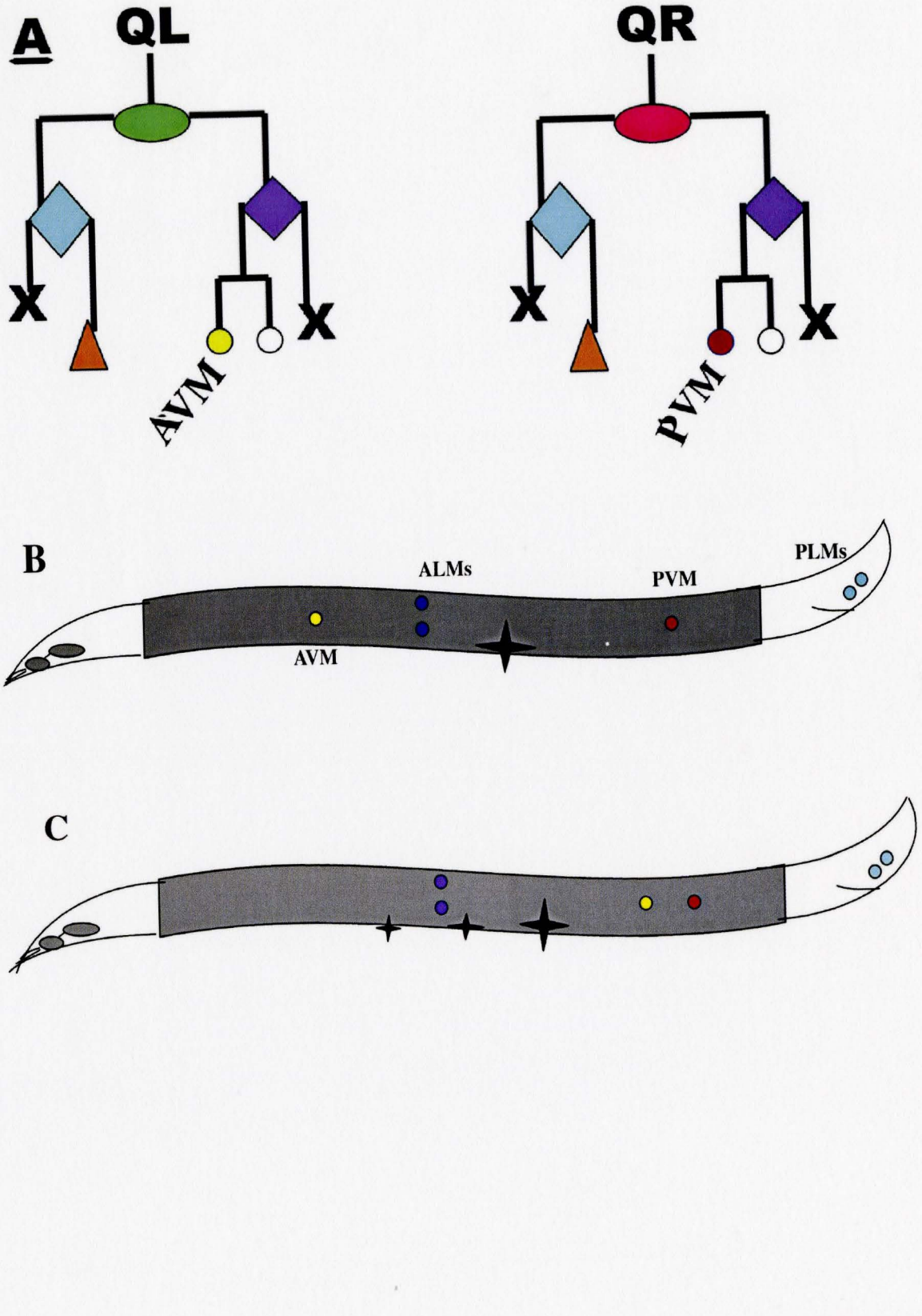
A
QL
QR
X
X
X
X
AVM
PVM
B
ALMs
PVM
PLMs
AVM
C

Figure 3.2: P11.p and P12.pa cell anatomy in N2 and in *Cel-pry-1 (mu38)* animals

(A) The positions and morphology of P11.p and P12.pa in AF16 animals. The P11.p nucleolus appears less dense and bigger in morphology compared to P12.pa, which was somewhat smaller and denser. (B) The positions and morphology of P11.p and P12.pa in *mu38* animals. The fate transformation of P11.p towards P12.pa is obvious in the mutant background, giving rise to two P12.pa like cells.

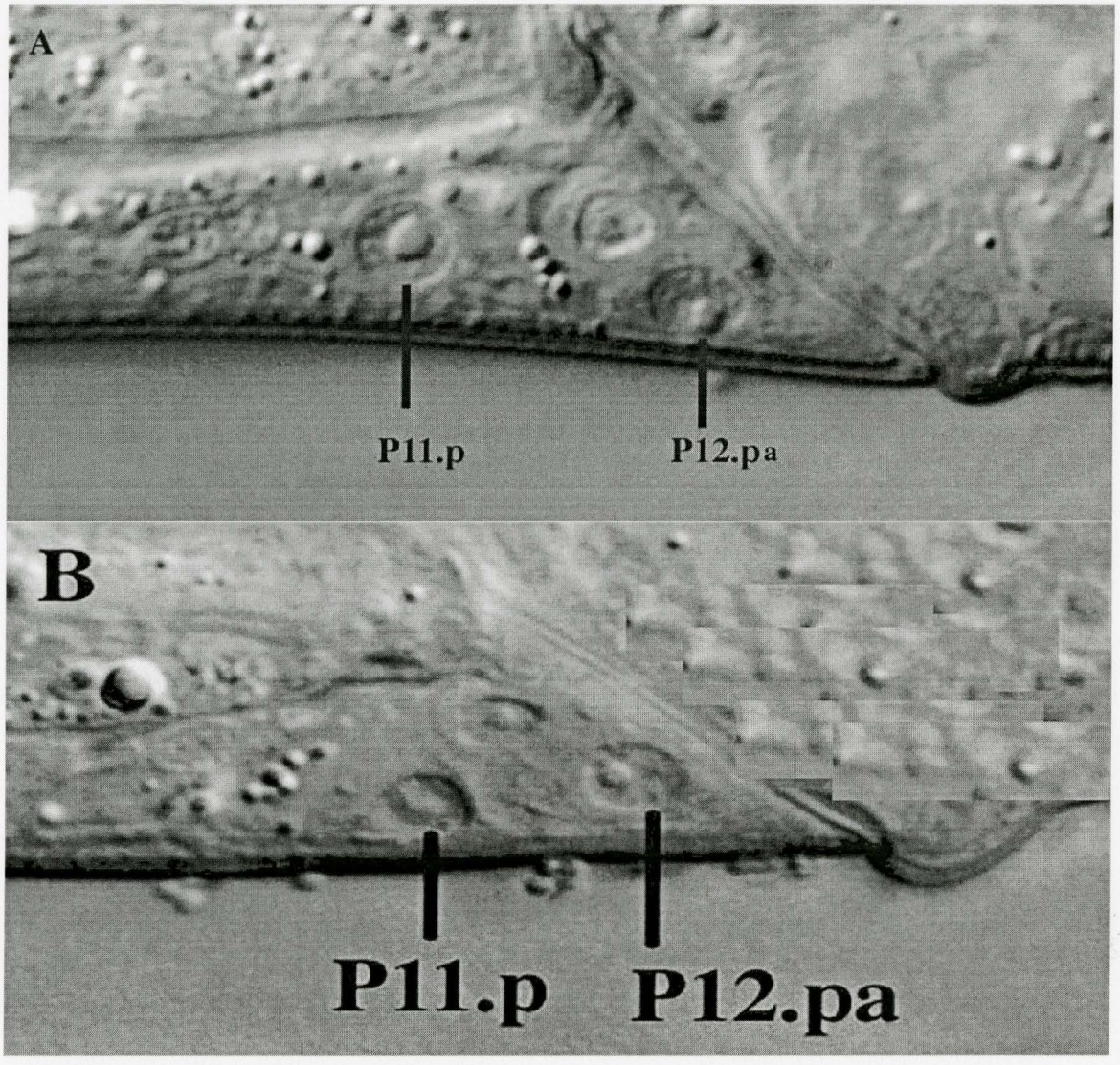
A
P11.p
P12.pa
B
P11.p
P12.pa

Figure 3.3: Genetic cross scheme for complementation test between *sy5270* and *sy5353*

P0: ♂AF-16 x *lin(sy5353)* ♀

F1: ♂ *sy5353/+* x *lev(sy5440):sy5270*♀ (UncMuv)

F2: The possible genotypes are:

lev(sy5440)/+; sy5270/+ -- wild type in phenotype and

sy5353/+; sy5270/+ (if they are not allelic and appear wild type) or *sy5353/sy5270* (present on same chromosome i.e., allelic and appear multivulva)

Figure 3.4: The genetic cross scheme for the Indel mapping of *sy5353*

P0: $+^{*}/0$ (males) x *lin(sy5353)/lin(sy5353)* (hermaphrodites)

F1: *lin(sy5353)/* $+^{*}$ (hermaphrodites) heterozygotes were selfed

F2: *lin(sy5353)/lin(sy5353)* : *lin(sy5353)/* $+^{*}$: $+^{*}/+^{*}$

1	**2**	**1**
Muv	non-Muv	
Only one PCR amplified band corresponding to *sy5353*	Two PCR bands corresponds to corresponding to *sy5353* and $+^{*}$	

$+^{*}$ - refers to HK104 wild type isolate

Figure 3.5: Validation of indel mapping of *sy5353* using bhP7 and bhP3 polymorphisms

(A) PCR amplifications of the genomic DNA of F2 generation sy5353 worms by GL 66 and 67 (Cb-in-1-2L/R) primer pair. They amplify 246 bp fragments in AF16 and 239 bp in HK104, corresponding to bhP7 polymorphism on chromsome 1. H refers to the heterozygote, *sy5353*/+*. (B) Both GL 66,67 and GL 43, 44 (Cb-in-3-1L/R) is presented. Numbers in white refer to Cb-in-1-2L/R and black to Cb-in-3-1L/R primer amplified products. (C) GL 43 and 44 (Cb-in-3-1L/R) amplified products are presented. They amplify 251 bp fragments in AF16 and 259 bp in HK104, corresponding to bhP7 polymorphism on chromsome 3.

A total of 3 out of 10 samples are amplified by Cb-in-1-2L/R (Solid white lines in A and B) and 11 out of 13 in case of Cb-in-3-1L/R (solid black lines in B and C). (Refer to Appendix C)

A

B

C

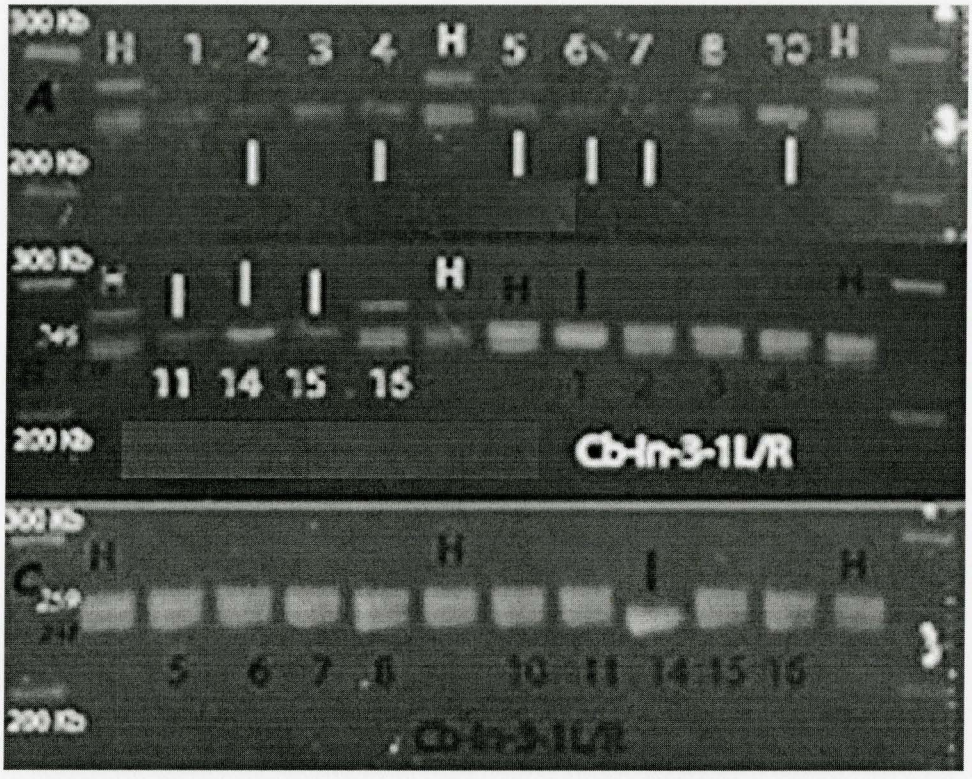
300 Kb
H 1 2 3 4 H 5 6 7 8 10 H
200 Kb
300 Kb
H H H
11 14 15 16
200 Kb
Cb-In-3-1L/R
300 Kb
H H H
5 6 7 8 10 11 14 15 16
200 Kb
Cb-In-3-1L/R

Figure 3.6: Genetic cross scheme for calculating recombination frequencY between *sy5353* and *sy5440*

(A) Obtaining the double mutant *[lin(sy5353) lev(sy5440)]*

P: AF16 ♂ X *lin(sy5353)* ♀

F1: *lin(sy5353)/+* ♂ x *lev(sy5440)*♀ (Both Muv in phenotype)

F2: cloned and selfed wild type looking *lin(sy5353) lev(sy5440)/ + +* worms.

F3: the double mutant *lin(sy5353) lev(sy5440)* [Muv Lev] was obtained and used for two factor mapping between *sy5353* and *sy5440*

(B) Calculating % recombination between *sy5353* and *sy5440*

P: AF16 ♂ X *lin(sy5353) lev(sy5440)* ♀

F1: cis-heterozygote, *lin(sy5353) lev(sy5440)/++* (wild type phenotype) allowed for selfing ♀

F2: The segregation of parental and recombinants or non-parental are as follows:

Parental - *lin(sy5353) lev(sy5440)/++* - wild type in phenotype

lin(sy5353) lev(sy5440) - MuvLev in phenotype

Recombinants - *lin(sy5353)/lin(sy5353) lev(sy5440)/+* - Muv non-Lev in phenotype

lin(sy5353)/+ lev(sy5440)/lev(sy5440) –non Muv Lev in phenotype

Figure 3.7: Expression pattern for *Cel-mec-7*::gfp in wild type *C. briggsae*

Anterior is towards left in all the images. All animals are observed at midL4 to early adults. (A) Expression pattern of *Cel-mec-7::gfp* in AF16 background. The actual positions of AVM and PVM were compared with *C. elegans mec-7::gfp* expression and were indicated by small white arrows. (C) The DIC image of the transgenic AF16 under observation.

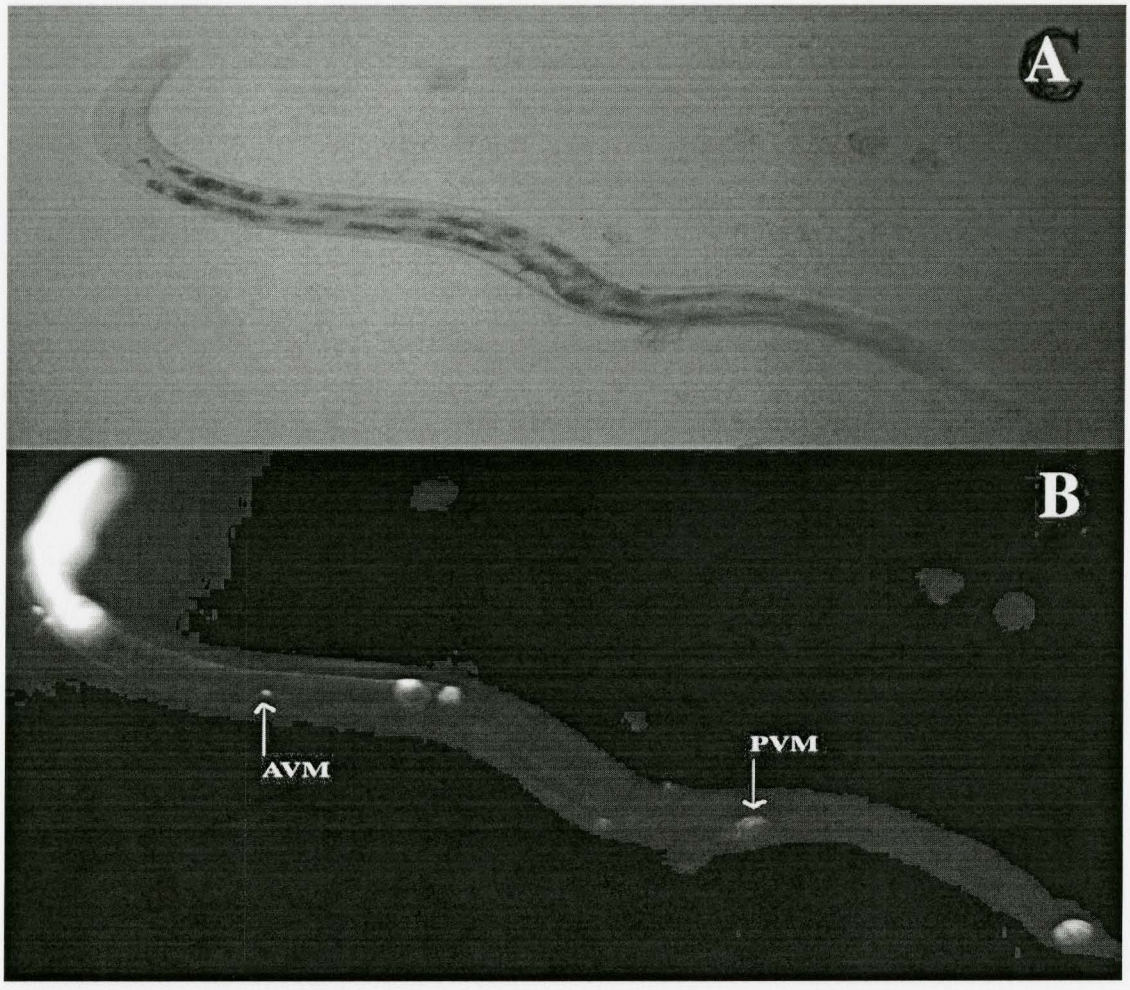
A
B
AVM
PVM

Figure 3.8: Expression pattern for *Cel-mec-7*::gfp in *sy5353* animals

(A) DIC image of the corresponding animal under observation. (B) Expression of *mec-7::gfp* in *sy5353* mutant animals. PVM is present at the expected position and the cell present between the vulva and PVM is confirmed as AVM by verifying the expression and positions of all the six chemosensory neurons.

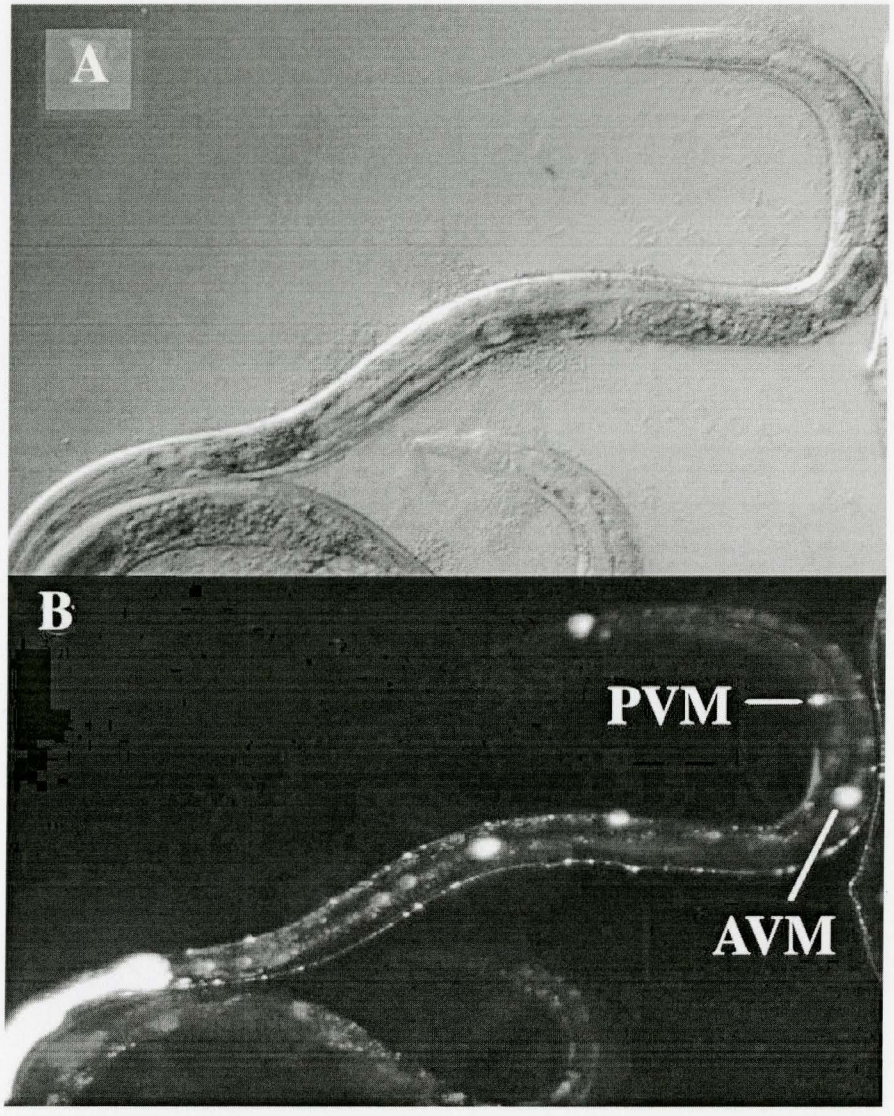
A
B
PVM
AVM

Figure 3.9: P7.p-P10.p morphology in wild type *C. briggsae* and *Cbr-pry-1* mutants

(A) This figure represents the posterior region of wild type *C. briggsae*, The morpholoigical features of the posterior Pn.p cells is presented. (B) This figure represents the posterior region of *lin(sy5353).* Morphology of P7.p-P10.p cells is shown and appears similar to P11.p – P12.pa fate transformations (as shown in Figure 1.3).

A

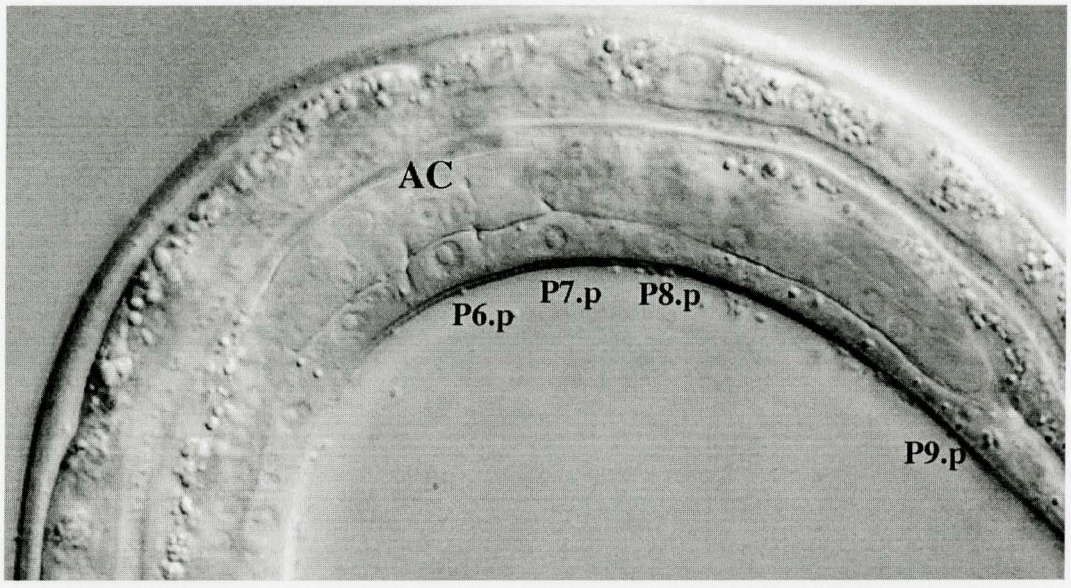

B

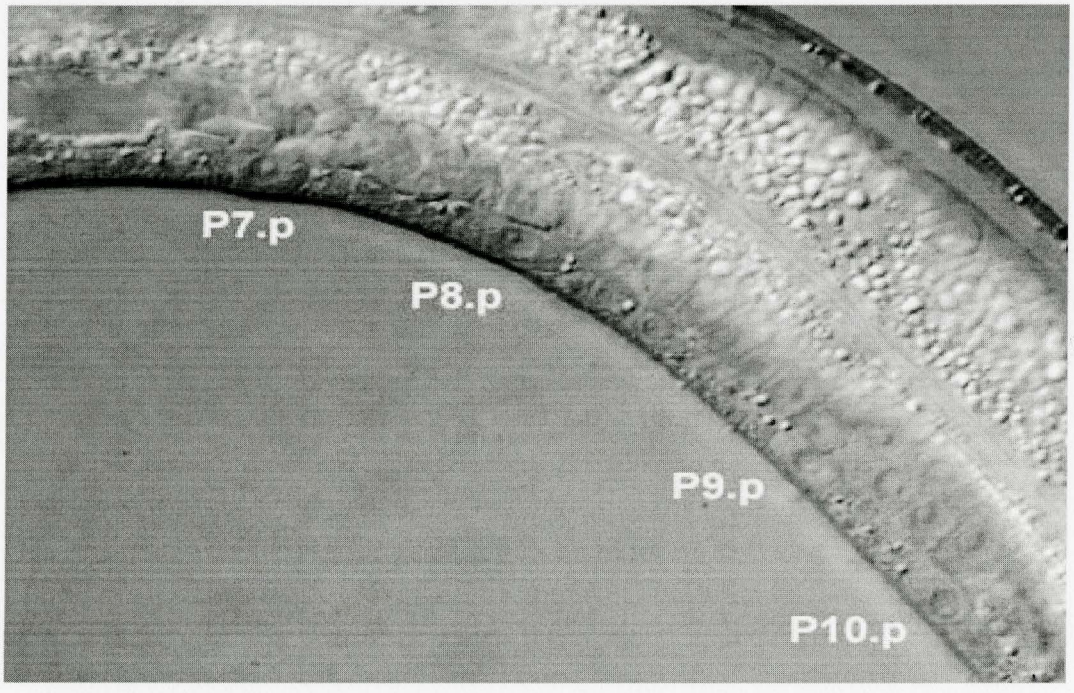

Figure 3.10: Male tail morphology in AF16 and *Cbr-pry-1* mutants

(A) The adult male tail of AF16 in lateral view. Only one pair of rays and fan is visible in this view. (B) The adult male tail of AF16 in ventral view. Obvious shield like hook was observed and both pairs of sensory rays were seen. The spicules are not obvious and referred by black lines (C) The adult male tail of *Cbr-pry-1* mutants in lateral view. The typical poly-ray phenotype of *Cel-pry-1* mutants was very obvious along the A/P axis (D) The adult male tail of *Cbr-pry-1* in ventral view. The crumpled nature of the spicules and missing sensory rays (2^{nd} pair) was very obvious in the mutant background.

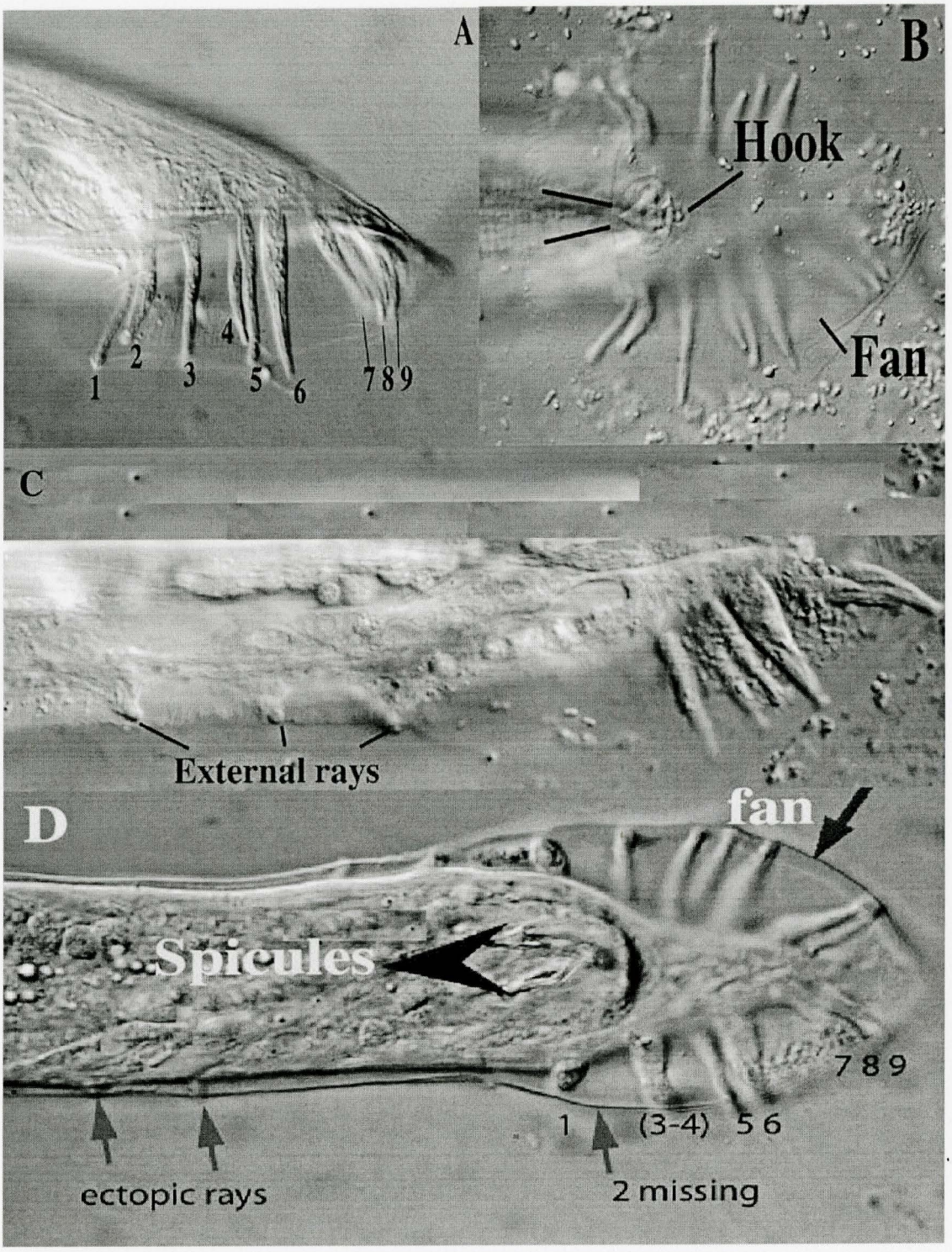
A
1
2
3
4
5
6
7 8 9
B
Hook
Fan
C
External rays
D
fan
Spicules
7 8 9
1
(3-4)
5 6
ectopic rays
2 missing

Chapter 4: Genetic analysis of *pry-1* function in *C. briggsae* vulval development

Background

Cell-cell communication during development is a vital process mediated through ligand-receptor (protein-protein) interactions, which then get relayed through signal transduction pathways (Barolo and Posakony 2002). Some of the key signal transduction pathways that operate during metazoan development include the NOTCH, RAS, WNT, JNK/STAT, and the TGF-β pathway (Cadigan 1997; Barolo and Posakony 2002; Bray 2006). These pathways are well conserved during evolution suggesting their fundamental role in mediating crucial biological processes (A.Pires-daSilva 2003).

Wnt family of secreted glycoproteins play a pivotal role in cell communication processes during development (Cadigan 1997). More recently, many components of this pathway have been linked to several types of cancers such as colon cancer, oral carcinoma, etc (Cadigan 1997). The Wnt proteins are well conserved among flies, vertebrates and *C. elegans* (Table 1.1) (Herman MA 2003). The components of the canonical Wnt pathway in worms regulate multiple developmental processes, such as the P12 cell fate, Q neuroblast migration, male and hermaphrodite reproductive systems (refer to Chapter 3). The analysis of Wnt signaling in vulval development in *C. elegans* has provided us with valuable insights regarding cell lineages, specification and commitment to cell fates during development (see chapter 1). Previous studies have identified four key Wnt proteins that function redundantly with each other in the canonical pathway to specify VPC fates. These include β-catenin homolog, BAR-1, TCF homolog, POP-1, APC homolog, APR-1 and the Axin homolog PRY-1. *bar-1* and *pop-1* positively regulate the specification of VPC cell fates, by regulating the expression of the Hox gene *lin-39* (Eisenmann, Maloof et al. 1998). Later, *pry-1* and *apr-1* were identified as negative regulators of VPC fate specification (Gleason et.al., 2002).

The *pry-1(lf)* mutation results in a multivulva phenotype which can be suppressed by *bar-1(lf)* and *pop-1 (lf)* mutations. Thus, *bar-1* and *pop-1* are epistatic to pry-1 with respect to vulval development (Gleason et al, 2002). Previously, the Wnt ligands acting on the VPCs were largely unknown. More recently, the genes *lin-44, cwn-1, cwn-2, egl-20* and *mom-2* were found to encode Wnt ligands and genes *lin-17, mom-5 and mig-1* to

encode the receptors (Gleason, Szyleyko et al. 2006). It has been observed that the triple mutant *lin-44; cwn-1; egl-20* exhibits the strongest defect in the VPCs, while no obvious defects were observed in single mutants (Gleason, Szyleyko et al. 2006). These observations revealed the extent of functional redundancy of wnt signaling in VPC fate specification.

Comparative studies between *C. elegans* and other related nematode species have revealed significant evolutionary variations with respect to the specification and regulation of cell fates during vulval development (see chapter 1). To analyze the evolution of Wnt pathway between *C. elegans* and *C. briggsae* vulval development, the effect of *Cbr-pry-1(lf)* was analyzed. This chapter covers the following objectives towards *pry-1*/Axin function in *C. briggsae* vulval development:

1. Characterization of vulval cell lineages, cell fate specification and competence through cell ablation studies in *Cbr-pry-1* alleles
2. Characterization of gonad-independent fate specification of the VPCs in *Cbr-pry-1* allelels
3. Specification of the genetic interactions of *Cbr-pry-1* with other vulval pathway genes (*lin-12/Notch, pop-1, mab-5 and bar-1*) in *C. briggsae,* through RNAi approach.

4.1 Vulval development in *Cbr-pry-1* mutants

4.1.1 Vulval induction properties of *Cbr-pry-1* alleles

Our preliminary analysis has revelaed that both P7.p and P8.p cells rarely assume the induced cell fate in *Cbr-pry-1* alleles (Table 3.1). To analyze this in greater detail, the number of progeny generated by Pn.p (n= 3-8) cells in *Cbr-pry-1* alleles was quantified (see Materials and Methods). Average vulval induction value for each allele was calculated. The order of average vulval induction in *Cbr-pry-1* alleles is as follows: *lin(sy5270)* > *lin(sy5411)* > *lin(sy5353)* (Table 4.1). A comparison of the VPC induction potential of *Cbr-pry-1* alleles with *Cel-pry-1(mu38)* revealed that P(7-8).p cells are more often induced in *Cel-pry-1(mu38)* compared to *Cbr-pry-1* mutants (Table 4.1). These studies also revealed that in *Cbr-pry-1* alleles, the anterior VPCs, P(3-6).p are more often induced compared to the posterior group. In addition, both P7.p and P8.p also displayed similar morphological features to P9-P12.pa cells (Table 4.1, Figure 4.2D and Figure 3.8).

4.1.2 VPC lineage analysis in *Cbr-pry-1* animals

To examine the induction potential of VPCs in *Cbr-pry-1* mutants in greater detail, I carried out a cell lineage analysis (see Materials and Methods). The VPC lineage analysis was done in AF16 (WT) and later in *sy5353* and *sy5270*. I found that in *Cbr-pry-1* mutants *sy5353* and *sy5270*, the P6.p cell that usually follows a TTTT pattern in WT animals, exhibited similar lineages in only 1 out of 7 animals (in *sy5353*) and 1 out of 8 (in *sy5270*) (Figure 4.4; Table 4.2 and 4.3). In addition, abnormal cell division of P5.p was also observed as revealed by unusual LLLN pattern in the mutant background compared to LLTN in wild type animals (Table 4.2 and 4.3). P3.p, P4.p and P8.p cells also adopted hybrid or incomplete lineages. In the case of the P7.p and P8.p, induced fates were observed only in 2 animals for P7.p and 1 animal for P8.p of the observed eight animals. Similar cell lineage analysis in *Cel-pry-1(mu38)* revealed higher penetrance of induced fates of P7.p and P8.p (Table 4.3).

4.1.3 VPC fate specification studies in *Cbr-pry-1* animals

Though the cell lineage analysis in *Cbr-pry-1* mutants provided us with details regarding cell division patterns of the VPCs, the observed lineage variations made it difficult in specifying their VPC cell fates. Hence I decided to analyze the expression of vulval cell fate markers, *Cbr-egl-17::gfp* (*mfIs5*) and *Cbr-zmp-1::gfp* (*mfIs8*) in *Cbr-pry-1* mutants (*sy5353* and *sy5270*). In wild type animals, *Cbr-egl-17::gfp* (*mfIs5*) predominantly expresses in Vul C and Vul D and *Cbr-zmp-1::gfp* (*mfIs8*) in Vul E (Figure 4.5 and Table 4.4) (Kirouac and Sternberg 2003). The ectopic VPCs that adopted vulval cell fates in the *Cbr-pry-1* mutants predominantly expressed mostly *Cbr-egl-17::gfp* and very rarely *Cbr-zmp-1::gfp* (Tables 4.5 and 4.6; Figures 4.6 and 4.7). These results suggest that VPCs in *Cbr-pry-1* mutants acquired 2^0 cell fate characteristics.

4.1.4 Vulval induction competence of P7.p and P8.p in *Cbr-pry-1* mutants

Previous cell ablation studies have shown that all six VPCs (P3-8.p) in *C. elegans* are competent to adopt 1^0 fate in response to the anchor cell signaling (Sulston and White 1980; Sternberg and Horvitz 1986). A single isolated VPC acquires the 1^0 fate while two isolated VPCs adopt 1^0 - 2^0 cell fates (Figure 4.1). To analyze the competence of P7.p and P8.p cells, all the anterior VPCs (P3-6.p) were ablated in AF16 and *sy5353* animals (see Materials and Methods). The cell ablations were carried out at mid L3 stage i.e., Pn.p stage of the VPCs and later analyzed for their cell fates during L4 stage. The expression of *Cbr-egl-17::gfp* reporter was used to analyze cell fate changes in both AF16 and *sy5353* animals. P7.p, and P8.p adopted 1^0 and 2^0 cell fates respectively in 2 of 6 cases in AF16 animals and none of the cases in sy5353 mutants (Table 4.7; Figure 4.8). (Table 4.7 and Figure 4.9). Thus, it can be inferred that in the *sy5353* background P7.p and P8.p were not competent to respond to the inductive signaling.

4.1.5 RNAi mediated knock down of *Cbr-pry-1* phenocopies *pry-1* alleles in *C. briggsae*

To correlate the observed vulval phenotypes of *Cbr-pry-1* alleles at the level of gene sequences, I analyzed VPC induction properties in AF16 and *Cbr-pry-1* background (see Materials and Methods). I observed a penetrance of 3.7% Muv (Adult animals) and 5.5 % Muv (L4 animals) in the F1 progeny of *Cbr-pry-1(RNAi)* animals (Table 4.14). These results further support the role of *Cbr-pry-1* in the negative regulation of vulval development in *C. briggsae*. However, P7.p and P8.p appear often induced in F1 progeny.

4.2 Gonad independent VPC fate specifications in *Cbr-pry-1* animals

Previous studies in *C. elegans* have revealed anchor cell independent fate specifications in certain multivulva mutants (Figure 4.1) (Sulston, Albertson et al. 1980; Sulston, Albertson et al. 1980; Sulston and White 1980; Sternberg and Horvitz 1986). This phenomenon has been proven to result from the constitutive activation of vulval genes that control cell proliferation. To analyze the role of anchor cell in mediating cell fate patterning in *Cbr-pry-1* multivulva mutants, I carried out gonad ablations in *sy5353* animals. The precursors of the somatic gonad, Z1- Z4 (that give rise to anchor cell in the L2 stage) were ablated in L1 worms in *sy5353* (see Materials and Methods). The ablated animals were initially confirmed with the success of the gonad ablations (as observed by the debris of gonad cells or absence of germline) and later analyzed for their VPC induction patterns in the L4 stage. It was observed that 75% (n=4) of the gonad-ablated *sy5353* worms exhibited Muv phenotype, suggesting that VPC inductions in *Cbr-pry-1* animals were independent of gonad signal or anchor cell signals (Table 4.8).

4.3 Genetic interactions of *Cbr-pry-1*with LIN-12/Notch and Wnt signaling pathway and their targets

4.3.1 LIN-12/Notch pathway

It was previously shown that both inductive and lateral signals cooperate to regulate the 2^0-1^0-2^0 cell fate patterns in P5.p-P6.p-P7.p VPCs (section 1.3.2). In *Cbr-pry-1* animals, P7.p and P8.p are not competent in responding to inductive signal from the anchor cell compared to the anterior VPCs (P3-6).p (section 4.1.4). These observations suggested that there is a possible malfunctioning of *lin-12*/lateral signaling in the posterior region (after P6.p) in *pry-1* background in *C. briggsae.* In order to analyze the effect of lateral signaling on VPC fates specification in these animals, *Cbr-lin-12 (RNAi)* was performed in AF16 and *sy5353* (see Materials and Methods) (Table 4.9). The *C. briggsae* wild type (AF16) plate level RNAi phenotypes were quantified and compared to the corresponding ortholog genes in *C. elegans* (www.wormbase.org) (Table 4.9) Cell fate transformations, such as, 2^0-1^0 and 3^0-$2^0/1^0$ were observed in AF16 (WT) animals in *Cbr-lin-12 (RNAi)* background (Figure 4.11). In case of the *Cbr-pry-1* mutants, we observed a different fate pattern for the VPCs (Table 4.10). First, the P6.p cell in these animals acquired both 1^0 and hybrid cell fates. Furthermore, P7.p acquired a significant increase in adopting vulval fates in *Cbr-pry-1* alleles in *Cbr-lin-12 (RNAi)* background (17% - 28%; Table 4.1 - Table 4.10). As a result a wide range of cell fates i.e., 1^0, 2^0 and hybrid cell fates were observed for P7.p in these animals (Figure 4.11). However, no significant change was observed in the case of P8.p lineages. The remaining VPCs (P3.p and P4.p) were also frequently in *Cbr-pry-1* alleles *Cbr-lin-12 (RNAi)* (Table 4.10).

4.3.2 Wnt pathway

4.3.2a *Cbr-bar-1*

To analyze the role of β-catenin *bar-1* in vulval development in *C. briggsae, Cbr-bar-1 (RNAi)* was performed in AF16 and *sy5353* (see Materials and Methods) (Table 4.9). The VPC cell fates were analyzed in the progeny of RNAi treated worms and P7.p cell fates were increased from 17% to 51% (Table 4.11). The remaining VPCs also

adopted variable cell fate patterns similar to that observed in *Cbr-lin-12 (RNAi)* animals (Table 4.11).

4.3.2b *Cbr-pop-1*

To analyze the role of TCF/LEF homolog *pop-1* in vulval development in *C. briggsae, Cbr-pop-1(RNAi)* was performed in AF16 and *sy5353* (see Materials and Methods) (Table 4.9). Initially I observed a strong vulvaless phenotype (80% Vul, n= 7) in AF16 animals (Table 4.12). However, further analysis suggested a somewhat weaker phenotype with an average vulval induction value of 2.5 (n=18) (Table 4.16). However, in both cases animals exhibited a 100% gonad morphology defect (Figure 4.12 D and E: Table 4.12). The vulval induction in *Cbr-pry-1(sy5353)* mutants in *Cbr-pop-1 (RNAi)* was significantly reduced from 3.4 to 2. Once again, 100% penetrance for gonad defects was observed (Table 4.13and 4.16).

4.3.3 The Hox gene *Cbr-mab-5*

The Hox genes, *lin-39* and *mab-5* are two known downstream targets of the Wnt signaling pathway during vulval development in *C. elegans* (section 1.4) (Clark, Chisholm et al. 1993; Clandinin, Katz et al. 1997; Eizinger and Sommer 1997; Eisenmann, Maloof et al. 1998; Chen and Han 2001). To analyze the role of these genes in *C. briggsae* vulval development, I carried out *Cbr-mab-5(RNAi)* in AF16 and *Cb-pry-1* mutants. Due to the lack of a visible phenotype, I was unable to examine interaction between *Cbr-pry-1* and *Cbr-mab-5*. Thus further experiment is required to confirm the role of *Cbr-mab-5* in Wnt pathway-mediated vulval development.

Discussion

This chapter summarizes work on analyzing the genetics *pry-1* mediated Wnt signaling in *C. briggsae* vulval development.

Cbr-pry-1 mutation is associated with a unique Muv-Vul phenotype in the vulva

In regards to vulval development, both *Cel-pry-1* and *Cbr-pry-1* mutants belong to Muv class of mutants. This phenotype relates to the ectopic vulvae or pseudovulvae observed in hermaphrodites along with the central vulva. However, in our comparisons of vuvlal induction patterns of P(3-8).p cells between *Cel-pry-1* and *Cbr-pry-1* mutants, it was observed that P7.p and P8.p cells are rarely induced in *Cbr-pry-1* mutants (section 4.1.1). In addition, the posterior VPCs, (P9-11.p) exhibited morphological similarities with P12.pa cell (section 4.1.1). Thus, it can be inferred that *Cbr-pry-1* alleles are associated with a simultaneous multivulva (resulting from induced fates of P(3-6).p) and vulvaless phenotypes (resulting from rare inductions of P(7-8).p). This phenotype is simply referred to as 'Muv-Vul phenotype'. Furthermore, VPC lineage and fate specification studies analyzed in *Cbr-pry-1* alleles supported 'Muv-Vul phenotype' (section 4.1.2 and 4.1.3). Thus, based on *Cbr-pry-1* Muv-Vul phenotype, it can be suggested that Wnt pathway in *C. briggsae* has evolved differently from *C. elegans* during vulval development. In *C. elegans*, *lin-39* is involved in the generation of Pn.p cells during L1, and the proper fate specifications (1^0, $2^0$and 3^0) of P(3-8).p cells during L3 stage (Clark, Chisholm et al. 1993; Wang, Muller-Immergluck et al. 1993; Clandinin, Katz et al. 1997; Maloof and Kenyon 1998). In addition, *mab-5* is involved in the fate specifications of the posterior Pn.p cells, P7.p to P11.p (Clandinin et al, 1997). It has been identified that these genes are downstream targets of Wnt pathway in the VPCs (section 1.4). If the mechanisms of Wnt signaling-mediated vulval development in *C. briggsae* is conserved then the Muv-Vul phenotype in *Cbr-pry-1* alleles may also result from the upregulation of *Cbr-mab-5* in the posterior VPCs P(7-11).p and to changes in the regulation of *lin-39* in P(3-8).p cells along the A/P axis. In future it would be desirable to analyze the function of the *Cbr-lin-39* and *Cbr-mab-5* in *C. briggsae* to postulate a model for Muv-Vul phenotype in *Cbr-pry-1* alleles.

Analysis of VPC competence in *Cbr-pry-1* mutants

To better understand the cellular basis of Muv-Vul phenotype in *Cbr-pry-1* mutants, competence of P7.p and P8.p in *Cbr-pry-1* mutants was analyzed. I wanted to determine whether P7.p and P8.p respond to inductive signaling in the absence of other VPCs in *Cbr-pry-1* animals. For this all the anterior VPCs P(3-6).p except P7.p and P8.p were ablated during L2 stage and animals were allowed to grow till L4 stage and vulval inductions were examined under Nomarski microscopy. Based on the studies in *C. elegans*, it was expected that isolated P7.p and P8.p cells will receive most of the signal from anchor cell and should adopt induced fates. However, isolated P7.p and P8.p did not adopt induced fates confirming that they lack competence to respond to inductive signaling (section 4.1.4). Similar experiments were carried out in AF16 animals and it has been observed that P7.p and P8.p are induced to adopt 1^0 or 2^o cell fates (section 4.1.4).

LIN-12/Notch pathway may cooperate with *Cbr-pry-1* to regulate competence of P7.p and P8.p

From the cell fate studies carried in *Cbr-pry-1* alleles, it has been observed that P(3-6).p cells adopt 2^0 vulval cell fates (section 4.1.3). In *C. elegans*, it has been previously known that *lin-12(gf)* mutation results in a Muv phenotype that was characterized by 2^0 cell fates adopted by all the six VPCs (Greenwald 1983). So, we hypothesized that 2^0 vulval fates adopted by the VPCs in *Cbr-pry-1* alleles are due to hyperactivation of *Cbr-lin-12* function. If so, then removing LIN-12 activity may suppress the Muv phenotype of *Cbr-pry-1* mutant animals. This hypothesis was tested by knocking down *Cbr-lin-12* by RNAi in *Cbr-pry-1* background. The results showed that reducing *Cbr-lin-12* activity had no effect on the induction potentials of anterior VPCs P(3-6).p in *lin(sy5353)* animals. Thus, *Cbr-pry-1* mediated Wnt signaling may utilize some unknown mechanism to regulate the competence of anterior VPCs (section 4.3.1). However, interestingly, the competence of posterior VPCs namely, P7.p and P8.p in *Cbr-pry-1* mutants was regained in *Cbr-lin-12(RNAi)* background (Table 4.10 and Figure 4.11). This suggests that *Cbr-lin-12* may be involved in regulating competence of posterior VPCs in *C. briggsae*

Cbr-pry-1 mediated canonical Wnt pathway in *C. briggsae* vulval development

Genetic analysis of Muv mutants in *C. elegans* has revealed that these genes negatively regulate VPC induction (Lesa and Sternberg 1997; Jacobs, Beitel et al. 1998; Fay and Han 2000; Moghal and Sternberg 2003). Wnt pathway in *C. elegans* vulval development is mediated by *bar-1, pry-1, apr-1 and pop-1* and their target genes that include the Hox genes, *lin-39* and *mab-5* (see chapter 1). *Bar-1* and *pop-1* are known to positively regulate vulval development whereas *pry-1* and *apr-1* act negatively (Eisenmann et.al., 1998; Gleason et al., 2002). To define Wnt pathway involved in *C. briggsae* vulva formation, I studied genetic interactions of *Cbr-pry-1* with the othrologs of *C. elegans* Wnt pathway genes and their down stream targets through RNAi (section 4.3). The results of my studies are presented in the Table 4.17.

In *C. elegans,* it has been shown that loss-of-function of either *pop-1* or *bar-1* results in the suppression of Muv phenotype of *pry-1* (Gleason, 2002) (Table 4.16). My studies in *C. briggsae* revealed a similar interaction between *Cbr-pop-1* and *Cbr-pry-1* (Table 4.13). However in contrast to *C. elegnas* where RNAi mediated knock-down to *pop-1* has no phenotype on its own, I found that in *C. briggsae pop-1(RNAi)* animals exhibit significantly reduced vulval induction. Thus, *Cbr-pop-1* appears to have acquired a different role in VPC fate specification when compared to *Cel-pop-1*. The role of *Cbr-bar-1(RNAi)* was examined in three independent RNAi experiments which showed no significant change in the Muv phenotype of *Cbr-pry-1* was observed compared to *C. elegans* (N, 3.4 to 3.3; Table 4.11 and 4.15). However, I observed significant variations in different batches of *Cbr-bar-1(RNAi)* experiments. Hence, it is necessary that *Cbr-bar-1* RNAi study should be repeated in order to carefully ascribe function to this gene in *C. briggsae* vulva formation. Likewise, the function of *Cbr-mab-5* also needs to be examined to deterime its role in *Cbr-pry-1* mediated vulval induction in *C. briggsae.*

In summary, the results described in this section demonstrate that a *Cbr-pry-1* and *Cbr-pop-1* mediated Wnt signaling pathway plays important role in *C. briggsae* vulval development and that both these genes have acquired some changes in their function compared to *C. elegans* orthologs.

Table 4.1: Percentage of VPCs adopting vulval fates in and *Cel-pry-1* and *Cbr-pry-1* mutants

Genotype	Percentage of VPCs adopting vulval fate						n	Average vulval induction (N)
	P3.p	P4.p	P5.p	P6.p	P7.p	P8.p		
AF16	0	0	100	100	100	0	67	3
				*Cbr-pry-1*animals				
lin(sy5411)	32	36	41	42	1	5	42	3.8
lin(sy5353)	39	82	100	100	17	21	41	3.4
lin(sy5270)	53	47	100	100	77[a]	32[b]	56	4.5
				Cel-pry-1animals				
mu38	19	10	100	100	75	10	48	3.2

n- number of L4 animals observed for the study

N- average vulval induction of each strain was obtained by, the number of VPC adopting vulval fate/n. The P3.p to P8.p cells exhibiting similar induction patterns compared to the 1^0 and 2^0 vulval fates in AF16 are counted as 1 cell induction or complete induction and other cases are considered as partial (0.5) or no (0) induction events. Thus the average induction potential of AF16 is described as 3 depending on P5.p – P7.p induction patterns (2^0-1^0-2^0) and for multivulva animals the value of N is always > 3.

a&b - The remaining percentage of P7.p and P8.p cells, 33 and 68, respectively, which are not adopting vulval fates exhibit similar morphological features to *lin(sy5353)* and *lin(sy5411)* as presented in figure 4.2D.

Table 4.2: VPC lineage pattern in *sy5353*

	VPC lineage pattern					
Genotype	**P3.p**	**P4.p**	**P5.p**	**P6.p**	**P7.p**	**P8.p**
AF16	S or SS	SS	LLTN	TTTT	NTLL	SS
lin(sy5353)						
1	SS	SS	LLON	TOTO	N	DNL
2	ONN	LNNT	LLTN	OOTT	N	N
3	TNNO	LNNO	LLLN	OOTO	N	N
4	LNNN	NNNN	LLON	TTTT	NTLL	N
5	LNN	LNNT	LLON	TOOT	NOLL	N
6	SL	SS	LLLN	ONTO	N	N
7	S	SS	LLLN	TLOO	N	N

All the VPC cell divisions were analyzed under Nomarski optics and the final round of cell division was carried out as follows: L, longitudinal division along the anterior-posterior axis; T, transverse division along the left/right axis; O, division along the oblique clevage axis; N, the cells that re not undergoing any kind of cell division; S, syncytial cell. The VPC lineages that are still attached to the cuticle (after the three rounds of cell divisions) are underlined.

Table 4.3: VPC lineage pattern in *sy5270* and *mu38*

	VPC lineage pattern					
Gentotype	**P3.p**	**P4.p**	**P5.p**	**P6.p**	**P7.p**	**P8.p**
lin(sy5270)						
1	LNNL	LNS	LLLN	OOTO	S	NO?L
2	SS	SS	LLLN	OOOO	NN	SS
3	S	NNNO	LLLN	OOOO	N	NONO
4	SS	SS	LLLN	OTTO	NOLL	SNN
5	SS	SS	LLLN	OTTO	S	NONLN
6	OTNO	LONO	LLON	TTTT	NLLN	SS
7	NNON	LNNT	LLON	OTOL	S	ONNL
8	SNN	LNN	LLON	OOO?	NTLL	SS
Cel-pry-1(mu38)						
1	STLL	SS	LLON	TLTT	NDLL	SS
2	SS	NLS	LLON	TLLT	NLLL	SS

Table legends were adopted similar to Table 4.2

? refers to a cell whose lineage could not be clearly identified.

Table 4.4: Vulval cell fate marker expression in AF16 animals

Cell fate markers							
	Cbr-egl-17::gfp				*Cbr-zmp-1::gfp*		
Pn.p Stages[a]	**% Cell type expression**[b]						
	AC and other[a]	**Vul E**	**Vul A**	**Vul A& E**	**Vul C**	**Vul D**	**Vul C&D**
Pn.px	4	0	0	0	0	0	0
Pn.pxx	13	0	0	0	0	0	0
Pn.pxxx	0	83	2	15	63	7	30
N	38	53			135		

Pn.px refers to first round of VPC divisions: Pn.pxx refers to second round and Pn.pxxx to third round of cell divisions, during vulva formation.
a- *Cbr-zmp-1::gfp* expression was observed in the AC and other uterine cell lineages
N- the number of animals observed for the expression patterns

Table 4.5: Vulval cell fate marker expression in *sy5353*

Expression pattern of *Cbr-egl-17::gfp* in *sy5353*																
Pn.p cells																
P1.p		**P2.p**		**P3.p**		**P4.p**		**P5.p**		**P6.p**		**P7.p**		**P8.p**		N
I[a]	U[b]	I	U	I	U	I	U	I	U	I	U	I	U	I	U	115
0	115	0	115	81	34	86	29	115	0	115	0	7	108	14	101	
0%	100%	0%	100%	70%	30%	75%	25%	100%	0	100%	0%	13%	87%	30%	70%	
Gfp expression[c]																
0%	13%	0%	13%	100%	0%	100%	0%	95%	0	0%	0%	100%	5%	100%	0%	
Expression pattern of *Cbr-zmp-1::gfp* in *sy5353*																
Pn.p cells																
P1.p		**P2.p**		**P3.p**		**P4.p**		**P5.p**		**P6.p**		**P7.p**		**P8.p**		N
I[a]	U[b]	I	U	I	U	I	U	I	U	I	U	I	U	I	U	92
0	0	0	0	54	38	65	27	92	0	92	0	4	88	8	84	
0%	0%	0%	0%	58%	42%	70%	30%	100%	0	100%	0%	4%	96%	8%	92%	
Gfp expression[c]																
0%	0%	0%	0%	2%	0%	2%	0%	0%	0	100%	0%	0%	0%	0%	0%	

a- refers to the induced state of the Pn.p cells

b-refers to the un-induced state of the Pn.p cells

c- the percentage of gfp expression

Table 4.6: Vulval cell fate marker expression in *sy5270*

Expression pattern of *Cbr-egl-17::gfp* in *sy5270*																
Pn.p cells																
P1.p		**P2.p**		**P3.p**		**P4.p**		**P5.p**		**P6.p**		**P7.p**		**P8.p**		N
I[a]	U[b]	I	U	I	U	I	U	I	U	I	U	I	U	I	U	110
0	110	0	110	75	35	51	59	110	0	110	0	103	7	33	77	
0%	0%	0%	0%	68%	32%	46%	54%	100%	0	100%	0%	94%	6%	30%	70%	
Gfp expression[c]																
0%	19%[d]	0%	19%[d]	100%	3%	100%	22%	100%	0	0%	0%	100%	14%	100%	0%	
Expression pattern of *Cbr-zmp-1::gfp* in *sy5270*																
Pn.p cells																
P1.p		**P2.p**		**P3.p**		**P4.p**		**P5.p**		**P6.p**		**P7.p**		**P8.p**		N
I	U	I	U	I	U	I	U	I	U	I	U	I	U	I	U	96
0	0	0	0	63	33	57	38	96	0	96	0	92	4	33	63	
0	0	0	0	85%	35%	59%	41%	100%	0	100%	0%	94%	6%	34%	66%	
GFP expression																
0	0	0	0	8%	0%	5%	0%	0%	0	100%	0%	0%	0%	9%	0%	

Table legends were adopted similar to Table 4.5

Table 4.7: Cell fates adopted by the isolated P7.p and P8.p in wild type and *Cbr-pry-1* animals

	VPC fate specifications					
Gentotype	**P3.p**	**P4.p**	**P5.p**	**P6.p**	**P7.p**	**P8.p**
mfIs5 (Cbr-egl-17::gfp)						
1	X	X	X	X	1^0	2^0
2	X	X	X	X	H	H
3	X	X	X	X	1^0	2^0
4	X	X	X	X	2^0	H
5	X	X	X	X	H	S
6	X	X	X	X	?	S
sy5353; Cbr-egl-17::gfp						
1-6	X	X	X	X	D	D
7	X	X	X	X	D	X
8	S	X	X	X	D	D

All cell ablations were carried out at mid L3 stage. X refers to the ablated cells and S to syncytial cell and D the unique degenerate morphology of the P7.p and P8.p in *sy5353*. The fate of the cells was determined as follows: 1^0, by the number of cells produced (8) by the VPC and which were not attached to the cuticle. 2^0, by the number of cells produced (7) and attachment to the cuticle (few of the daughters that typically follow L divisions, where L refers to longitudinal division) and the expression of *Cbr-egl-17::gfp*. The fate adopted by the VPCs that produce only two or four daughters were considered as intermediate or hybrid (H).

Table 4.8: Gonad independent VPC inductions in *Cbr-pry-1(sy5353)* animals

Genotype	Plate level observation	
	Gonad intact	**Gonad ablated**
Wt (AF16)	0% Muv (67)	0% Muv (2)
Cbr-pry-1(sy5353)	98% Muv (41)	75% Muv (4)

Table 4.9: Summary of plate level phenotypes observed during RNAi experiments for *Cbr-pry-1* animals

Target gene	Pvul	Rup	Vul	Wt	N
Cbr-lin-12[a]	67.7%			32.2%	239
Cbr-bar-1[b]	32%	22.7%		45%	290
Cbr-pop-1[c]	15%		85%		131

Adult animals were placed on the RNAi plates and their corresponging RNAi plate level phenotypes were analyzed under dissecting microscope

a-The data collected from two independent RNAi experiments

b- The data collected from five independent RNAi experiments

c- The data collected refers to only one RNAi experiment

Pvul, Protruding vulva; Rup, Ruptured vulva; Vul- Vulvaless; Wt- wild type

N- the number of animals observed

Table 4.10: VPC cell fates observed upon *Cbr-lin-12* inactivation by RNAi in *lin(sy5353);*JU1018

Genotype	VPC induction pattern						
	P3.p	P4.p	P5.p	P6.p	P7.p	P8.p	N[a]
JU1018	3^0	3^0	2^0	1^0	2^0	3^0	many
Cbr-lin-12(RNAi) in *lin(sy5353)*;JU1018: Adult animals							
L4 animals							
	U	I	1^0	1^0	I	?	1/39
	U	I	1^0	1^0	2^0	?	1/39
	U	I	1^0	1^0	?	H	1/39
	I	I	1^0	1^0	?	?	4/39
	I	I	H	H	H	?	1/39
	I	U	1^0	1^0	?	?	6/39
	U	U	U	1^0	?	?	1/39
	U	H	1^0	1^0	?	?	1/39
	H	U	1^0	1^0	?	?	1/39
	I	U	1^0	1^0	1^0	H	1/39
	I	I	H	H	?	?	I/39
	H	H	H	H	?	?	1/39
	I	I	I	I	?	?	1/39
	H	U	H	H	?	?	1/39
	I	I	2^0	1^0	2^0	?	1/39
	I	I	I	I	H	?	1/39
	U	H	1^0	1^0	1^0	?	1/39
	I	I	2^0	1^0	H	?	1/39
	I	U	1^0	1^0	?	I	1/39
	I	I	2^0	1^0	2^0	2^0	1/39
	I	?	?	?	?	?	1/39
	I	I	1^0	1^0	?	H	1/39
	I	I	I	I	I	I	1/39
	I	1^0	1^0	1^0	?	H	1/39
	U	2^0	1^0	1^0	1^0	2^0	1/39
	I	U	1^0	1^0	H	?	1/39
	I	U	1^0	1^0	?	H	1/39
	U	I	I	I	?	?	2/39
	I	U	I	I	?	?	2/39
Percentage	74.3%	56.4%	95%	100	31%	23%	

The morphology of vulval invaginations and the number of cells produced and the attachment of daughter cells to the hyp7 was used as a criterion to determine the cell fates. The VPCs that were induced and was unable to specify their fate were referred by '?'. H refers to the hybrid fate adopted by a VPC, U the VPC that was not induced and I refers to induced fates. N- the number of animals exhibiting the respective cell fate patterns.

Table 4.11: VPC cell fates observed upon *Cbr-bar-1* inactivation by RNAi in *lin(sy5353)*;JU1018

Genotype	VPC induction pattern												
	P3.p		P4.p		P5.p		P6.p		P7.p		P8.p		N
JU1018	S or SS/ non-vulval/3^0		SS/non-vulval /3^0		Vulval/2^0/ LLTN		Vulval/1^0/ LLTN		Vulval/2^0/ NTLL		SS/non-vulval /3^0		many
Cbr-bar-1(RNAi) in *lin(sy5353)*;JU1018: Adult animals													
L4 animals	V	NV/S	V	NV/S	V	NV/S	V	NV/S	V	NV/S or D	V	NV/S or D	
1	25	25	31	19	49	2	50	0	31	19	8	42	50
%cell fates	50%	50%	62%	38%	98%	2%	100%	0%	62%	38%	16%	84%	
2	11	6	10	7	17	0	17	0	4	13	1	15	17
%cell fates	64%	36%	59%	41%	100%	0%	100%	0%	23%	77%	5.8%	88.2 %	
3	7	28	14	21	31	4	34	1	24	11	4	21	35
%cell fates	20%	80%	40%	60%	88.5%	11.5%	97.2%	2.8%	68.6%	31.4%	11.5%	60%	
% average	44%		53%		95.5%		99%		51%		22%		102
sy5353 % cell fates	39%		82%		100%		100%		17%		21%		41

The data represents three independent RNAi studies. V refers to the vulval fate and NV/S to the nonvulval /syncytial fate adopted by the respective VPC and D to the degenerate morphology of P7.p and P8.p in *sy5353* background. N – number of animals observed. *sy5353* % vulval cell fates adapted from Table 3.7.

Table 4.12: VPC cell fates and gonad defects observed upon *Cbr-pop-1* inactivation by RNAi in JU1018

Genotype	VPC induction pattern						Gonad	P12.pa defect
	P3.p	P4.p	P5.p	P6.p	P7.p	P8.p		
JU1018	S/ SS	SS	LLTN	TTTT	TNLL	SS	Normal	No
Cbr-pop-1(RNAi) in JU1018: Adult animals								
1[a]	S	SS	I	I	I	S	D	No
2	SS	SS	SS	SS	SS	SS	D	No
3[b]	?	?	?	?	SS	SS	D	No
4[c]	-	-	-	-	-	-	D	No
5	S	SS	SS	SS	SS	SS	D	No
6	SS	SS	SS	SS	SS	SS	D	No
7	?	?	SS	SS	SS	SS	D	No
%N	80%						100%	0%

a- In this case I refer to the induced fate of the cells analyzed by the presence of daughter cells.

b- only some of the VPC lineages are able to analyze without ambiguity

c- severe gonad defect was observed in this animal and I was unable to observe the VPC lineages.

%N – Percentage of the observed phenotypic defects

The percentage of VPC induction defects was calculated from the 5 of 7 cases where lineages are observed clearly.

Table 4.13: VPC cell fates and gonad defects observed upon *Cbr-pop-1* inactivation by RNAi in *lin(sy5353)*;JU1018

Genotype	VPC induction pattern							Gonad	P12.pa defect
	P3.p	P4.p	P5.p	P6.p	P7.p	P8.p	N		
JU1018	S/ SS	SS	LLTN	TTTT	TNLL	SS	many	Normal	No
Cbr-pop-1(RNAi) in *lin(sy5353)*;JU1018: Adult animals									
L3 animals	S	SS	SS	SS	D	D	3/10	d	Yes
			I	I	D	D	1/10	d	Yes
		I	I	I	D	D	3/10	d	Yes
			I	I	I	D	2/10	d	Yes
			I	I	D	D	1/10	d	Yes
Cbr-pop-1(RNAi) in *lin(sy5353)*;JU1018: L4 animals									
L4 animals		I	I	I	D	D	1/4	d	Yes
			I	I	D	SS	2/4	d	Yes
			SS	SS	D	D	1/4	d	Yes
Cbr-pop-1(RNAi) in *lin(sy5353)*;JU1018: L4 animals									
L4 animals	I	I	I	I	D	D	1/8	d	Yes
				I	I	D	1/8	d	Yes
			I	I	D	D	3/8	d	Yes
		I	I	I	D	D	2/8	d	Yes
	SS	SS	SS	SS	D	D	1/8	d	Yes
Average % of vulval fates	77% (average vulval induction = 2.0)						22		

N- the number of animals exhibiting the respective cell fate patterns

D refers to the degenerate morphology of P7.p and P8.p in *sy5353* background and, d - the defective gonad and S - syncytial fate I refer to the induced fate of the cells analyzed by the presence of daughter cells.

Table 4.14: RNAi phenotype of *Cbr-pry-1* in *C. briggsae*

Cbr-pry-1(RNAi) in JU1018						
S. N	Plate level observation (Adults)			Nomarski optics (L4 animals)		
	Wt	Muv	n	Wt	Muv	n^b
1	8	0	8	15	1	16
2	7	0	7	24	1	25
3	24	3	27	38	3	41
4	10	2	12	8	0	8
N	129	5	134	85	5	90
% Muv	3.7			5.5		

Adult animals are placed on the RNAi plates and observed their progeny at adult and L4 stages. RNAi phenotypes were observed from four independent studies

N- the total number of animals observed in each case

Table 4.15: Summary of *bar-1* and *lin-12* RNAi interactions of *Cbr-pry-1* and its comparisons to *Cel-pry-1*

Genotype	n	% overinduced	% Wild type	% underinduced	N
		bar-1* and *pry-1			
Cel-pry-1[a]	376	37	46	4	3.2 (56)
Cel-pry-1; Cel-bar-1[a]	105	4	46	50	2.7 (50)
lin(sy5353)	46	92	2	6	3.4
lin(sy5353);Cbr-bar-1(RNAi)	103	44	46	13	3.3
		Hyperinductive vulval pathway genes and *pry-1*			
Cel-pry-1[a]	376	37	46	4	3.2 (56)
Cel-pry-1;Cel-let23[a]	103	87	0	4	4.4
lin(sy5353)	46	92	2	6	3.4
lin(sy5353);Cbr-lin-12(RNAi)	41	20	17	4	3.5

a- Gleason et al., 2002

Table 4.16: Summary of *pop-1* RNAi interactions of *Cbr-pry-1* and its comparisons to *Cel-pry-1*

Genotype	n	% overinduced	% Wild type	% underinduced	N
Cel-pry-1	376	37	46	4	3.2 (56)
Cel-pop-1	103	0	71	1	3.0
Cel-pop-1; Cel-pry-1	121	0	90	3	3.0 (121)
lin(sy5353)	46	92	2	6	3.4
Cbr-pop-1(RNAi)	18	0	15	3	2.5
lin(sy5353);Cbr-pop-1(RNAi)	23	1	7	15	1.9

a- Gleason et al., 2002

Table 4.17: Model for *Cbr-pry-1* VPC competence

Genotype	P3.p	P4.p	P5.p	P6.p	P7.p	P8.p
AF16 (+)	3^0	3^0	2^0	1^0	2^0	3^0
A model of regulation of cell competence in *Cbr-pry-1*						
Cbr-pry-1(-)	2^0	2^0	2^0	1^0	NC	NC
Cbr-lin-12(+)	UP	UP	+	+	NC	NC
Cbr-mab-5(+)	+	+	+	+	UP	UP
Cbr-pry-1 VPC competence changes in genetic interactions						
Cbr-pry-1(-)	2^0	2^0	2^0	1^0	NC	NC
Cbr-pry-1(-); Inductive signal (-)	3^0	3^0	3^0	2^0/H	2^0/H	2^0/H
Cbr-pry-1(-); Cbr-lin12 (-)	H/I	H/I	1^0	+	UP	NC
Cbr-pry-1(-); Cbr-bar-1 (-)	I	I	2^0	1^0	UP	NC/S
Cbr-pry-1(-); Cbr-pop-1 (-)	I	I	I	I	NC	NC

UP- refers to the possible up regulation of the corresponding genes

NC- Non – competent VPCs

+ wild-type gene product

- mutant gene product, H- hybrid, I – induced fates

Figure 4.1: Changes in VPC fates upon cell ablations in *C. elegans*

All VPCs are differentiated by separate color backgrounds. The thick black circle refers to 1^0 cell fate, brown to the 2^0 and white to the 3^0. Ablated anchor cell was presented by black arrow. Dashed black circles represent the ablated VPCs. A) If the AC is ablated then all the VPCs adopt 3^0 fate and no functional vulva is formed, B) The VPC isolated through ablating all other VPCs acquires 1^0 fate, C) & D) If two VPCs isolated they adopt alternate 1^0 - 2^0 cell fates E) In Muv animals, gonad independent specification of VPC fates were observed. Picture was modified and adapted from worm book chapter: vulval development (Paul Sternberg) (www.wormbook.org).

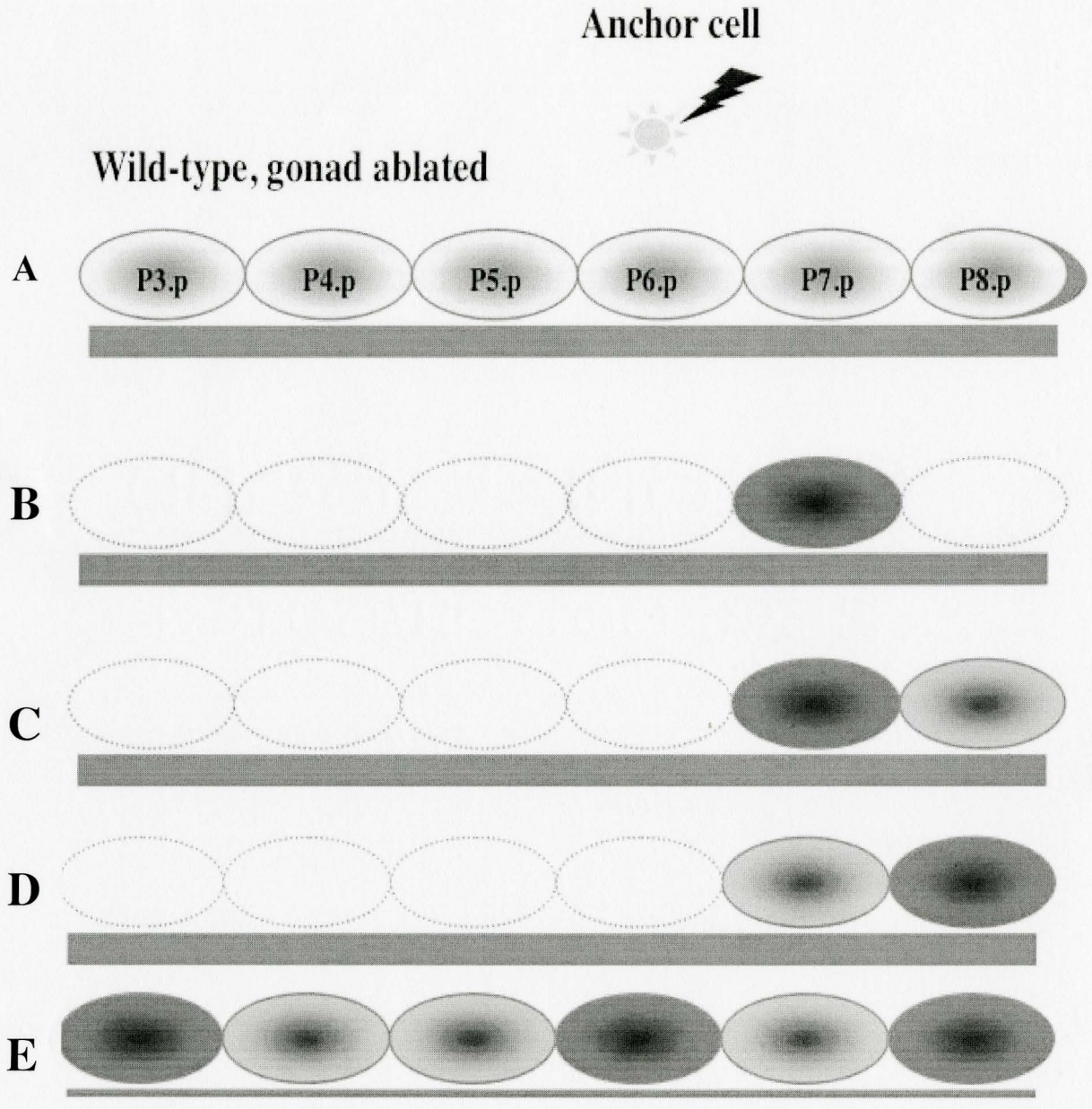
Anchor cell
Wild-type, gonad ablated
A
P3.p
P4.p
P5.p
P6.p
P7.p
P8.p
B
C
D
E

Figure 4.2: Morphological features of the vulval phenotypes of AF16 and *Cbr-pry-1* mutants

Adult morphology of the vulva in AF16 and *lin(sy5353)* is presented. (A) The morphology of the central vulva in adult AF16 animals. (B) The multivulva phenotype of the adult *lin(sy5353)*. The ectopic vulva resulted from P8.p induction along with the central vulva is presented. (C) Mild L4 *lin(sy5270)*. Central vulva was observed similar to AF16 and ectopic invagination was due to the result of P4.p being half induced. One of the daughters of P4.p fused with the syncitium (S) and the daughters formed from the remaining cell acquired vulval fates to form partial invagination. This is typically referred as 0.5 induction or half induction. (D) Mid L4 *lin(sy5353)*. Unique vulval invagination was seen where only P5.p and P6.p gave rise to the vulval opening and P7.p being not involved and very interestingly not induced at all. The distinct morphological feature of the P7.p (one cell) and P8.p (two cells) can be observed where the nucleoli appears very small compared to wild type animals.

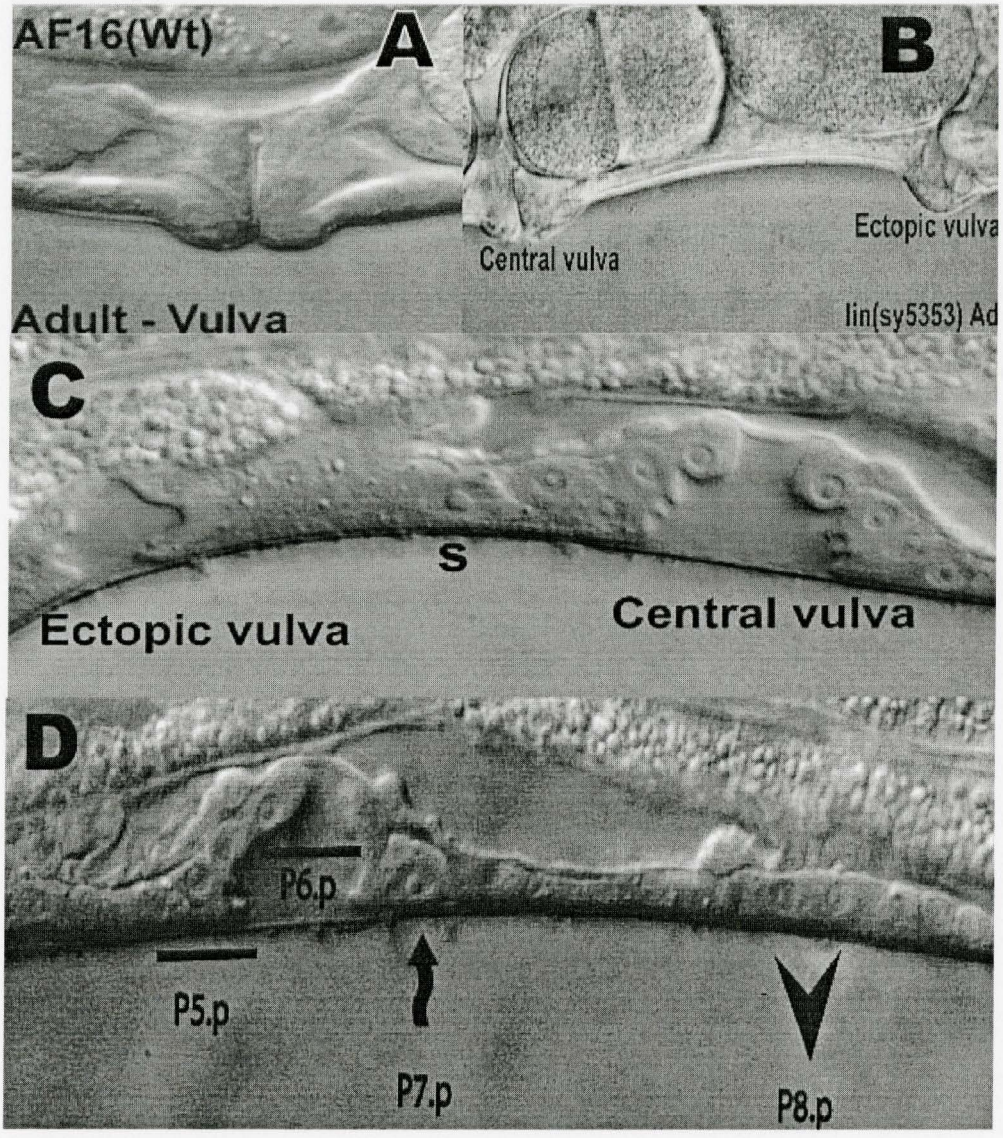
AF16(Wt)
A
B
Central vulva
Ectopic vulva
Adult - Vulva
lin(sy5353) Ad
C
S
Ectopic vulva
Central vulva
D
P6.p
P5.p
P7.p
P8.p

Figure 4.3: DIC images of the VPC cell lineage analysis in AF16

VPC cell lineages are analyzed from late L3 stage to early L4 stages. Cell division pattern of each VPC was observed under continuous Nomarski optics. Most of the cell divisions are confirmed at 1-2 hours after the L3-to-L4 lethargus. Pn.p refers to VPCs; Pn.px immediate daughters of VPCs; Pn.pxx granddaughters and Pn.pxxx great granddaughters. S refers syncytial cell.

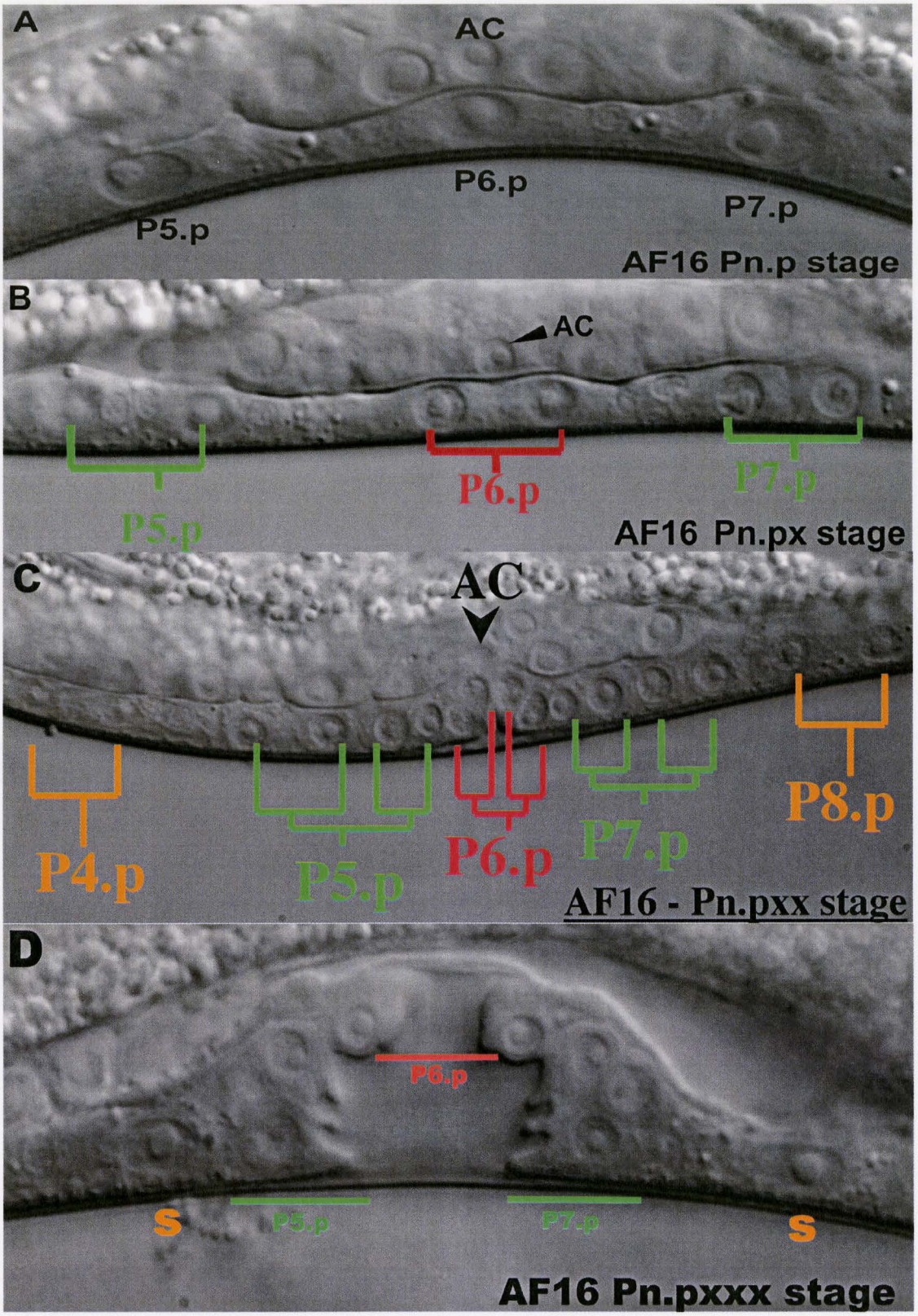
A
AC
P6.p
P7.p
P5.p
AF16 Pn.p stage
B
AC
P6.p
P7.p
P5.p
AF16 Pn.px stage
C
AC
P8.p
P4.p
P5.p
P6.p
P7.p
AF16 - Pn.pxx stage
D
P6.p
S
P5.p
P7.p
S
AF16 Pn.pxxx stage

Figure 4.4: VPC cell lineage analysis in *sy5353*

AC refers anchor cell and in all the images anterior is towards left. The VPC morphology and position is referred with the corresponding time frame of observations on the top right side of the respective images. Only P5.p to P8.p VPC cell lineages are represented in the images. (A) This figure represents *lin(sy5353)* worms at the Pn.pxx (four-cell stage) of P5.p and P6.p VPCs. (B) In this present time frame, two of the P5.p granddaughters have undergone longitudinal division and the cell represented by '?' is undergoing the process of cell division. N represents the P5.p granddaughter that has not divided, at all. The white stars represent granddaughters of P6.p, which were beginning to divide. (C) The complete lineages of P5.p are depicted in the present reference time giving rise to LLLN pattern for P5.p in the present animal. The P6.p cell divisions are completed in 5-10' after P5.p and all of them divided in TTTT fashion. Thus within a time frame of 2 to 2.5 hrs complete cell lineage analysis was analyzed.

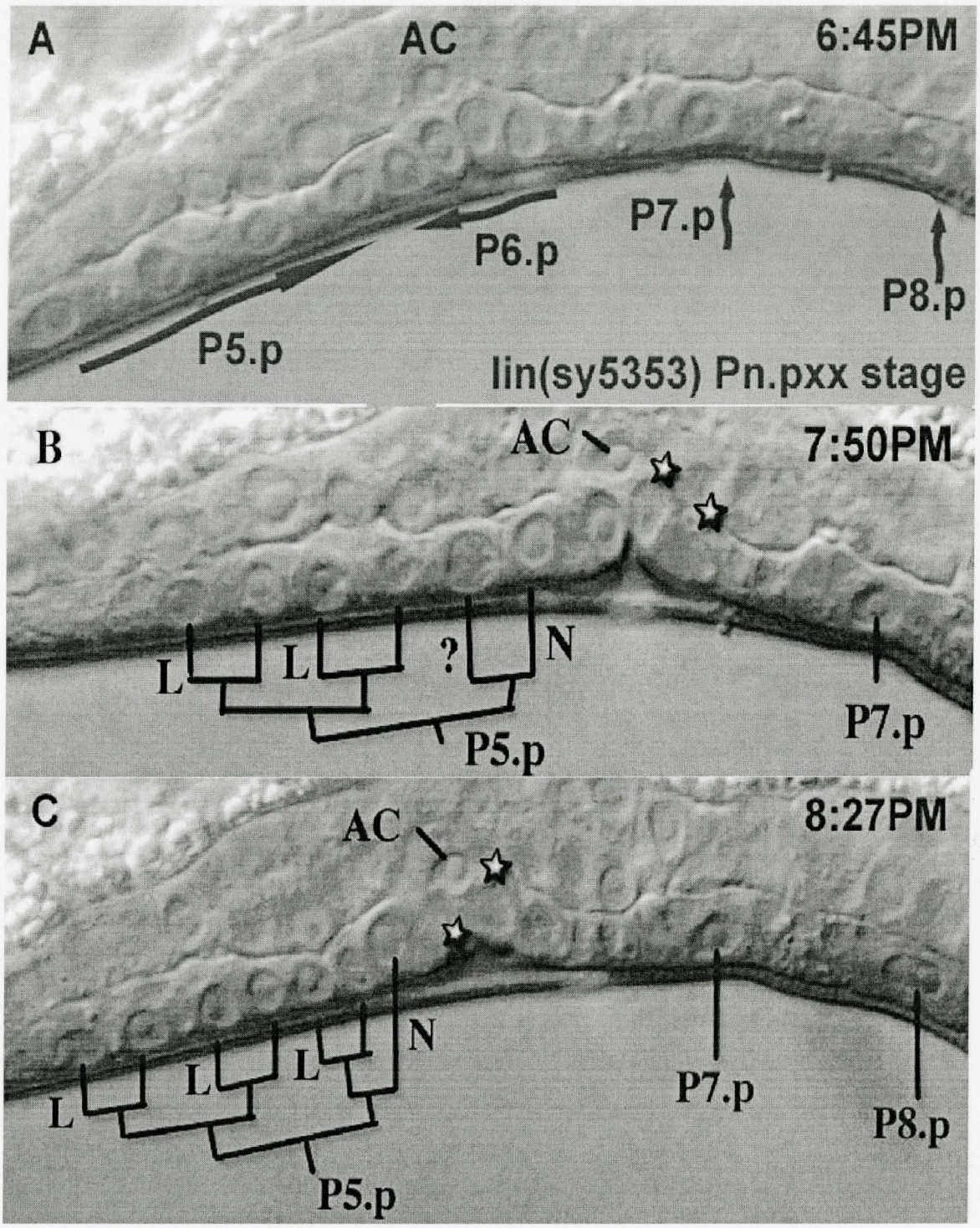
A
AC
6:45PM
P7.p
P6.p
P8.p
P5.p
lin(sy5353) Pn.pxx stage
B
AC
7:50PM
L
L
?
N
P5.p
P7.p
C
AC
8:27PM
N
L
L
L
P5.p
P7.p
P8.p

Figure 4.5: Expression of 1^0 and 2^0 cell fate markers, *Cbr-zmp-1::gfp* and *Cbr-egl-17::gfp*, respectively in AF16

All the animals were observed at mid L4 to late L4 stage. 1^0 cell fate marker expresses in VulE and Vul A cell types and 2^0 cell fate marker in VulC and VulD (A) Nomarski image of AF16 carrying *Cbr-egl-17::gfp*. VulC and VulD cell type specific expression was referred in the corresponding fluorescent image in (B). (C) Nomarski image of AF16 carrying *Cbr-zmp-1::gfp* and Vul E cell type specific expression was referred in the corresponding image in (D).

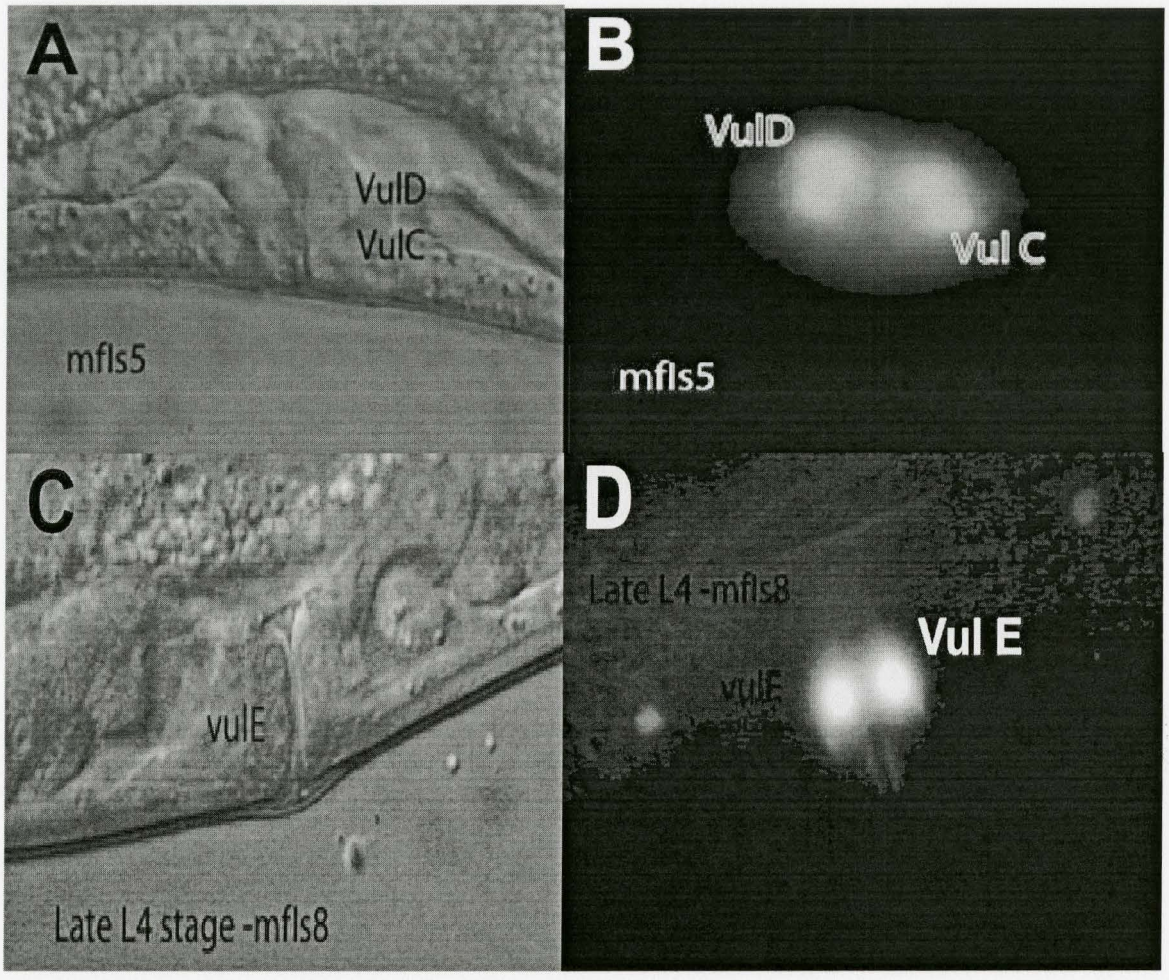
A
VulD
VulC
mfls5
B
VulD
Vul C
mfls5
C
vulE
Late L4 stage -mfls8
D
Late L4 -mfls8
Vul E
vulE

Figure 4.6: Expression pattern of *Cbr-egl-17::gfp* in *sy5353* animals

Animals were analyzed at midL4 stage. Anterior is towards right. (A) Nomarski image of *lin(sy5353)* at midL4 stage. The central vulva refers to 2^0-1^0-2^0 cell pattern of VPCs P5.p to P7.p, respectively. P4.p acquired vulval induction potential and is induced to form a pseudo vulval invagination. Figure (B) shows the expression of VulD in central vulva and ectopic expression of VulC and VulD in P4.p lineages.

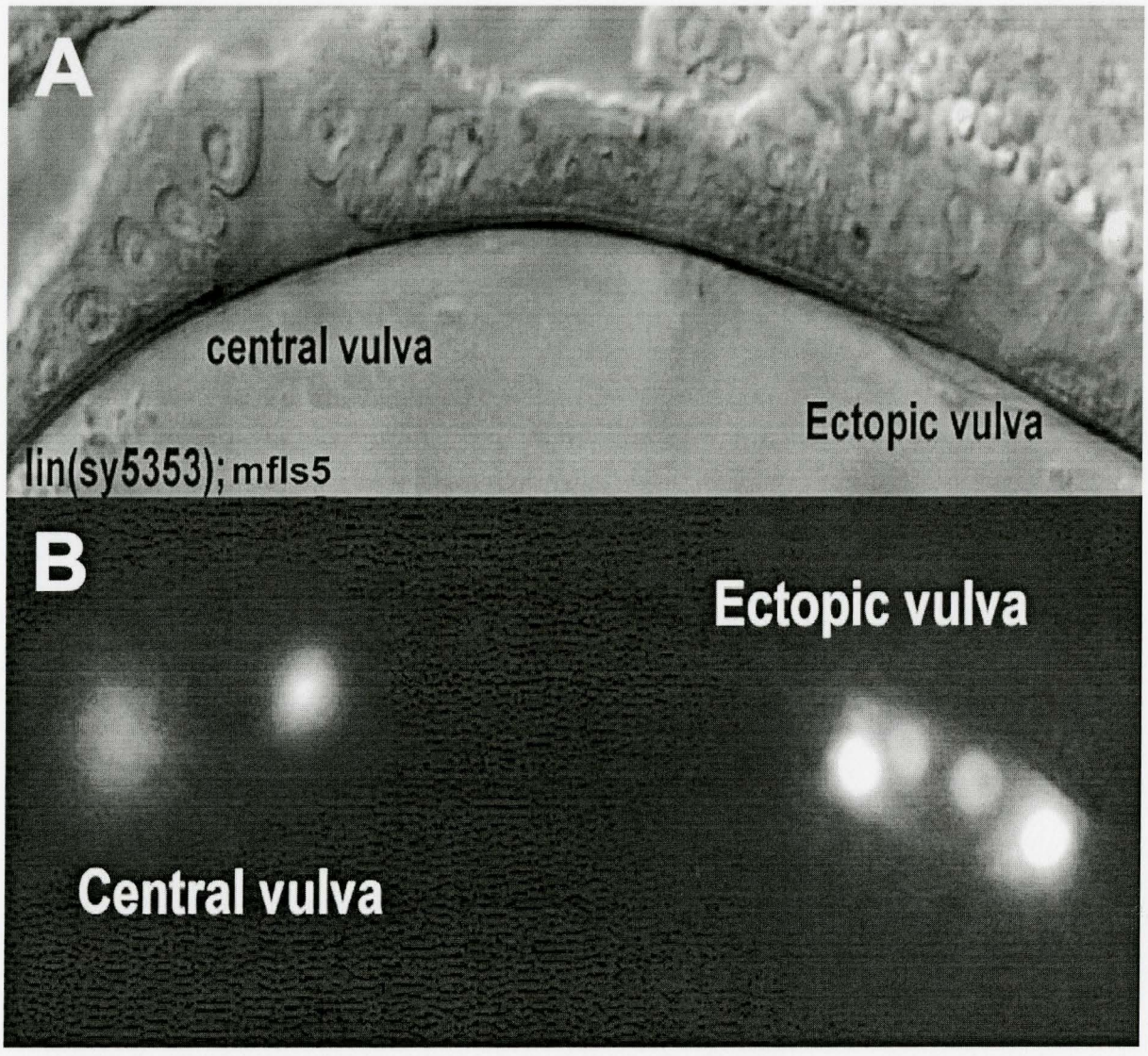
A
central vulva
Ectopic vulva
lin(sy5353); mfls5
B
Ectopic vulva
Central vulva

Figure 4.7: Expression pattern of *Cbr-egl-17::gfp* in *sy5270* animals

Animals are analyzed at midL4 stage. Anterior is towards left. (A) Nomarski image of *lin(sy5270)* at midL4 stage. The central vulva refers to 2^0-1^0-2^0 cell pattern of VPCs P5.p to P7.p, respectively. P8.p acquired vulval induction potential and is induced to form a pseudo vulval invagination

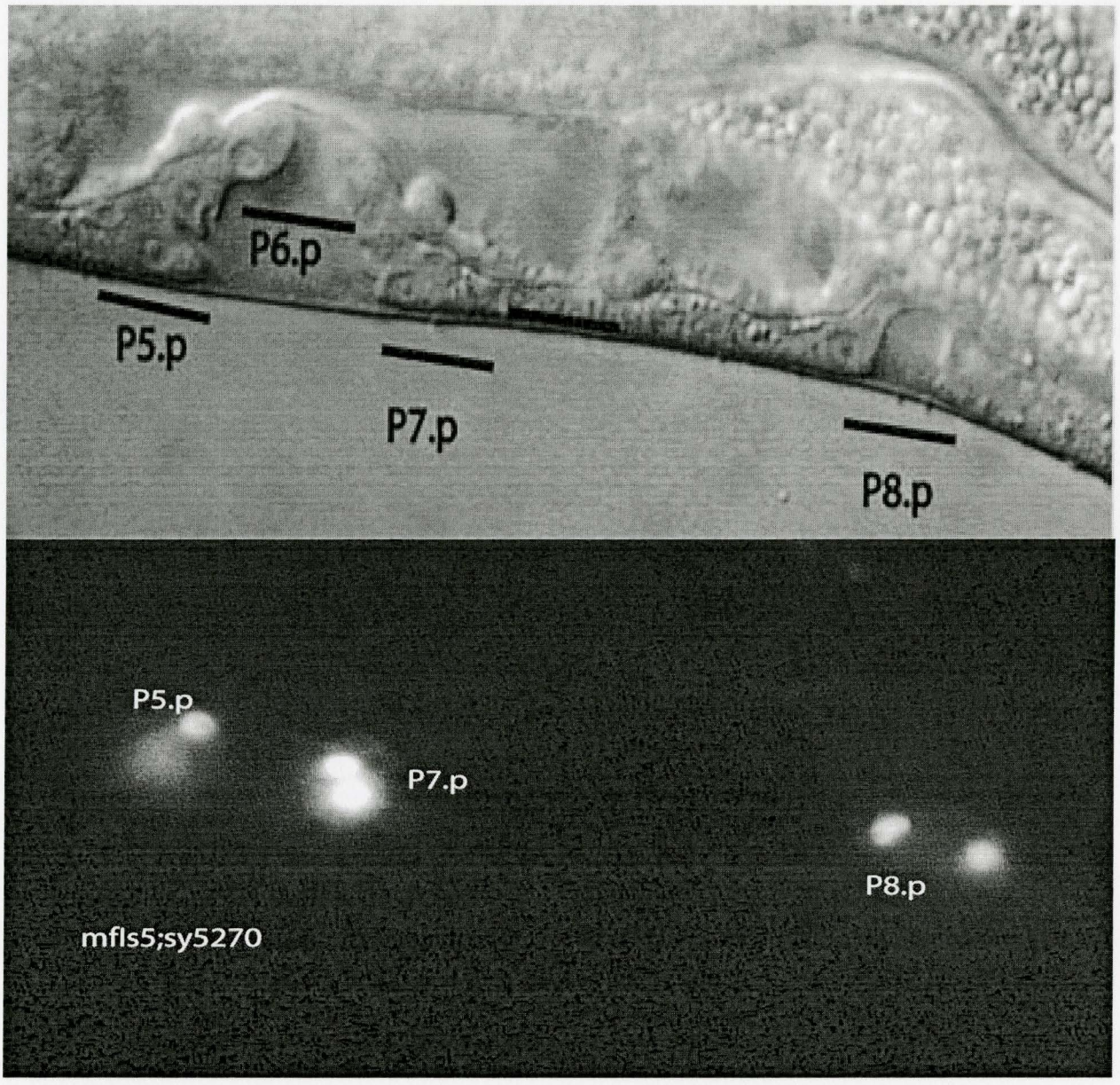
P6.p
P5.p
P7.p
P8.p
P5.p
P7.p
P8.p
mfls5;sy5270

Figure 4.8: *Cbr-egl-17::gfp* expression pattern in isolated P7.p and P8.p cells in AF16

All VPCs were ablated at mid L3 stage in except P7.p and P8.p cells in wild type *C. briggsae* animals carrying *Cbr-egl-17::gfp* reporter gene. (A) P7.p acquired 1^0 and P8.p 2^0 fates. The white line drawn refers to the absence of other Pn.p cells or their progeny, which confirms successful ablation. (B) The 2^0cell fate expression pattern of P8.p is very obvious in VulC and VulD cell types.

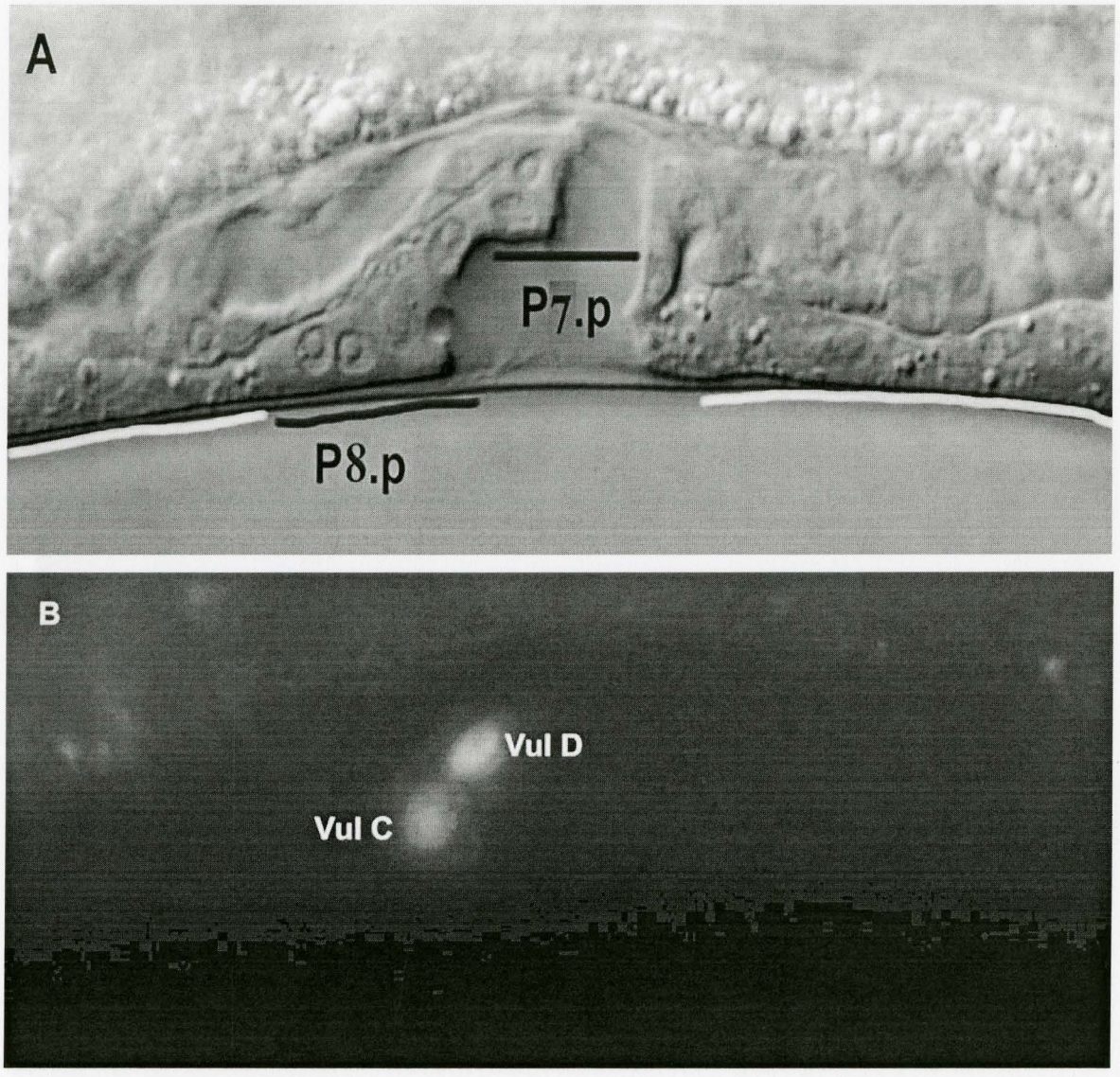
A
P7.p
P8.p
B
Vul D
Vul C

Figure 4.9: DIC images of isolated P7.p and P8.p VPCs in *sy5353* showing non-competence towards inductive signal

All the cells of the Vulval Equivalence Group are ablated at mid L3 stage in *Cbr-pry-1* worms, isolating P7.p and P8.p cells. The cells are observed for any cell division and cell fate expression pattern during the later stages. The yellow stars represent P7.p and P8.p cells and they remain the same in morphology and no cell division was observed. The black line refers to the absence of anterior Pn.p cells confirming that the ablations are successful.

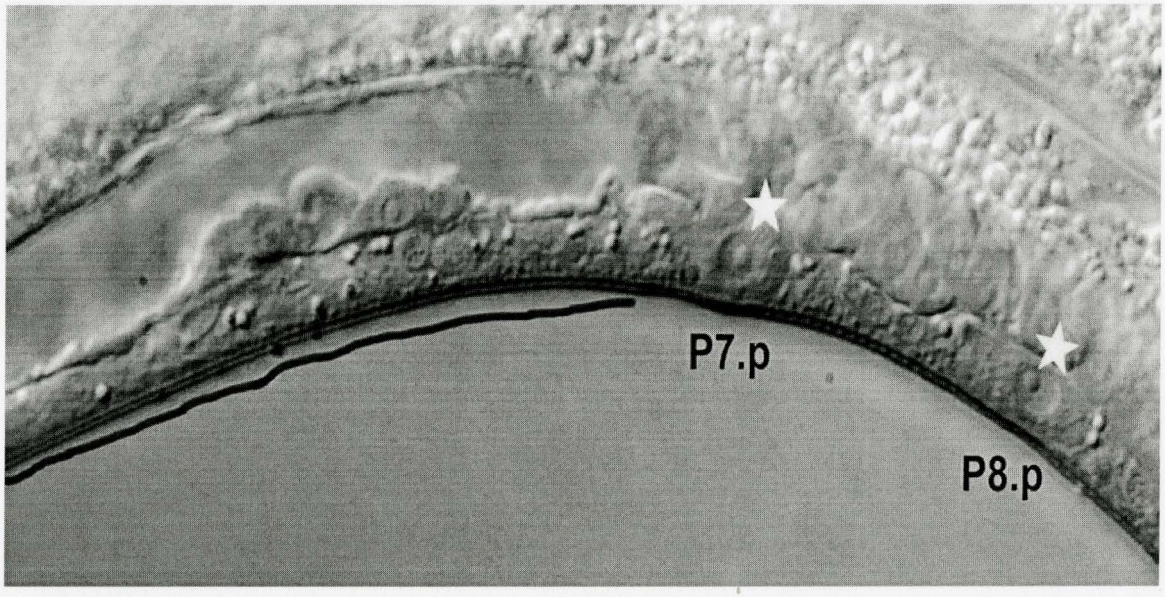
P7.p
P8.p

Figure 4.10: Gonad independent vulval fate specifications in *sy5353* animals

Anterior is towards left in all the figures. (A) Early L1 *lin(sy5353)* carrying *Cbr-egl-17::gfp* reporter gene. The positions of somatic gonadal precursors, Z1/Z4 that produce DTCs (Distal Tip Cells) are presented. The white dots represent the cells that are in the process of cell division. The primordial germ cells Z2/ Z3 (One of them will give rise to anchor cell) are clearly shown. (B) Mid L3 gonad ablated *lin(sy5353)* carrying *Cbr-egl-17::gfp* reporter gene. All the four gonadal precursors Z1 – Z4 are ablated in L1 stage and the horizontal solid line refers to the ablated-gonad. The positions of Pn.p cells are shown. (C) Mid L4 gonad ablated *lin(sy5353)* carrying *Cbr-egl-17::gfp* reporter gene. Nomarski figure showing partial invagination formed due to P6.p induction. The 2^0cell fate expression of P6.p daughters was shown in (D). (E) Adult gonad ablated *lin(sy5353)* carrying *Cbr-egl-17::gfp* reporter gene.

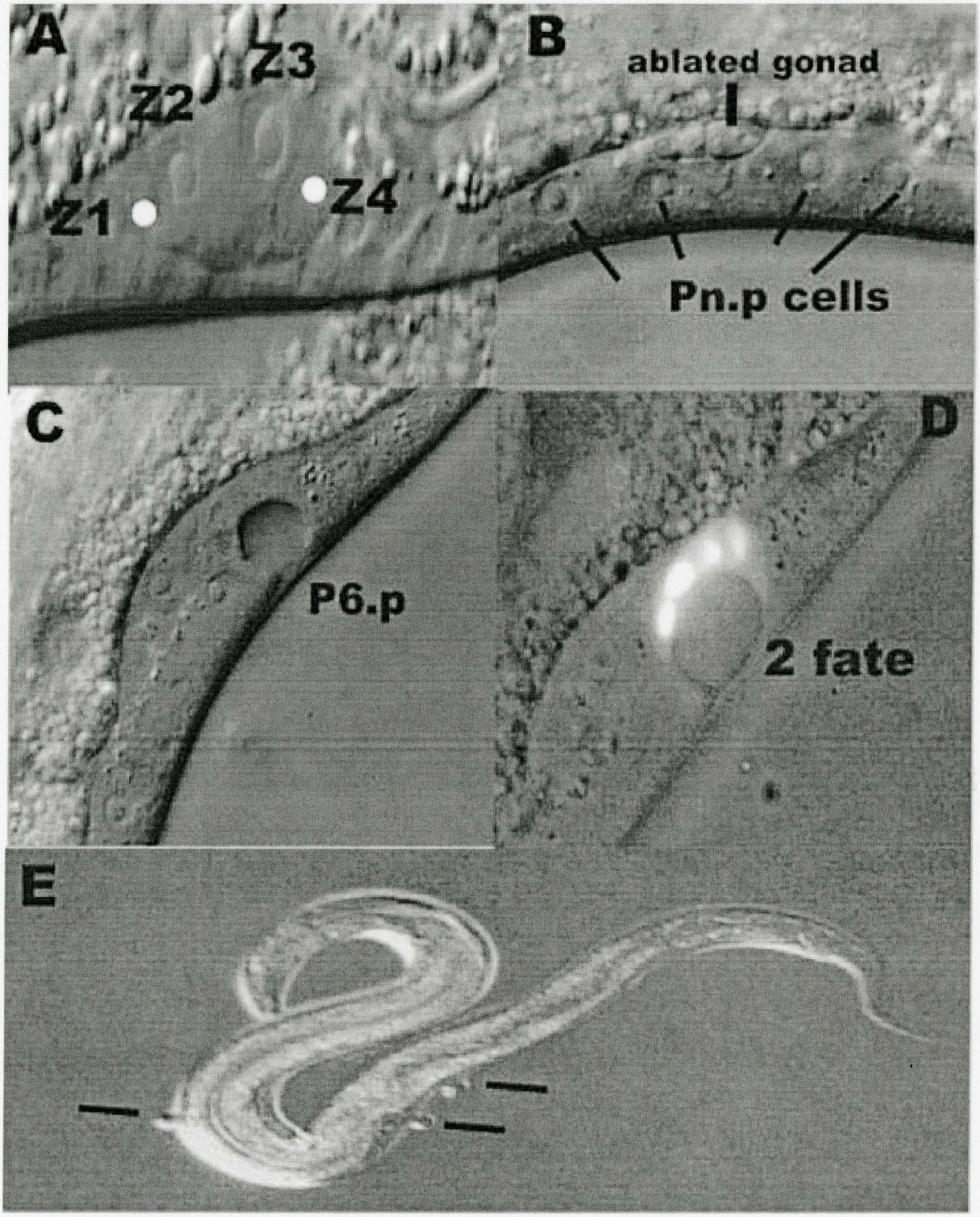
A
Z1
Z2
Z3
Z4
B
ablated gonad
Pn.p cells
C
P6.p
D
2 fate
E

Figure 4.11: RNAi phenotypes of JU1018 and *Cbr-pry-1* mutants in *lin-12*/Notch pathway background in *C. briggsae*

Partial inactivation of lin-12 results in adjacent fate transformation as 3^0 - 2^0 and 2^0- 1^0. (A) Mid L4 JU1018. Partial invagination was observed with aberrant vulval fate pattern with adjacent 1^0 fates for P5.p and P6.p. P7.p and P4.p retained their normal 2^0 and 3^0 fates, respectively. (B) Mid L4 *lin(sy5353)*. Broad vulval invagination was observed compared to JU1018 with P5.p – P7.p acquiring 1^0 fates. P4.p acquired 2^0 fate.

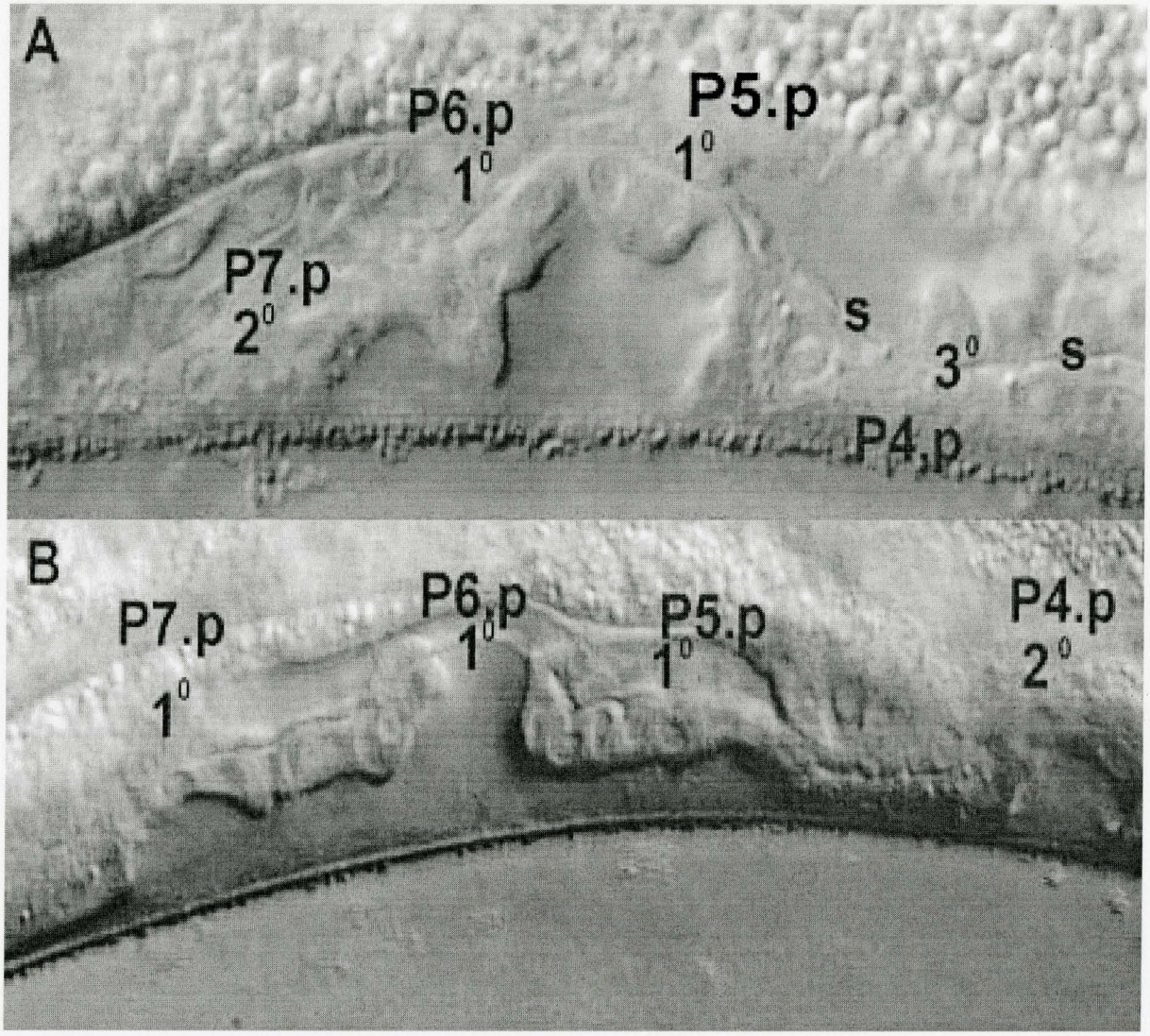
A
P6.p
1°
P5.p
1°
P7.p
2°
s
3°
s
P4.p
B
P7.p
1°
P6.p
1°
P5.p
1°
P4.p
2°

Figure 4.12: RNAi phenotypes of JU1018 and *Cbr-pry-1* mutants in wnt pathway background in *C. briggsae*

(A) Mid L4 *lin(sy5353).* Vulval cell fate patterns in observed in *Cbr-bar-1(RNAi)*background. P6.p acquired 1^0 fate and P5.p and P7.p have given rise to four-syncytial like cell (S). (B) P12.p like fate transformation of P11.p was observed for *lin(sy5353)* in *Cbr-bar-1(RNAi)* background in addition to (A). (C) Adult JU1018, one gonadal arm and vulva are shown in *Cbr-bar-1(RNAi)* background. Minor migration defect of gonadal arm was observed and the vulval morphology appears normal. (D) Adult JU1018 in *Cbr-bar-1(RNAi)*background. VPC induction was not observed and the typical gonadal defect (E) *lin(sy5353)* L4 worm in *Cbr-pop-1* background. VPC induction was obvious along with gonadal defects (D).

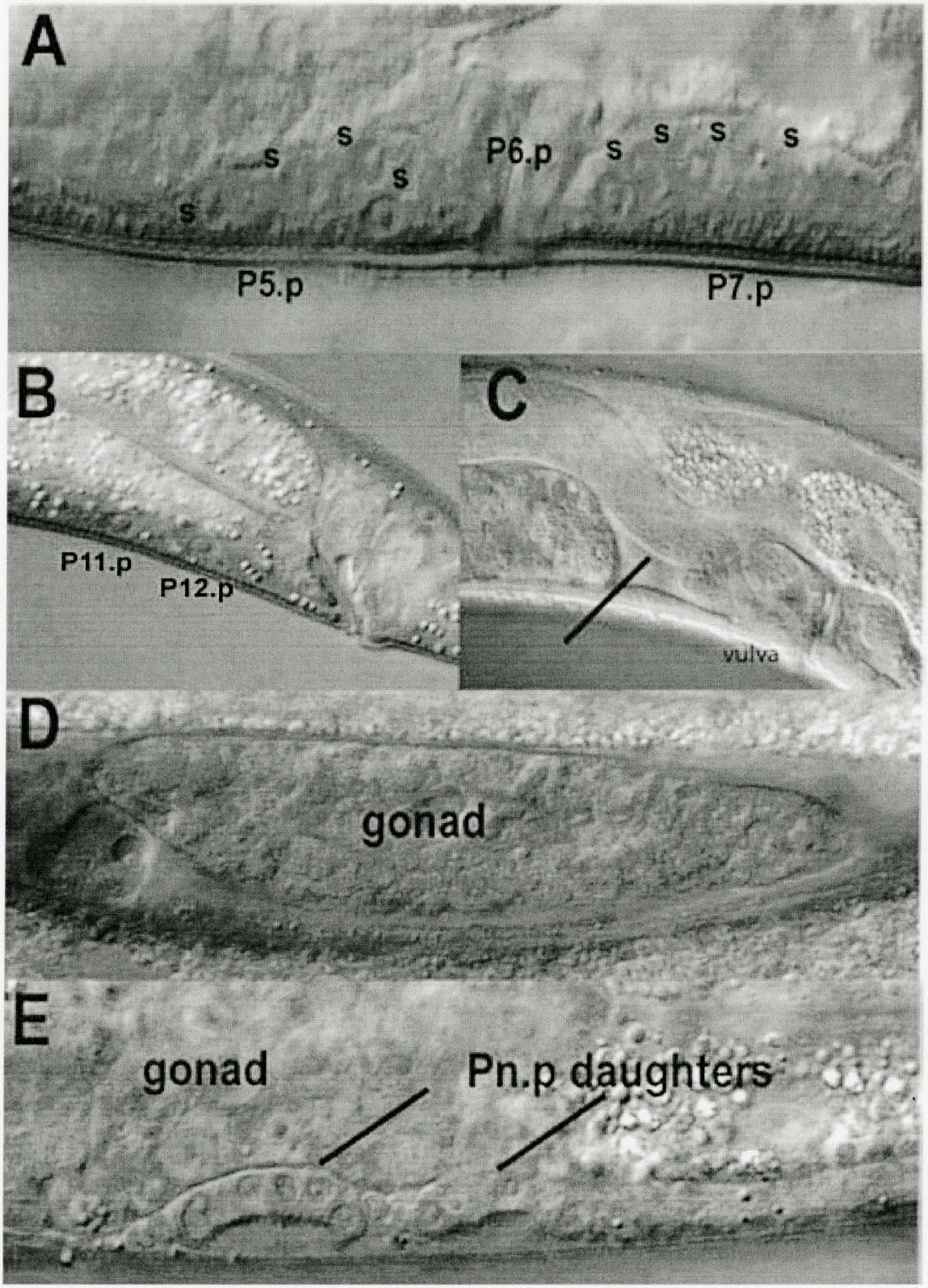
A
s
s
s
s
P6.p
s
s
s
s
P5.p
P7.p
B
P11.p
P12.p
C
vulva
D
gonad
E
gonad
Pn.p daughters

Summary

C. briggsae has become an established model for comparative studies in *Caenorhabditis* gensus (Kiontke and Fitch). *C. briggsae* diverged from *C. elegans* roughly 80-110 Mya ago (Stein, Bao et al. 2003). Due to its complete genome sequence and the ease of genetic manipulations, *C. briggsae* is being increasingly used in understanding changes in gene function and the mechanism of animal development. This thesis describes experiments on the *Cbr-pry-1* and Wnt pathway in the formation of *Caenorhabditis briggsae* reproductive system. Three alleles of *Cbr-pry-1* locus, *lin(sy5353), lin(sy5411) and lin(sy5270)* are mapped to LG I. Phenotypic characterization of these alleles confirmed that *Cbr-pry-1* belongs to unique Muv-Vul class of vulval mutants in *C. briggsae* compared to *C. elegans*. Further analysis of *Cbr-pry-1* Muv-Vul phenotype suggested that compared to *C. elegans* utilizes conserved Wnt signaling pathway components with some alterations in their function to regulate the competence of VPCs. I also observed that *Cbr-lin-12* might contribute to the posterior VPC competence in *C. briggsae*. Further experiments on the role of Wnt pathway genes *C. briggsae* will provide a better understanding of the evolutionary changes in developmental mechanisms in conferring cell fates and cell proliferations.

Future Experiments

Genetics:

1. Allele sequencing
2. Genetic suppression screens to identify genes that interact with *Cbr- pry-1*

Cell biology:

1. Cell fate transformations and fusion properties of Pn.p cells in the *Cbr-pry-1*animals should be examined by ajm-1 expression which marks the cell junctions (Mohler, Simske et al. 1998). Additionally, the VPC specific marker genes, *Cbr-lip-1* or *Cbr-dlg-1* expression analysis can also provide more details regarding the VPC identities.

Molecular biology:

1. Expression analysis can provide insights into the function of *Cbr-pry-1*
2. The expression of *Cbr-lin-39, Cbr-mab-5* and *Cbr-egl-5* can provide more details about the vulval defects, P12 cell fate and Q neuroblast migrations defects in *Cbr-pry-1* mutants.
3. Identification of Wnt receptors and lignad will help to better understand the role of Wnt signaling in *C. briggsae* vulval development

Appendix A: Preliminary phenotypic characterization of *C. briggsae* Muv mutants

In addition to analyzing *Cbr-pry-1* mutants I also carried out preliminary phenotypic characterization of some of the Muv mutants isolated in *C. briggsae* (Table 3.1). Specifically I observed their male tail defects and vulval defects. Interestingly, P3.p is never induced at all in *sa993*, suggesting the evolution of vulval equivalence group in *C. briggsae* (Table A.2). Male tail defects were observed in the morphology and defective ray patterns along with crumpled spicule (Table A.1).

Table A.1: Morphological defects in male tail development in *C. briggsae* Muv mutants

Mutant	**Defective ray pattern**	**crumpled Spicule**	**N**
lin(sa993)	11	10	13
lin(sy5216)	1	2	2
lin(sy5342)	2	1	2

Table A.2: VPC induction patterns in *C. briggsae* Muv mutants

Genotype	Percentage of VPCs adopting vulval fate						n
	P3.p	P4.p	P5.p	P6.p	P7.p	P8.p	
AF16	0	0	100	100	100	0	67
sy5342	68	73	100	100	99	71	23
sa993	0	35	100	100	100	50	20

Appendix B: Genetic mapping of integrants *mfIs5* (*Cbr-egl-17::gfp)* and *mfIs8 (Cbr-zmp-1::gfp)*

I also carried out genetic mapping of cell fate markers *mfIs5* and *mfIs8* on the six linkage groups in *C. briggsae* in a similar way to *Cbr-pry-1* genetic study. But I utilized the gfp expression of the marker genes as a criterion for the mapping technique rather than the phenotype to analyze mendelian segregation patterns. From the mapping data mfIs8 was assigned to LG V and *mfIs5* to LG II (Table B.1 and B.2).

Genetic cross:

P0: ♂ AF-16 x *mfIs5*(gfp) ♀

F1: ♂ *mfIs5*/+ x *cby-15* (LGII) (dpy)♀

F2: (*mfIs5*/+; *cby-15*/+) (both wt and expressing gfp)

(*mfIs5*/+;+/+)

↓

Cloned 10-12 L4 worms from the plates which segregate both dpy and gfp worms i.e., coming from the genotype (*mfIs5*/+; *cby-15*/+)

↓

From the progeny of the double heterozygote cloned 40-60 dpy worms under dissecting microscope and observed for the following segregation pattern

↓

(*cby-15*/*cby-15*) -- pure dpy worms -- -- 25%

(*cby-15*/*cby-15; mfIs5*/+) -- dpygfp (low) --- 50%

(*cby-15:mfIs5*) -- dpygfp (high) ----- 25%

Deviations from the above ratios correspond to the linkage to that phenotypic marker.

Table B.1: Genetic mapping data for the integrant *mfIs8*

Genotype	LG	Phenotypic marker	F2 phenotype scored	% segregation of double mutants from F2 (desired phenotype/total)
mfIs8	I	*lev(sy5440)*	Unc non-GFP	12/46 (25%)
	II	*dpy(sy5148)*	Dpy non- GFP	13/40 (32%)
	III	*dpy(s1281)*	Dpy non- GFP	11/43 (25.5%)
	IV	*unc (s1270)*	Unc non- GFP	15/46 (32%)
	V	*unc(sa997)*	Unc non- GFP	18/57 (25%)
	V	*unc(Sy5415)*	Unc non- GFP	5/37 (14%)

Table B.2: Genetic mapping data for the integrant *mfIs5*

Genotype	LG	Phenotypic marker	F2 phenotype scored	% segregation of double mutants from F2 (desired phenotype/total
mfIs5	II	*dpy(sy5148)*	Dpy non-GFP	6/60 (10%)
	II	*Cb-unc-4 (sy5341)*	Unc non-GFP	3/40 (7.5%)
	III	*dpy(sy1281)*	Dpy non-GFP	8/42 (19%)
	IV	*unc(s1270)*	Unc non-GFP	11/43(32%)

Appendix C: Primers used in the present study

Chromosome specific indel primers are utilized for indel mapping of *sy5353* for Cb1 and Cb 3 chromosomes. GL 66 and 67 are the up and down primers, respectively, applied for Cb1. They amplify 246 bp fragment in AF16 and 239 bp in HK104. GL 43 and 44 are the up and down primers, respectively, applied for Cb3. They amplify 251 bp fragments in AF16 and 259 bp in HK104. Refer to indel mapping procedure for more details (see Materials and Methods).

Table C: Primers used in Indel mapping of *sy5353*

Primer	Sequences	Chromosome	Polymorphisms
GL 66	GTGTCATGTCATACTCTGAAACA (up)	Cb1	bhP7
GL 67	ATGAATTCTCCATTCATCTATCA (down)	Cb1	bhP7
GL 43	ACAATAAGCATCTTCTTCACAAT (up)	Cb3	bhP3
GL 44	TCTAACTTTTTCAATCTCACATTC (down)	Cb3	bhP3

References

A.Pires-daSilva, R. J. S. (2003). "The Evolution of Signalling Pathways in Animal Development." Nature Genetics **4**: 39-49.

Aroian, R. V., M. Koga, et al. (1990). "The let-23 gene necessary for Caenorhabditis elegans vulval induction encodes a tyrosine kinase of the EGF receptor subfamily." Nature **348**(6303): 693-9.

Barolo, S. and J. Posakony (2002). "Three habits of highly effective signaling pathways: principles of transcriptional control by developmental cell signaling." Genes and Development **16**: 1167-1181.

Beitel, G. J., S. G. Clark, et al. (1990). "Caenorhabditis elegans ras gene let-60 acts as a switch in the pathway of vulval induction." Nature **348**(6301): 503-9.

Berset, T., E. F. Hoier, et al. (2001). "Notch inhibition of RAS signaling through MAP kinase phosphatase LIP-1 during C. elegans vulval development." Science **291**(5506): 1055-8.

Blaxter, M. (1998). "Caenorhabditis elegans is a nematode." Science **282**(5396): 2041-6.

Bray, S. (2006). "Notch signalling: a simple pathway becomes complex." Nat Rev Mol Cell Biol **7**: 678–689.

Brenner, S. (1974). "The genetics of Caenorhabditis elegans." Genetics **77**: 71-94.

Cabrera, C. V., M.C. Alonso, P. Johnston, R.G. Phillips, and P.A. Lawrence (1987). "Phenocopies induced with antisense RNA identify the wingless gene." Cell **50**: 659-663.

Cadigan, K. M., and Reol Nusse (1997). "Wnt signaling: a common theme in animal development." Genes & Development **11**(24): 3286-3305.

Ceol, C. J., F. Stegmeier, et al. (2006). "Identification and classification of genes that act antagonistically to let-60 Ras signaling in Caenorhabditis elegans vulval development." Genetics **173**(2): 709-26.

Chen, Z. and M. Han (2001). "C. elegans Rb, NuRD, and Ras regulate lin-39-mediated cell fusion during vulval fate specification." Curr Biol **11**(23): 1874-9.

Clandinin, T. R., W. S. Katz, et al. (1997). "Caenorhabditis elegans HOM-C genes regulate the response of vulval precursor cells to inductive signal." Dev Biol **182**(1): 150-61.

Clark, S. G., A. D. Chisholm, et al. (1993). "Control of cell fates in the central body region of C. elegans by the homeobox gene lin-39." Cell **74**(1): 43-55.

Delattre, M. and M. Felix (2001). "Polymorphism and evolution of vulval precursor cell lineages within two nematode genera, Caenorhabditis and Oscheius." Curr Biol **11**: 631 - 643.

Delattre, M. and M. A. Felix (2001). "Polymorphism and evolution of vulval precursor cell lineages within two nematode genera, Caenorhabditis and Oscheius." Curr Biol **11**(9): 631-43.

Eisenmann, D. Wnt signaling. WormBook. T. C. e. R. Community, WormBook.

Eisenmann, D. M. and S. K. Kim (2000). "Protruding vulva mutants identify novel loci and Wnt signaling factors that function during Caenorhabditis elegans vulva development." Genetics **156**: 1097-1116.

Eisenmann, D. M., J. N. Maloof, et al. (1998). "The β-catenin homolog BAR-1 and LET-60 Ras coordinately regulate the Hox gene lin-39 during Caenorhabditis elegans vulval development." Development **125**(18): 3667-80.

Eizinger, A. and R. J. Sommer (1997). "The homeotic gene lin-39 and the evolution of nematode epidermal cell fates." Science **278**(5337): 452-5.

Fay, D. S. and M. Han (2000). "The synthetic multivulval genes of C. elegans: functional redundancy, Ras-antagonism, and cell fate determination." Genesis **26**(4): 279-84.

Felix, M. A. and P. W. Sternberg (1996). "Symmetry breakage in the development of one-armed gonads in nematodes." Development **122**: 2129-2142.

Ferguson, E. L. and H. R. Horvitz (1985). "Identification and characterization of 22 genes that affect the vulval cell lineages of the nematode Caenorhabditis elegans." Genetics **110**(1): 17-72.

Ferguson, E. L. and H. R. Horvitz (1989). "The multivulva phenotype of certain Caenorhabditis elegans mutants results from defects in two functionally redundant pathways." Genetics **123**(1): 109-21.

Ferguson, E. L., P. W. Sternberg, et al. (1987). "A genetic pathway for the specification of the vulval cell lineages of Caenorhabditis elegans." Nature **326**(6110): 259-67.

Fitch, D. H. and S. W. Emmons (1995). "Variable cell positions and cell contacts underlie morphological evolution of the rays in the male tails of nematodes related to Caenorhabditis elegans." Dev Biol **170**(2): 564-82.

Fixsen, W., P. Sternberg, et al. (1985). "Genes that affect cell fates during the development of Caenorhabditis elegans." Cold Spring Harb Symp Quant Biol **50**: 99-104.

Fraser, A. G., R. S. Kamath, et al. (2000). "Functional genomic analysis of C. elegans chromosome I by systematic RNA interference." Nature **408**(6810): 325-30.

Gleason, J. E., H. C. Korswagen, et al. (2002). "Activation of Wnt signaling bypasses the requirement for RTK/Ras signaling during C. elegans vulval induction." Genes Dev **16**(10): 1281-90.

Gleason, J. E., E. A. Szyleyko, et al. (2006). "Multiple redundant Wnt signaling components function in two processes during C. elegans vulval development." Dev Biol **298**(2): 442-57.

Greenwald, I. (1989). "Cell-cell interactions that specify certain cell fates in C. elegans development." Trends Genet **5**(8): 237-41.

Greenwald, I. (1997). Development of the vulva. C. elegans II. D. L. Riddle, T. Blumenthal, B. J. Meyer and J. R. Priess. New York, Cold Spring Harbor Laboratory Press: 519-541.

Greenwald, I. S., P. W. Sternberg, et al. (1983). "The lin-12 locus specifies cell fates in Caenorhabditis elegans." Cell **34**(2): 435-44.

Gupta, B. P., R. Johnsen, et al. (2007). Genomics and biology of the nematode Caenorhabditis briggsae. WormBook. T. C. e. R. Community, WormBook.

Gupta, B. P., J. Liu, et al. (2006). "sli-3 negatively regulates the LET-23/epidermal growth factor receptor-mediated vulval induction pathway in Caenorhabditis elegans." Genetics **174**(3): 1315-26.

Hamelin, M., I. M. Scott, et al. (1992). "The mec-7 beta-tubulin gene of Caenorhabditis elegans is expressed primarily in the touch receptor neurons." Embo J **11**(8): 2885-93.

Han, M., R. V. Aroian, et al. (1990). "The let-60 locus controls the switch between vulval and nonvulval cell fates in Caenorhabditis elegans." Genetics **126**(4): 899-913.

Hedgecock, E. M., J. G. Culotti, et al. (1987). "Genetics of cell and axon migrations in Caenorhabditis elegans." Development **100**(3): 365-82.

Herman MA (2003). Wnt signaling in *C. elegans*. Wnt signaling in development. M. Kuhl. Georgetown, Landes Biosciences: 187-212.

Herman, M. A. and H. R. Horvitz (1994). "The Caenorhabditis elegans gene lin-44 controls the polarity of asymmetric cell divisions." Development **120**(5): 1035-47.

Herman, M. A., L. L. Vassilieva, et al. (1995). "The C. elegans gene lin-44, which controls the polarity of certain asymmetric cell divisions, encodes a Wnt protein and acts cell nonautonomously." Cell **83**(1): 101-10.

Herman, R. K. and E. M. Hedgecock (1990). "Limitation of the size of the vulval primordium of Caenorhabditis elegans by lin-15 expression in surrounding hypodermis." Nature **348**(6297): 169-71.

Hill, R. J. and P. W. Sternberg (1992). "The gene lin-3 encodes an inductive signal for vulval development in C. elegans." Nature **358**(6386): 470-6.

Hillier, W. L., et.al, (2007). "Comparison of C. elegans and C. briggsae Genome Sequences Reveals Extensive Conservation of Chromosome Organization and Synteny." PLoS Biol **5**(7).

Horvitz, H. R. and J. E. Sulston (1980). "Isolation and genetic characterization of cell-lineage mutants of the nematode Caenorhabditis elegans." Genetics **96**(2): 435-54.

Hunter, C. P. and C. Kenyon (1995). "Specification of anteroposterior cell fates in Caenorhabditis elegans by Drosophila Hox proteins." Nature **377**(6546): 229-32.

Jacobs, D., G. J. Beitel, et al. (1998). "Gain-of-function mutations in the Caenorhabditis elegans lin-1 ETS gene identify a C-terminal regulatory domain phosphorylated by ERK MAP kinase." Genetics **149**(4): 1809-22.

Jiang, L. I. and P. W. Sternberg (1998). "Interactions of EGF, Wnt and HOM-C genes specify the P12 neuroectoblast fate in C. elegans." Development **125**(12): 2337-47.

Kamath, R. S. and J. Ahringer (2003). "Genome-wide RNAi screening in Caenorhabditis elegans." Methods **30**(4): 313-21.

Kenyon, C. (1986). "A gene involved in the development of the posterior body region of Caenorhabditis elegans." Cell **46**: 477 - 488.

Kiontke, K. and D. H. A. Fitch The phylogenetic relationships of Caenorhabditis and other rhabditids. WormBook. T. C. e. R. Community, WormBook.

Kirouac, M. and P. W. Sternberg (2003). "cis-Regulatory control of three cell fate-specific genes in vulval organogenesis of Caenorhabditis elegans and C. briggsae." Developmental Biology **257**: 85-103.

Kornfeld, K. (1997). "Vulval development in Caenorhabditis elegans." Trends Genet **13**(2): 55-61.

Korswagen, H. C. (2002). "Canonical and non-canonical Wnt signaling pathways in Caenorhabditis elegans: variations on a common signaling theme." Bioessays **24**(9): 801-10.

Korswagen, H. C., M. A. Herman, et al. (2000). "Distinct beta-catenins mediate adhesion and signalling functions in C. elegans." Nature **406**(6795): 527-32.

Lesa, G. M. and P. W. Sternberg (1997). "Positive and negative tissue-specific signaling by a nematode epidermal growth factor receptor." Mol Biol Cell **8**(5): 779-93.

Maloof, J. N. and C. Kenyon (1998). "The Hox gene lin-39 is required during C. elegans vulval induction to select the outcome of Ras signaling." Development **125**(2): 181-90.

Maloof, J. N., J. Whangbo, et al. (1999). "A Wnt signaling pathway controls hox gene expression and neuroblast migration in C. elegans." Development **126**(1): 37-49.

Michael A. Miller et.al. (2004). "Clustered organization of reproductive genes in the *C. elegans* genome." Current Biology **14**: 1284-1290.

Moghal, N. and P. W. Sternberg (2003). "A component of the transcriptional mediator complex inhibits RAS-dependent vulval fate specification in C. elegans." Development **130**(1): 57-69.

Mohler, W. A., J. S. Simske, et al. (1998). "Dynamics and ultrastructure of developmental cell fusions in the Caenorhabditis elegans hypodermis." Curr Biol **8**(19): 1087-90.

Myers, T. R. and I. Greenwald (2005). "lin-35 Rb acts in the major hypodermis to oppose ras-mediated vulval induction in C. elegans." Dev Cell **8**(1): 117-23.

Natarajan, L., N. E. Witwer, et al. (2001). "The divergent Caenorhabditis elegans beta-catenin proteins BAR-1, WRM-1 and HMP-2 make distinct protein interactions but retain functional redundancy in vivo." Genetics **159**(1): 159-72.

Rachael Ainscough et.al. (1998). "Genomne Sequence of the Nematode *C. elegans*: A Platform for Investigating Biology." Science **282**: 2010-2018.

Rudel, D. and J. Kimble (2001). "Conservation of *glp-1* regulation and function in nematodes." Genetics **157**: 639-654.

Rudel, D. and J. Kimble (2002). "Evolution of discrete Notch-like receptors from a distant gene duplication in *Caenorhabditis*." Evol. Dev. **4**: 319-333.

Salser, S. J. and C. Kenyon (1992). "Activation of a C. elegans Antennapedia homologue in migrating cells controls their direction of migration." Nature **355**(6357): 255-8.

Salser, S. J. and C. Kenyon (1994). "Patterning C. elegans: homeotic cluster genes, cell fates and cell migrations." Trends Genet **10**(5): 159-64.

Sharma-Kishore, R., J. G. White, et al. (1999). "Formation of the vulva in Caenorhabditis elegans: a paradigm for organogenesis." Development **126**(4): 691-9.

Shaye, D. D. and I. Greenwald (2002). "Endocytosis-mediated downregulation of LIN-12/Notch upon Ras activation in Caenorhabditis elegans." Nature **420**(6916): 686-90.

Simpson, P. (2002). "Evolution of development in closely related species of flies and worms." Nature Rev. Gen. **3**(12).

Sommer R.J (2005). Evolution of development in nematodes related to C. elegans. WormBook. T. C. e. R. Community, WormBook.

Sommer, R. J. and P. W. Sternberg (1996). "Evolution of nematode vulval fate patterning." Dev Biol **173**(2): 396-407.

Stein, L. D., Z. Bao, et al. (2003). "The genome sequence of Caenorhabditis briggsae: a platform for comparative genomics." PLoS Biol **1**(2): E45.

Sternberg, P. W. and M. Han (1998). "Genetics of RAS signaling in C. elegans." Trends Genet **14**(11): 466-72.

Sternberg, P. W. and H. R. Horvitz (1986). "Pattern formation during vulval development in C. elegans." Cell **44**(5): 761-72.

Sulston, J., D. Albertson, et al. (1980). "The Caenorhabditis elegans male: Postembryonic development of nongonadal structures." Dev Biol **78**: 542 - 576.

Sulston, J. and H. Horvitz (1977). "Post-embryonic cell lineages of the nematode, Caenorhabditis elegans." Dev Biol **56**: 110 - 156.

Sulston, J. E., D. G. Albertson, et al. (1980). "The Caenorhabditis elegans male: postembryonic development of nongonadal structures." Dev Biol **78**(2): 542-76.

Sulston, J. E. and H. R. Horvitz (1977). "Post-embryonic cell lineages of the nematode, Caenorhabditis elegans." Dev Biol **56**(1): 110-56.

Sulston, J. E. and J. G. White (1980). "Regulation and cell autonomy during postembryonic development of Caenorhabditis elegans." Dev Biol **78**(2): 577-97.

Tabara, H., A. Grishok, et al. (1998). "RNAi in C. elegans: soaking in the genome sequence." Science **282**(5388): 430-1.

Van Ooyen, A., et.al, (1984). "Structure and nucleotide sequence of the putative mammary oncogene int-1; proviral insertions leave the protein-encoding domain intact." Cell **39**: 233-240.

Varmus, H. E., et.al (1982). "Many tumors induced by the mouse mammary tumor virus contain a provirus integrated in the same region of the host genome." Cell **31**: 99-109.

Wang, B., M. Muller-Immergluck, et al. (1993). "A homeotic gene cluster patterns the anteroposterior body axis of Caenorhabditis elegans." Cell **74**: 29 - 42.

Wang, X. and H. M. Chamberlin (2002). "Multiple regulatory changes contribute to the evolution of the Caenorhabditis lin-48 ovo gene." Genes Dev **16**(18): 2345-9.

White, J. G., E. Southgate, et al. (1986). "The structure of the ventral nerve cord of Caenorhabditis elegans." Philos Trans R Soc Lond B Biol Sci **314**: 1-340.

Wood, W. B., Ed. (1988). The Nematode *Caenorhabditis elegans*. Cold Spring Harbor New York, Cold Spring Harbor Laboratory Press.

Wu, Y. and M. Han (1994). "Suppression of activated Let-60 ras protein defines a role of Caenorhabditis elegans Sur-1 MAP kinase in vulval differentiation." Genes Dev **8**(2): 147-59.

Wu, Y., M. Han, et al. (1995). "MEK-2, a Caenorhabditis elegans MAP kinase kinase, functions in Ras-mediated vulval induction and other developmental events." Genes Dev **9**(6): 742-55.

Yoo, A. S., C. Bais, et al. (2004). "Crosstalk between the EGFR and LIN-12/Notch pathways in C. elegans vulval development." Science **303**(5658): 663-6.